UNIVERSITY OF OKLAHOMA
GRADUATE COLLEGE

THE EFFECT OF TEMPERATURE AND PH ON 2-METHACRYLOYLOXYETHYL PHOSPHATE HYDROGEL

A THESIS
SUBMITTED TO THE GRADUATE FACULTY
in partial fulfillment of the requirements for the
Degree of
MASTER OF SCIENCE

By
Yokly Leng
Norman, Oklahoma
2022

THE EFFECT OF TEMPERATURE AND PH ON
2-METHACRYLOYLOXYETHYL PHOSPHATE HYDROGEL

A THESIS APPROVED FOR THE
SCHOOL OF BIOLOGICAL, CHEMICAL AND MATERIALS ENGINEERING

BY THE COMMITTEE CONSISTING OF

Dr. John Klier, Chair
Dr. Keisha B. Walters, Co-chair
Dr. Jie Gao
Dr. Ngoc Bui

Table of Contents

Acknowledgment

I would like to thank Dr. Keisha Walters for her support, encouragement, understanding, and patience during this process. No words can describe her kindness and compassion. Especially Dr. Walters, I can not thank you enough for helping me and being there for me during such a difficult time. Thank you for pushing me beyond what I thought I could do and believing in me when I doubt myself. Thank you for the advice, never letting me give up, and always checking in on me with deadlines and daily life.

None of this could ever happen without Dr. Collin Britten. I have been working with him since day 1 in the lab and although I was behind, he has always been there for me to give guidance and supervise me throughout the year. A huge ‘thank you to him. Thank you for always being nice and open and finding a time to talk whenever I needed.

I would like to also thank Dr. Emi Kiyotake and, Peggy Keefe from Dr. Michael Detamore’s translational regenerative medicine lab for helping out with the cytotoxicity study, Vinit Sheth from Dr. Stefan Wilhelm’s lab for the expansion microscopy study, Chris Billing from Dr. Yingtao Liu’s lab for mechanical properties studies, Lucas Condes for showing me how to run contact angle measurements, and Hesham Aboukeila for showing me how to collect and analyze DSC data.

I would like to thank the Dolese Fellowship program, United World Scholar Program, and scholarship donors for financially supporting me throughout my time here at OU. Thanks to Dr. Kim Wolfinbarger and my mentor in the Jerry Holmes Leadership Program Mr. Steve Rogers for providing such great guidance in the past few years.

Thanks to Brandon Abbott and Kayla Foley for always being there for me, talking to me, and discussing issues with me. I could not imagine doing this without them. Thank you to Luis Mario Trevisi for being such a great friend over the years and always being there when I have questions. I would also like to thank all my roommates and friends for building such a supportive community around me and never giving up on me, even when I was not the best version of myself.

Thank you to my committee members, Dr. Jie Gao, Dr. Ngoc Bui, and especially Dr. John Klier for stepping in to help when needed. Thanks to the University of Oklahoma for continuous support and for providing resources for my education.

Lastly, I would like to thank both of my parents, siblings, and family for always being there for me whenever I needed them. I would not be who I am today without all of you. Although we do not say those 3 words, but we know them by heart. I could not be happier without any of you.

Abstract

Aqueous activators regenerated by electron transfer atomic transfer radical polymerization (aqueous ARGET-ATRP) is a well-understood polymerization technique that gives good control of the molecular weight of the final product. The regeneration of catalyst during polymerization reduces the amount of catalyst needed for the process. Reducing agents such as ascorbic acid are introduced and have shown great result with high oxygen tolerance. The polymerization conditions including pH, temperature, and solution composition could affect the final product of the polymerization. Aqueous ARGET-ATRP has shown great progress in polymerizing 2-methacryloyloxyethyl phosphate (MOEP). Current studies focused on the formation, gelation time and degree of swelling of poly(2-methacryloyloxyethyl phosphate) PMOEP.

In this study, the focus remained to be the degree of swelling of PMOEP, but in different solvents to better understand the interactions between PMOEP functional groups and solvents. It was found that salt solutions can be used to induce swelling of PMOEP with potassium chloride and sodium chloride showed similar rate of deswelling at 0.1M, but much lower than 0.1M calcium chloride and magnesium chloride solutions. Furthermore, the degree of swelling highly reduced when 0.1 M, 0.5M and 1M of sodium chloride, potassium chloride, calcium chloride and magnesium chloride solutions were used as solvent. The data shows that calcium chloride solution gives the lowest degree of swelling following by magnesium chloride, potassium chloride and sodium chloride, respectively. The increase in concentrations further decreased the rate and degree of swelling until a certain point at which concentrations do not affect the rate and degree of swelling anymore. It was also observed that after the first hour, the weight of hydrogels reduced significantly to lower than its initial weight when swelling in calcium chloride solutions. Scanning electron microscopy (SEM) and energy dispersive spectroscopy (EDS) were used to determine the

structure and compositions of the dried hydrogel. PMOEP interacted with cations of salt solutions and cations were observed across the surface. Potassium chloride salt were observed on the surface of PMOEP swelled in all concentration of KCl solutions.

PMOEP has shown to have very little response to pH of the solvent. The change in pH at acidic conditions, very little change of degree of swelling was observed. However, the degree of swelling increased significantly around neutral pH of 7 and remain constant at higher basic pH. The increase in temperature resulted in a decrease in degree of swelling as well. However, temperature significantly affected the rate of swelling of PMOEP in calcium chloride solutions. The collapse of hydrogel was observed at 30 °C and 40 °C.

PMOEP was polymerized with 4T1 mouse breast cancer cells via aqueous ARGET-ATRP to show its ability to expand cells as part of the expansion microscopy study. The result did not show fruitful data due to its low-quality image. However, it was estimated that PMOEP could expand cells by two-fold, which could be very useful since the preparation of PMOEP is much easier and less time consuming compared to the method currently practiced.

The polymerization conditions were altered to better understand their impact on the properties of the PMOEP hydrogel. The study involved reactions performed at 30, 40, and 50 °C with 40%, 50% and 60% by v/v MOEP and at the native pH along with pH values of 1 and 1.5. Results for PMOEP made with 50% MOEP showed excellent shape retention across the temperature and pH ranges investigated. Except at 50 °C where the PMOEP gels showed multiple fractures and the gel color was light brown, which is different from the usual clear hydrogels observed at other synthesis temperatures. Compression testing showed that PMOEP polymerized at 40 °C with 50% MOEP and native pH had the highest measured strain and could show the original compressive strength even after multiple cycles if the force is below the stress to break

the gel. Rat bone marrow stem cells (rBMSCs) were used for cytotoxicity study. rBMSCs were exposed and let to grow with the presence to PMOEP for 24 hours. rBMSCs showed great response to the gel with very few dead cells observed while continued to grow. This showed that PMOEP is not toxic tot cells.

Table of Figures

Chapter 1 Introduction

1.1. ATRP and Aqueous ARGET-ATRP

Preparation of hydrogel could be done in many ways. Some hydrogels can be found in nature while some require specific polymerization method to obtain such gels. Atomic transfer radical polymerization is a living polymerization technique relying on the catalyst to control the molecular weights and polydispersity of the products [1]. Common catalysts in ATRP are transition metals such as copper. The oxidation of the catalyst is very important to maintain the control of the reaction; therefore, ATRP is usually conducted in an oxygen free environment to prevent catalyst from oxidizing. ATRP usually requires high catalyst load to compromise with the oxidized catalyst during the reaction time. Alkyl halide structures also affect the reaction. The formation of alkyl halide radical by homolytic cleavage of the C-X bond allows the radical to bond with another carbon of an alkene group and form a new radical and a halogen radical [1]. However, finding a stable radical cold be difficult since it depends on multiple factors including steric, polar and resonance factors.

Recent development of ATRP focuses on the regeneration of activator by addition of reducing agents and photoinduced, electrochemical, and mechanochemical stimuli which make ATRP tolerance to oxygen for a certain amount [2]. Activators regenerated by electron transfer (ARGET) ATRP uses a reducing agent such as ascorbic acid to control the oxidation of the catalyst in which activator is constantly regenerated by electron transfer [3]. The addition of excess reducing agent should allow ATRP to tolerate higher amount of oxygen. This means that ARGET-ATRP could be done without deoxygenation process and therefore opens for everyone to do without special skill or fitted container for oxygen control. Aqueous ARGET-ATRP has shown to

work with many hydrophilic monomers. Aqueous ARGET-ATRP was previously reported being done with continuous fed of the reducing agent, ascorbic acid [4].

1.2. Hydrogel

Hydrogel has been synthesized and used in many applications. Hydrogels are a class of polymer that can absorb water due to its physical or chemical cross-links and/or chain entanglements [5, 6]. Factors limiting the ability of a hydrogel to absorb water include degree of crosslinking, crystallinity and tacticity [7]. pH of the solution can influence the swelling ratio and degree of swelling due to the interaction of the water molecules. Hydrogen bonding forms between water molecules at pH 7 which results in more space for hydrogel to swell [8].

Ionic strength of a solution can be affected by the amount of salt present in the solution. Hydrogel is also found to reduce its swelling ability in salt solutions comparing to its swelling in deionized water [9]. The interaction between cations of salt solution and polyelectrolytes hydrogels results in a decrease of hydrogel porosity, thus decreasing the ratio of swelling and degree of swelling. The higher the ionic strength, the lower the porosity will be. For example, for sodium alginate/Poly(vinyl alcohol) hydrogels, potassium chloride solution gives the highest swelling following by sodium chloride, calcium chloride and magnesium chloride, respectively. Similarly, among these four salt solutions, wheat straw cellulose based semi-interpenetrating polymer networks (semi-IPNs) shows the highest swelling in sodium chloride solution, following by potassium chloride, magnesium chloride and calcium chloride respectively [10].

1.3. From Monomer to Hydrogel: 2 - Methacryloyloxyethyl Phosphate

2-(methacryloyloxy)ethyl phosphate (MOEP) is an anionic monomer containing phosphate-pendant. MOEP has been used to prevent size change of 2-hydroxyehtyl methacrylate (HEMA) and methacrylamide propyltrimethylammonium chloride (MAPTAC) soft contact lens (SCLs). While cationic functional groups of HEMA and MAPTAC has the ability to store anionic drug such as azulene, the addition of MOEP has shown to help controlling the size change of the contact lens prior and after drug is released [11]. Similarly, the phosphate groups of MOEP was synthesized with HEMA to form SCLs for Naphazoline drug-released study [12].

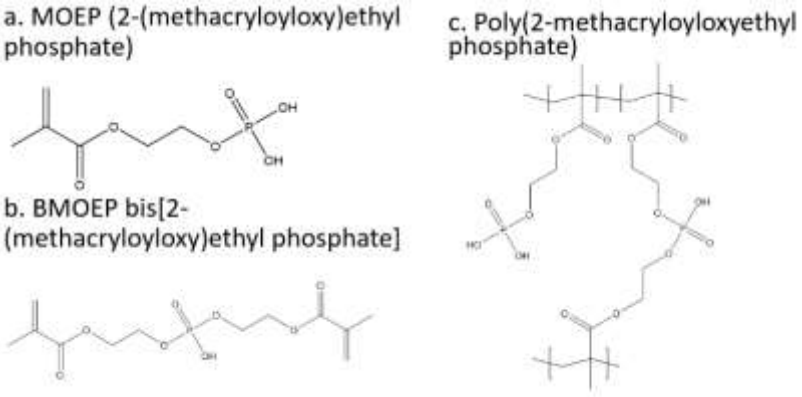

Figure 1-I: Structure of MOEP, BMOEP, and PMOEP.

The impurity of commercialized MOEP in the market is an essential in the formation of PMOEP hydrogel. The impurity usually contains 25% of bis[2-(methacryloyloxy)ethyl phosphate), a diene that can be used as crosslinker in a polymerization process. Structures of MOEP, BMOEP and PMOEP are shown in Figure 1-1 (a) MOEP, (b) BMOPE and (c) PMOEP. The alkene groups at both ends of BMOEP could react to different polymer chains and therefore crosslinks all the PMOEP polymer chains together forming a macros structure of hydrogel. Recently, aqueous ARGET-ATRP was used to polymerized MOEP together and crosslinked via its impurity, BMOEP to form a macro structure of PMOEP hydrogel. The degree of swelling was previously studied and showed up to 6000% increase in mass after fully swollen comparing to its

dried weight. PMOEP has been used in multiple applications especially in contact lens and drug release system.

1.4. Motivations and Study Goals

The goal of this study is to further investigate the properties of 2-methacryloyloxyethyl phosphate (MOEP) and its behaviors in solvent. While MOEP is used in many applications, but PMOEP hydrogel is fairly studied, especially as a polyelectrolyte polymer network. The anion groups of PMOEP could interact with many other functional groups and cations. The interaction could change the property of PMOEP hydrogel such as degree of swelling and their mechanical properties. Moreover, temperature and pH are very crucial to responsive polymers. This study will provide a better understanding of the behavior of PMOEP in different solvents at different temperatures.

Furthermore, the polymerization conditions are aimed to better understand the effect of temperatures, pH and concentration on the polymerization of PMOEP via aqueous ARGET-ATRP and how the degree of swelling changed upon the change in these polymerization conditions. The understanding of mechanical and biological properties of PMOEP is investigated using different equipment and methods for different polymerization conditions. Most importantly, PMOEP hydrogel could be used in many new applications that had never done before such as expansion microscopy which is a crucial imaging solution in biomedical field. Further investigation of PMOEP properties and its application should be done to expand the applicability of PMOEP in industrial and academic.

Chapter 2 Swelling Behavior and Degree of Swelling of PMOEP Hydrogels in Different Solutions

2.1. Abstract

Poly(2-methacryloyloxyethyl phosphate) hydrogel was polymerized via aqueous activators regenerated by electron transfer – atomic transfer radical polymerization (aqueous ARGET-ATRP) targeting the degree of polymerization of 300. The study of swelling behavior and degree of swelling of this hydrogel was conducted. After swollen in PBS and water, PMEOP significantly decreased its mass when exposed to chloride salt solutions. Potassium and sodium salt showed lower ratio of deswelling compared to calcium and magnesium slat solutions. The degree of swelling in salt solutions was also significantly reduced compared to the degree of swelling obtained from swelling in water and PBS. Calcium showed the lowest degree of welling followed by magnesium, potassium and sodium, respectively. PMOEP collapsed in calcium chloride solutions. SEM and EDS showed the presence of cations on the surface of dried PMOEP. pH of solvent did not affect the degree of swelling as much. It was observed that the degree of swelling changed drastically around neutral pH while remained very consistent at low acidic pH or high basic pH. An increase in temperature reduces the ratio and degree of swelling.

2.2. Introduction

Hydrogel is a three-dimensional network of monomers that connect via chemical crosslinking or chain entanglement [5, 13]. This allows hydrogel to swell in water without breaking its physical structure. At swollen state, hydrogel contains a huge amount of water comparing to its dried stage. It is considered a smart material due to its responsiveness to its environment [14]. The responsiveness of a hydrogel affects the swelling behavior and degree of swelling of the hydrogel.

It also allows hydrogel to be used in many applications including sensors and actuators, contact lenses, cardiac patch, drug delivery and in many more areas.

The induced swelling and degree of swelling of hydrogels is one of the important properties of hydrogel and have been studied extensively to understand the behavior of the hydrogels in different solutions and conditions of solvent. Physical properties affecting degree of swelling of a hydrogel include the degree of crosslinking or crosslinking density, molecular weight between crosslinkers, dangling and more. Temperature, ionic strength, pH etc. of solvents are some factors that limit the degree of swelling of hydrogels [9]. The degree of swelling of a hydrogel is determined by its swollen and dried weights showing how much the hydrogel can uptake water. This helps to understand how much water a hydrogel can absorb at equilibrium. The ratio of swelling on the other hand is determined based on the weight at time t and its initial weight before exposing the hydrogel to solvent. This shows how fast water can diffuse into the hydrogel for a given period of time.

Similarly, ionic strength can also affect the ability to swell of a hydrogel. Polyelectrolyte hydrogels accounts for any hydrogel with acidic or basic pendant groups [13]. The groups create repulsion forces within the hydrogel network which allows water to be absorbed even more [15]. The ionization of acidic and basic pendant groups influences the swelling ability of the hydrogel. Strong acid and base pendant groups can completely ionize, therefore the hydrogels containing these groups are able to swell at any pH of solvent. In contrast, hydrogels with weak acid or base pendant groups cannot swell at all pH range due to its inability to ionize at certain pH [13, 16].

Temperature is another factor influenced the degree of swelling in water. At low temperature, water becomes more viscos due to the increase in hydrogen bonding strength between water molecules, limiting the ability of water molecules to travel and diffuse into the hydrogel

[17]. As temperature increases, water molecules are less viscos allowing more water to be absorbed by the hydrogel.

2(methacryloyloxy)ethyl phosphate (MOEP) is a hydrophilic, anionic monomer containing phosphate-pendant groups. This allows MOEP to interact with any cations present in its environment. Beside its interaction with cationic drug such as Azulene in soft contact lens [11], this anionic monomer can also interact with other cation metals such as Na^{+}, K^{+}, Mg^{2+} and Ca^{2+}. Moreover, Stancu et al. copolymerized MOEP with 1-vinyl-2-pyrrolidinone and (diethylamino)ethyl methacrylate to grow hydroxyapatite on their surface [18]. The result shows that the growth of calcium layer on the surface is greatly affected by the phosphate content in the copolymer as phosphate content increases with an increase in MOEP concentration. The negative charge of phosphate group in MOEP is useful for implant calcification [19]. MOEP has also been electrosynthesized on titanium substrate with 2-hydroxiyethyl methacrylate (HEMA) to support the calcification in body fluid which is an indication of bone restoration ability. Additionally, Calcium phosphate mineral layers has been proven to form on PMOEP gel in a form of brushite or monetite depends on the Ca/P ratio as well as with a hydroxyapatite globular morphology [20].

This study reports the swelling behaviors of PMOEP hydrogels in different salt solutions and pH of solvent at different temperature. PMOEP is synthesized via aqueous ARGET-ATRP using the commercialized phosphoric acid 2-hydroxyethyl methacrylate easter that contains MOEP diene, bis[2-(methycryloyloxy)ethyl] phosphate impurity. This diene serves as the crosslinker in the hydrogel network. The swelling behaviors of PMOEP was measured at different time. SEM is used to confirm the present of each cation on the dried hydrogel after drying for 24 hours in the vacuum oven. The induced swelling of fully swelled PMOEP hydrogel is also reported.

2.3. Materials and Methods

2.3.1. Materials

Phosphoric acid 2-hydroxyethyl methacrylate ester (CAS 52628-03-2; 90%), potassium bromide (CAS 7758-02-3, 99%), α-bromophenylacetic acid (BPAA, CAS 4870-65-9; 98%), potassium dihydrogen phosphate, 99% (ACS) (CAS 7778-77-0), potassium chloride (CAS 7447-40-7), hexane, mixture of isomers (CAS 107-83-5; 98.5%), magnesium chloride (CAS 7786-30-3), calcium chloride (CAS 10043-52-4), sodium hydroxide (CAS 1310-73-2), and ascorbic acid (CAS 50-81-7) were purchased from Sigma-Aldrich. Sodium chloride (CAS 7647-14-5, 98%), hydrochloric acid (CAS 7647-01-0; 36.5%-38%), tris(2-pyridylmethyl)amine (TPMA, CAS 16858-01-8, 98%) were purchased from VWR. Type 1 ultrapure water was used directly from Millipore Synergy UV Water Purification System.

2.3.2. Purification of MOEP

Commercialized MOEP is has BMOEP impurity which makes up to about 25% on the molar basis. To reduce this crosslinker density, a 500 mL round bottom flask was used to extract BMOEP using hexane. 25 mL of MOEP, 25 mL of Type I ultrapure water and 100 mL of hexanes were added into the flask and rigorously stirred for an hour on a magnetic stir plate. This mixture was then separated using separation funnel. Aqueous MOEP/H2O went to the bottom of the funnel and then was transferred to a new clean 500 mL round bottom flask. This MOEP/H2O solution was further purified to extract hexane using reduced pressure Rotavap. The volume of purified solution was measured and transferred to a closed container and stored in the freezer until needed for synthesis.

2.3.3. Synthesis of PMOEP via Aqueous ARGET ATRP

An effort to determine the most stable PMOEP hydrogel was previously done. The degree of polymerization of 300 showed the highest degree of swelling with fewest fractures of the gel. The target degree of polymerization of 300 is used to examine the swelling behavior of PMOEP hydrogel. To obtain 300 degree of polymerization, 9.40 mg of αBPAA, 1.30 mg of TPMA, 1.00 g of $CuBr_2$, 59.5 mg of KBr, and 61.5 mg of Ascorbic acid were added to a clean and dry 20 mL scintillation vial. 5 mL of 50:50 by volume of purified MOEP solution was then added to the vial and was gently twirl to dissolve the ingredients. The homogenized solution was then transferred to a preformed mold and covered with a glass slide. This mold was then placed in a sealed vessel filled with nitrogen gas. The vessel is then transferred into an oven at 30 °C with continuous nitrogen flow for 8 hours to complete the polymerization. The glass cover is then carefully removed from the mold and the cylindrical-shaped hydrogels can be removed from the mold for swelling.

2.3.4. Swelling and Equilibration of Hydrogels

These hydrogels were then put on pre-weighed metal mesh weigh boats to obtain the initial mass of the hydrogel before swelling. The boats were then dipped into a dish filled with homemade Dulbecco's pH 7.4 phosphate buffer solution (PBS). Briefly, 8.0 g of NaCl, 1.15g of Na_2HPO_4 anhydrous, 0.2g KCl and 0.2 g of KH_2PO_4 were placed in a 1 L beaker and Type 1 ultrapure water was added to 800 mL on a magnetic stir plate and let to stir with a stirring rod for at least 10 minutes. When everything is dissolved, Type 1 ultrapure water was then added to obtain 1 L of pH 7.4 PBS solution with a pH meter attached to observe the final pH.

The degree of swelling is calculated using the swollen weight and dried weight as followed:

$$S = \frac{W_W - W_D}{W_D}$$

where:

- S is the swelling ratio;
- W_W is the swollen weight (in grams); and
- W_D is the swollen weight (in grams).

Similarly, the ratio of swelling is calculated in percentage using the formula below:

$$\%DS = \frac{W_t - W_0}{W_0} \times 100\%$$

where:

- %DS is the swelling ratio expressed in percentage;
- W_t is the swollen weight (in grams) at time t; and
- W_0 is the initial weight (in grams) before swelling.

2.3.5. Hydrogel Morphology Using ESEM

Environmental Scanning Electron Microscopy (ESEM) was also used to study the swollen morphology of the hydrogel. After swelling with PBS and Type 1 ultrapure water, a small piece of hydrogel was gently punched using a biopsy punch (2 mm in diameter). The height of the punched hydrogel was later adjusted with a shape blade to no more than 4 mm. The prepared hydrogel was then put into the ESEM chamber for morphology study.

2.3.6. Induced swelling of PMOEP

After synthesis, PMOEP hydrogels were swelled in pH 7.4 PBS for 12 hours and Type 1 ultrapure water for 12 hours while replacing each solvent every 4 hours. Then, the solvent is

removed and 0.1 M NaCl, KCl, $CaCl_2$ and $MgCl_2$ were added to swollen hydrogels and let to interact for 48 hours with a replacement of salt solutions at 9 hours. Mass of the hydrogels were measured accordingly. The induced swelling ratio can be calculated using the formula:

$$\%IS = \frac{W_S - W_t}{W_0} \times 100\%$$

where:

- %IS is the induced swelling ratio expressed in percentage;
- W_t is the swollen weight (in grams) at time t; and
- W_s is the initial weight (in grams) after swelling with PBS and Type 1 ultrapure water.

A sample was then punched by a biopsy punch to 4 mm and cut into 3 pieces: top facing salt solutions, center of the hydrogel and bottom exposing to the plate. The samples were then dried for scanning electron microscopy (SEM) and energy dispersive spectroscopy (EDS) analysis.

2.3.6.1. *Salt Solutions*

Sodium chloride (NaCl), potassium chloride (KCl), magnesium chloride ($MgCl_2$) and calcium chloride ($CaCl_2$) salt solutions were made with dissolving their solid salts in Type 1 ultrapure water based on the mass needed to get to the concentrations of 0.1 M, 0.5 M and 1M. For example, to make 0.1 M of NaCl solution, 1.1688 g of NaCl pellets were added to a 200 mL beaker on a magnetic stir plate. Type 1 ultrapure water was filled to 200 mL and let to stir for 30 minutes with a magnetic stirrer. Calcium chloride and magnesium chloride were added into water slowly to avoid over heating as the dissociations of these two salts in water are exothermic. Weighed boat and hydrogel was added to a plate and these solutions were then added to the plate. Mass of the hydrogels were measured accordingly.

2.3.6.2. *pH Adjustments*

200 mL of pH 7.4 PBS described previously was added to a 200 mL beaker. To lower the pH, hydrochloric acid was added to reach pH 1.5, 4 and 6.5. To increase the pH, 10 M of sodium hydroxide solution was made by dissolving 40 g of NaOH in 100 mL of Type 1 ultrapure water. This 10 M of sodium hydroxide was then added to the pH 7.4 PBS until the pH meter reads 10. Type 1 ultrapure water was used directly from the Millipore Synergy UV Water Purification System. pH meter read 5.662 for Type 1 ultrapure water. Weighed boat and hydrogel was added to a plate and these adjusted pH solutions were then added to the plate. Mass of the hydrogels were measured accordingly.

2.3.6.3. *Temperature for Selected Salt Solutions and pH*

0.1M NaCl and 1 M $CaCl_2$, Type 1 ultrapure water and PBS solutions at pH 1.5, 6.5 and 10 were selected to further investigate at temperatures of 30 °C and 40 °C. Selected solutions were placed in an oven for at least 30 minutes to heat up to targeted temperature before adding to the weighed boat and hydrogel plates. These plates stay in the oven for 24 hours for this study. Mass of the hydrogels were measured accordingly at selected time period.

2.3.6.4. *DSC Analysis*

Furthermore, Differential Scanning Calorimetry (DSC) were used to study the heat flow into the samples. Two different samples preparation were done for this study. A small sample of PMOEP hydrogel was cut by a sharp blade and placed in a weighed DSC cell. DSC cell with sample was then weigh and placed in the DSC chamber for thermo analysis. The second sample was done similarly except the addition of Type 1 ultrapure water into the DSC cell before measuring the mass samples. Each sample was gone through a heating process with 10 °C per minutes from 40 °C to 150 °C and then cooled back down to 40 °C at the rate of 10 °C per minutes.

2.3.7. Determination the Present of Cation on Dried Hydrogels using SEM and EDS

After each hydrogel was swollen in their respective salt solutions, gels were then left to dry in a vacuum oven for 24 hours to remove water as much as possible. After drying, scanning electron microscopy (SEM) was used to determine the surface structure and EDS was used to determine material compositions of the hydrogel.

2.4. Results and Discussions

The swelling ratio and degree of swelling of PMOEP in different salt solutions and concentrations, pH and temperature are reported below.

2.4.1. PMOEP Surface Morphology

Hydrogel is a highly porous network that allows solvent to diffuse inside. Environmental scanning electron microscopy (ESEM) was used to study the structure of the hydrogel. Though, ESEM shows only a small area of the hydrogel as pressure-limiting aperture were used [21].

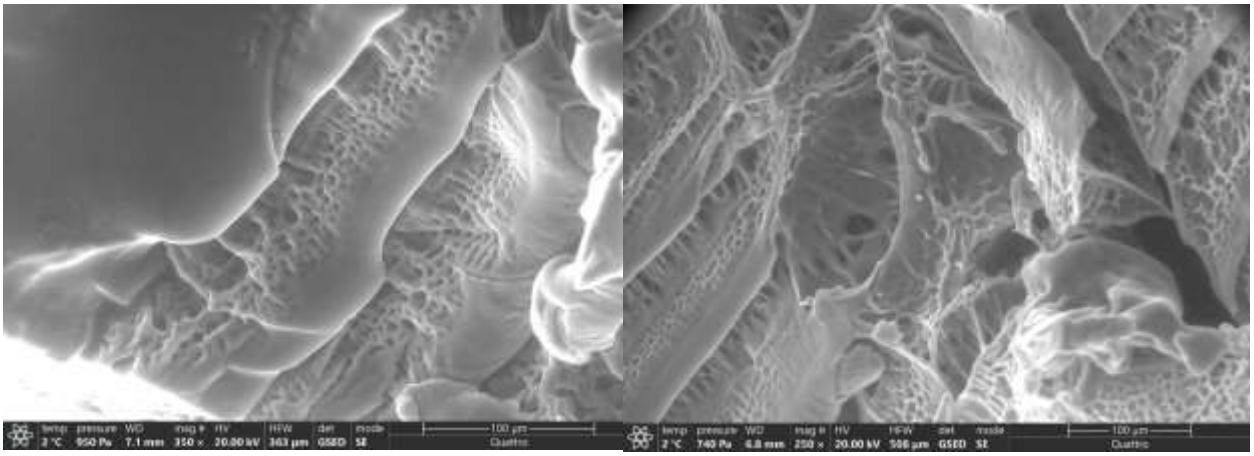

Figure 2-I: ESEM Images showing swollen PMOEP structure when pulling out water.

Due to the nature of ESEM, multiple images were needed to show the 3D structure of hydrogel. Figure 2-I showed a complex porous structure of ESEM images of PMOEP hydrogel. Each pore spaced very nicely between the hydrogel structure. This showed a good connectivity within the surface of the hydrogel, reflecting its overall internal architecture of the hydrogel. Good

stable uniform porosity system of a hydrogel gives better understanding especially in drug delivery and released [22]. ESEM images show that PMOEP has uniform and stable porous system showing the potential to be used in such system and other pharmaceuticals applications.

2.4.2. Induced Swelling of Hydrogels in Salt Solutions

PMOEP hydrogel was reported to have the ability to swell more than 6000% of its dried weight when swelling in PBS and water. When allowing to reach equilibrium, a balance between the electrochemical potentials of the hydrogel and the chemical potential of solvent is created [23]. However, polyelectrolyte hydrogels are known to have great response to slight changes of its surrounding (e.g. solvent solutions). This means that the hydrogel will create a new equilibrium system when exposing equilibrated hydrogels to a new solution.

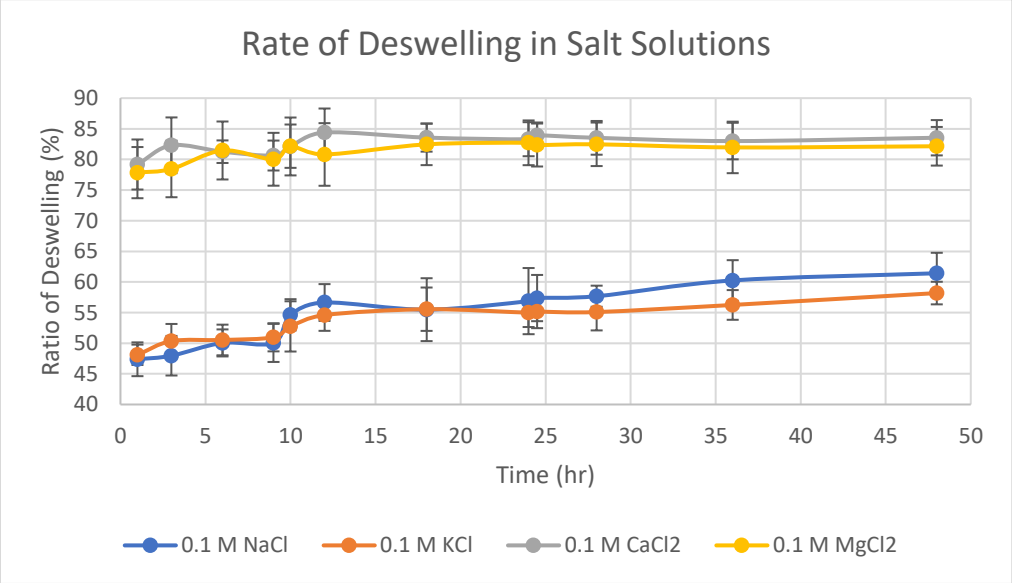

Figure 2-II: Induced swelling of PMOEP hydrogel in different salt solutions.

The shift in equilibrium of PMOEP hydrogel due to solvents was studied. PMOEP was swelled in PBS and water for 24 hours. The swollen hydrogels were exposed to different salt solutions (0.1 M of NaCl, KCl, $MgCl_2$ and $CaCl_2$) for 48 hours to observe weigh changes. The result showed significant decrease in mass after exposing the swollen hydrogel to salt solutions.

Figure 2-II shows the ratio of deswelling of PMOEP hydrogel. 0.1M of $CaCl_2$ and $MgCl_2$ shows the highest ratio of deswelling. This is due to their divalent cations, which could interact with the anions of the PMOEP hydrogel stronger than monovalent cations like Na^+ and K^+. The deswelling happens mostly within the first hour of the exposure and the equilibrium was reached after about 5 hours as the deswelling ratio plateau. A change of salt solutions introduced more cations to the environment around the hydrogel causing a jump in deswelling ratio at 10 hours. A new equilibrium is reached about 3 hours after these salt solutions were replaced. The result showed that 0.1 M $CaCl_2$ and $MgCl_2$ solutions reduced the mass of the swollen hydrogel by about 80% of its swollen mass while 0.1 M KCl and NaCl solutions can reduce the mass by more than 55% and 60% respectively. It was also noticed that only one out of each 6 samples swelled in $CaCl_2$ and KCl showed some fractures while at least half of the samples fractured during swelling in NaCl and $MgCl_2$.

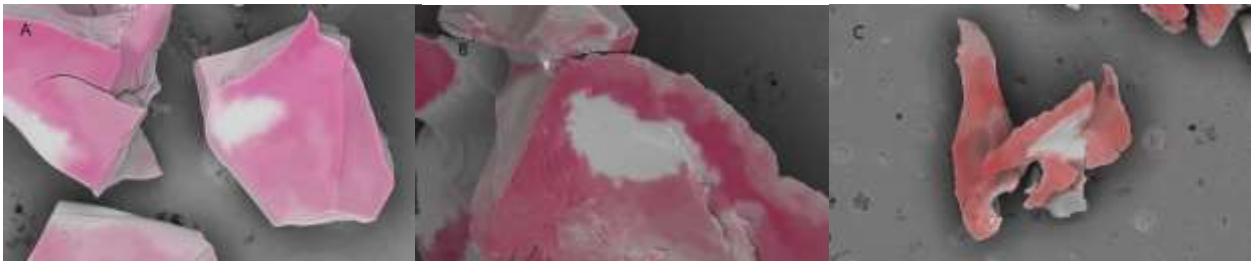

Figure 2-III: SEM image and EDS data showing uniform calcium presents (a) on the surface, (b) center (c) bottom of dried PMOEP.

SEM and EDS were used to determine the composition of the dried hydrogel after deswelling in 0.1M $CaCl_2$ solutions. The result showed a uniform composition of calcium across the hydrogel as shown in Figure 2-III. The blank spots appeared due to the angle of the camera on the samples. EDS data showed that calcium was made up to 8.7 ± 0.1 atomic % across the hydrogel and about 17.93 ± 0.2 weight %. This shows that calcium permanently stays on the hydrogel. Theoretically, calcium interacts with phosphate pendant group. A detail EDS spectra and compositions of each component can be found in Appendix A.

2.4.3. Effect of Salt Concentrations on Swelling Behavior and Degree of Swelling

In water, salt dissolved and formed their cations and anions. When polyelectrolyte hydrogels with anions are dipped in salt solution, the cations of salt and anions of hydrogel interacts. This leads to a decrease electrostatic repulsion interaction between anion and anion in the hydrogel network. This result in a decrease in osmotic pressure between the hydrogel and solution with the amount and types of salts presented in the solution. The effect of salt solutions and concentrations on the ratio of swelling and degree of swelling of PMOEP hydrogel was studied.

In general, monovalent cations allow PMOEP hydrogel to swell more than divalent cations, but less than water. This is due to the charge contributions to the swelling of PMOEP hydrogel. Divalent cations provide more charge which increases the interactions between anions of the hydrogel and cations. It results in a larger decrease in the repulsion force within the anions of hydrogel network allowing less solvent to diffuse into the hydrogel. Noticeably, as shown in Figure 2-2-a, potassium and sodium salt solutions give similar ratio of swelling. Magnesium and calcium salt solutions also give similar ratio of swelling. This indicates that salt solutions with similar

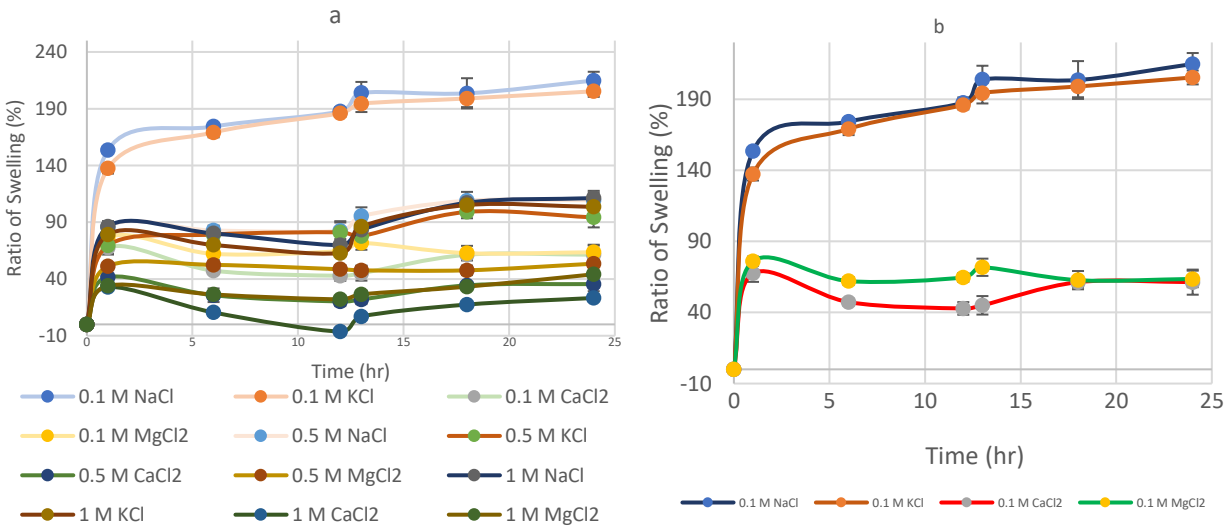

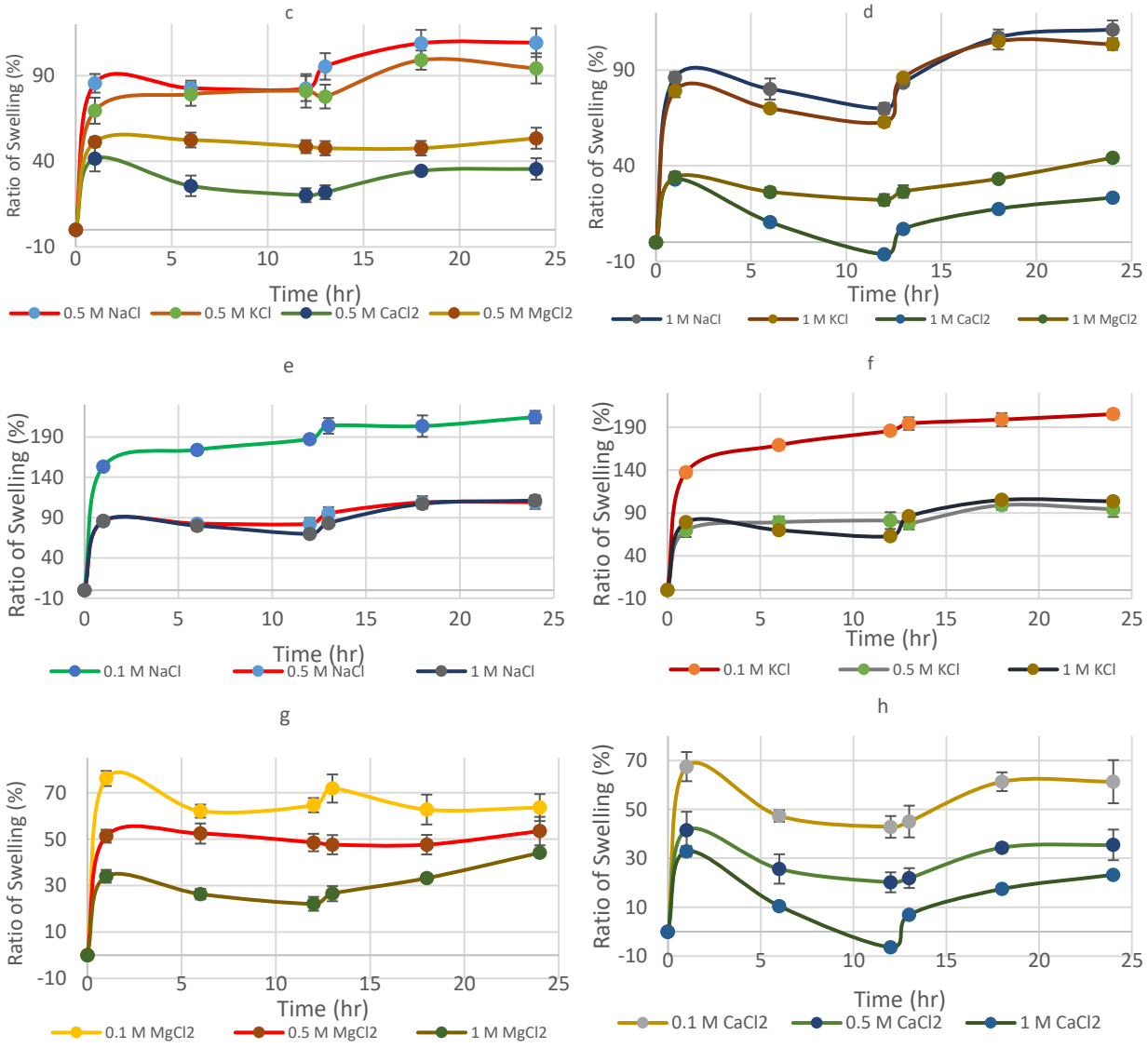

Figure 2-IV: Rate of swelling of PMOEP in different salt solutions: (a). all salt solutions studied, (b). different salt at 0.1 M, (c). different salt at 0.5 M, (d). different salt at 1M, (e). NaCl at different Concentrations, (f). KCl at different concentrations, (g)$MgCl_2$ at different concentrations, (h). $CaCl_2$ at different concentrations.

cations (e.g Na and K both are monovalent, Ca and Mg are both divalent) would similarly affect the ratio of swelling of PMOEP hydrogels at low concentration as shown in Figure 2.IV-b.

Figure 2-IV-e and f shows the swelling behavior of PMOEP in KCl and NaCl salt solutions at different concentrations. It was observed that the lower the salt concentration is, the higher the swelling ratio will be. However, the increasing in concentration do not affect the swelling behavior

as much. As shown at 0.5M and 1M concentrations, the swelling behavior are very close to each other. This is due to the saturation of the salt on the hydrogel surface limiting the ability of the solvent to diffuse further into the hydrogel. Figure 2-IV-g and h shows the swelling behavior of PMOEP in $MgCl_2$ and $CaCl_2$. The data shows that the increase in concentrations will decrease the ratio of swelling. Noticeably, both Mg^{2+} and Ca^{2+} decrease the swelling ratio after an hour. One possible explanation for this is that divalent cations diffuse into the hydrogel after solvent molecules and interact with anions of the hydrogel. Moreover, divalent cations can chelate the COO- group within the hydrogel network causing further decrease in swelling. At high Ca^{2+} concentration, the hydrogel collapsed. This shows a strong interaction between Ca^{2+} and the hydrogel. It is possible that the interaction is strong enough to push the initial solvent in MOEP solution from the hydrogel causing further decrease in volume to a negative value.

2.4.3.1. *Present of Cations on Dried Hydrogel*

SEM and EDS were used to confirm the present of salt on the surface after swelling in the salt solutions. Figure 2-V shows the atomic% and weight% of each cation on the surface of PMOEP hydrogels. Sodium content increased with increase in concentration while potassium and calcium salts showed the highest atomic% and weight % at 0.5M. The drop in potassium and calcium content at high concentration is most likely due to the osmotic pressure balance between the hydrogel surface and solvent has reached equilibrium and saturated the surface of the hydrogel preventing potassium and calcium from further link with the hydrogel network. As a result, hydrogel can no longer accept the cations. The atomic sizes of each cation can further restrict the ability to diffuse. As shown in figure 2-V, sodium has the lowest atomic size which continued to grow on the hydrogel when increasing in concentrations. Potassium and calcium have higher atomic size resulting in the decrease in their contents on the hydrogel. Magnesium contents did

not increase when increasing the concentration from 0.5M to 1M. This shows a trend at which an increase in atomic size will decrease the cation contents on the hydrogel. SEM images show even distribution of cations on the surface of dried PMOEP hydrogel form each salt and concentration as shown in Figure 2-VI. EDS spectra can be found in Appendix A-II.

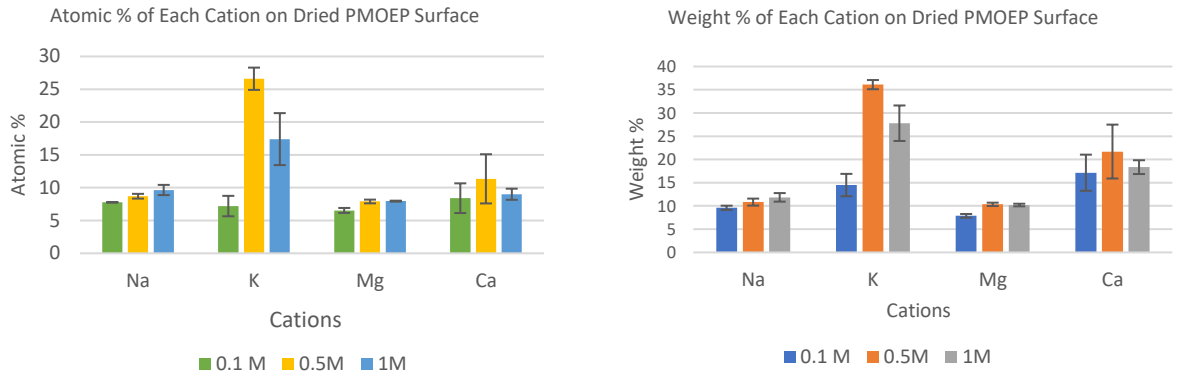

Figure 2-V: EDS data showing Atomic % (left) and weight % (right) of salt cations presented on the surface of PMOEP dried hydrogel.

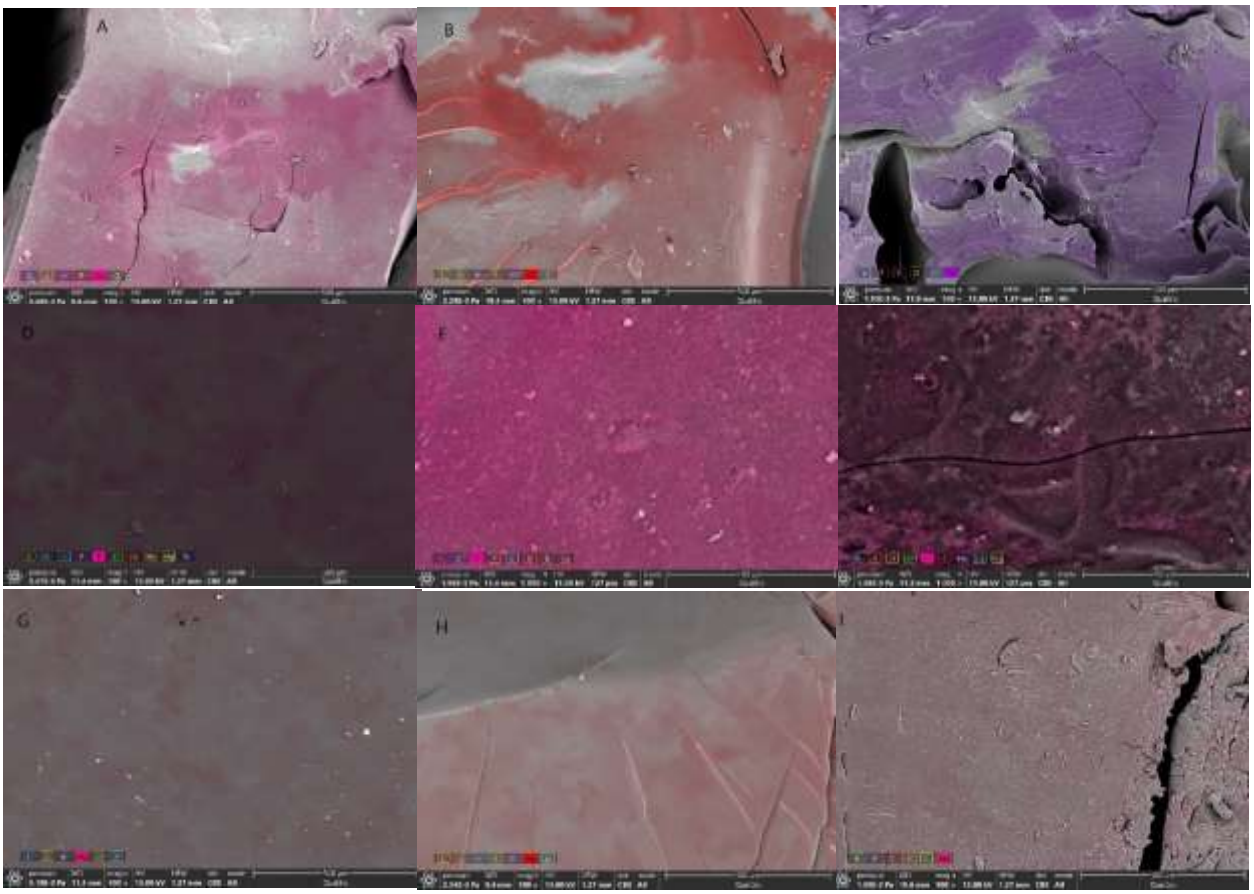

Figure 2-VI: SEM Images showing distributions of cations on dried PMOEP hydrogel surfaces after swelling in (A) 0.1M $CaCl_2$, (B) 0.5 M $CaCl_2$, (C) 1 M $CaCl_2$, (D) 0.1M KCl, (E) 0.5M KCl, (F) 1M KCl, (G) 0.1M $MgCl_2$, (H) 0.5M $MgCl_2$, (I) 1M $MgCl_2$, (J) 0.1M NaCl, (K) 0.5M NaCl, (L) 1M NaCl.

Potassium chloride salts were observed across the samples swelled in potassium chloride salt solutions. The amount of potassium chloride salt increases with the increase in concentration of potassium chloride solution. This could result from the precipitated potassium chloride salt during swelling or potassium chloride were not completely dissolved when making the solutions. The swollen hydrogels were then dried in vacuum under reduced pressure for 24 hours and dried weight were measured to calculate the degree of swelling of the samples. The data shows that sodium chloride gives the highest degree of swelling following by potassium, magnesium, and calcium salt respectively. Figure 2-VII shows the degree of swelling of PMOEP in different salt solutions.

As previously discussed, monovalent cations show less interaction with anions of the hydrogel system, resulting in lower intermolecular forces. This allows more water to diffuse. In contrast, divalent cations such as Ca^{2+} and Mg^{2+} provide more charges and therefore, higher intermolecular interactions. This will limit the ability of water to diffuse as the interaction also affect the pore size and space within the hydrogel network. Increasing in concentration would allow more cations to interact with the hydrogel network resulting in less repulsions between anions of the hydrogel, and therefore less water molecules can diffuse into the hydrogel system. As a result, a decrease in degree of swellings were observed for all salt solutions. The increase

from 0.5M to 1M of $CaCl_2$ and $MgCl_2$ does not affect the degree of swelling as much. This could result from the saturation of each cation across the hydrogel network as a whole, rather than only saturation on the surface.

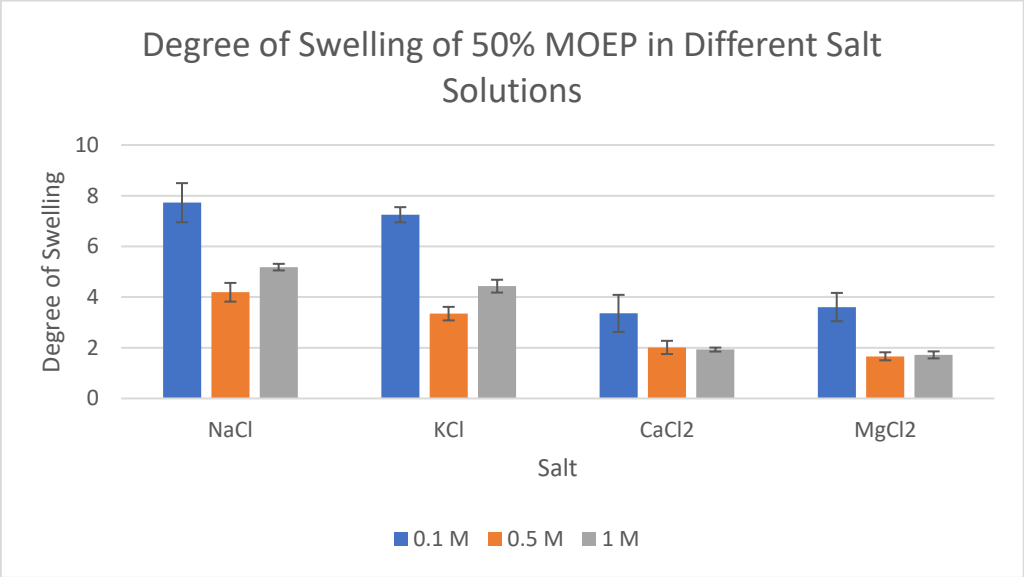

Figure 2-VII: Degree of swelling of PMOEP after swelling in different salts solutions.

2.4.4. Effect of pH on Swelling Behavior and Degree of Swelling

An effort to understand the swelling behavior of PMOEP in solutions with different pH was conducted. pH 1.5, 4, 6.5, 7.4 and 10 were chosen based on the pKa's of the phosphate pendant group. Moreover, the pH was also chosen based on the pH of gastric juice which is acidic in nature with pH between 1 to 2.5 [24] which then increased rapidly to 6 at the duodenum. The pH keeps increasing to 6.6 in the small intestine and it reaches 7.5 at the terminal ileum [24]. to study the capability of swelling of PMOEP in such condition. Therefore, these pH's were adjusted using hydrochloric acid, the main acid found in gastric juice and 10 M sodium hydroxide to imitate the gastric juice condition as close as possible.

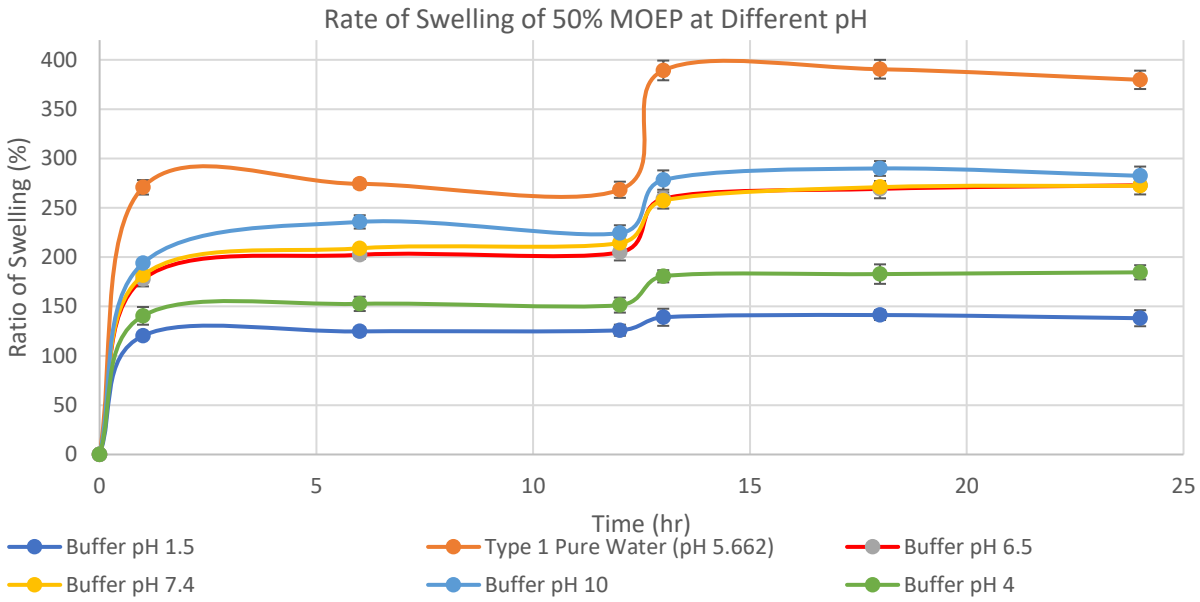

Figure 2-VIII: Rate of swelling of PMOEP in solutions with different pH.

Figure 2-VIII shows the ratio of swelling of the hydrogel. Water showed the higher ratio of swelling. This is due to the hydrogen bonding between water molecules and PMOEP network creating more space for water to swell, thus higher swelling ratio. The increase in pH resulted in increase in swelling ratio. The increase in pH above 7 decrease the swelling ratio from what observed for water. At low pH, anionic groups of PMEOP ionized resulting in higher interaction between cations of the acid and anion of PMOEP. This leads to lower swelling ratio. In contrast, basic solutions have OH- groups which help increase the repulsion forces between anionic group. As a result, basic solutions showed higher ratio of swelling than acidic solutions.

Type 1 ultrapure water shows the highest degree of swelling while the pH 6.5 buffer showed the highest degree of swelling among pH solutions as seen in Figure 2-IX. However, the degree of swelling became nearly constant when increasing pH from 7.4 to 10 or increasing from 1.5 to 4. This shows that the degree of swelling of MOEP is not affected as much at acidic pH or basic pH. However, PMOEP shows a great change in degree of swelling around neutral pH.

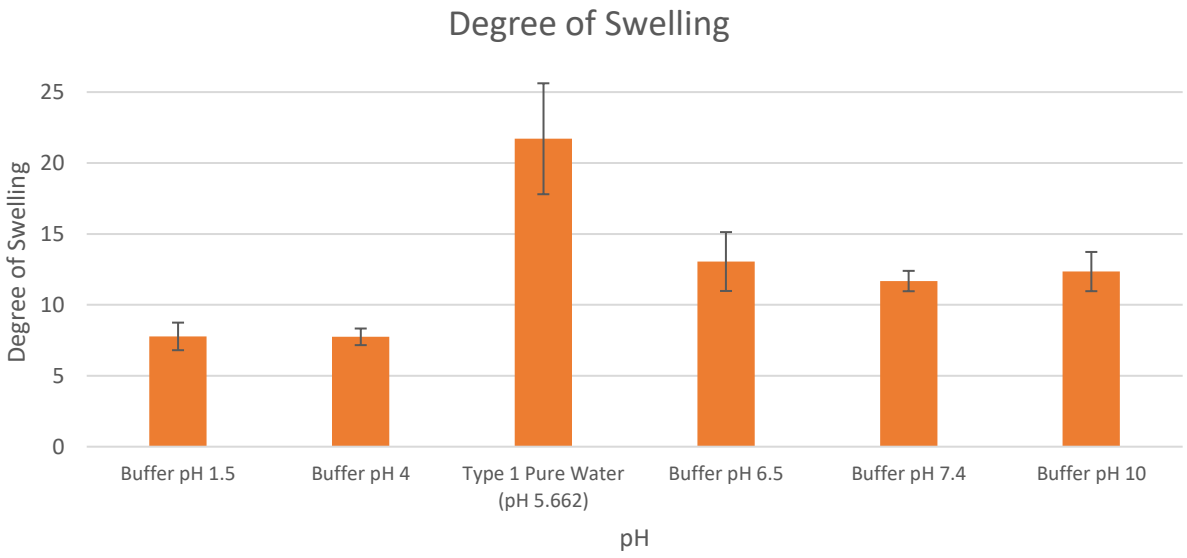

Figure 2-IX: Degree of swelling of PMOEP in solutions at different pH.

2.4.5. Effect of Temperature of Selected Salt Concentration and pH on Swelling Behavior and Degree of Swelling

To further investigate the swelling behaviors, six solutions: Buffer pH 1.5, Buffer pH 6.5, Buffer pH 10, Type 1 Ultrapure water, 0.1M NaCl and 1M NaCl were allowed to swell at higher temperature. The swelling behavior of a polymer with increasing in temperature could fall into one of the 3 categories: (1) the swelling increases with temperature (e.g. poly(dihydroxypropyl methacrylate)), (2) swelling decreases with increasing in temperature (e.g. poly(hydroxypropyl acrylate), and (3) the combination of (1) and (2) (e.g. PHEMA) [25].

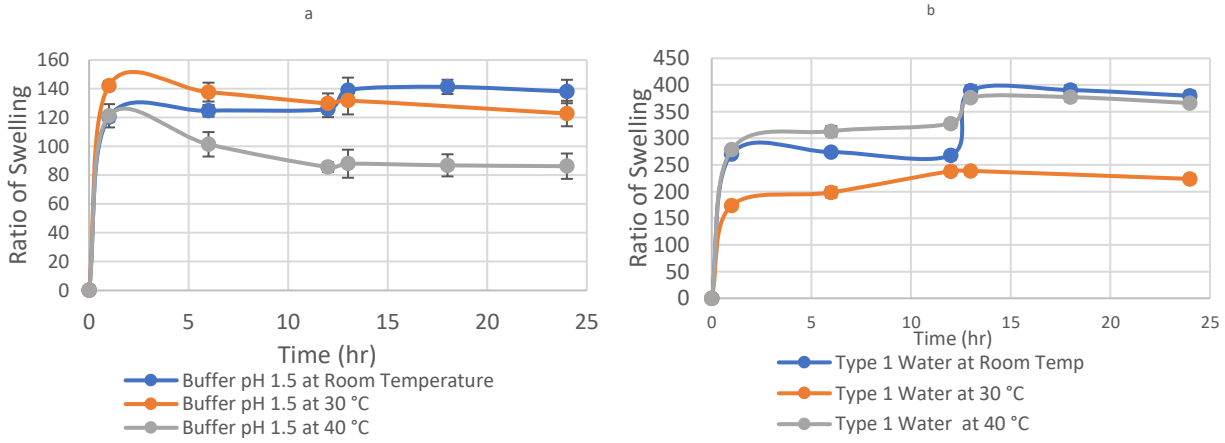

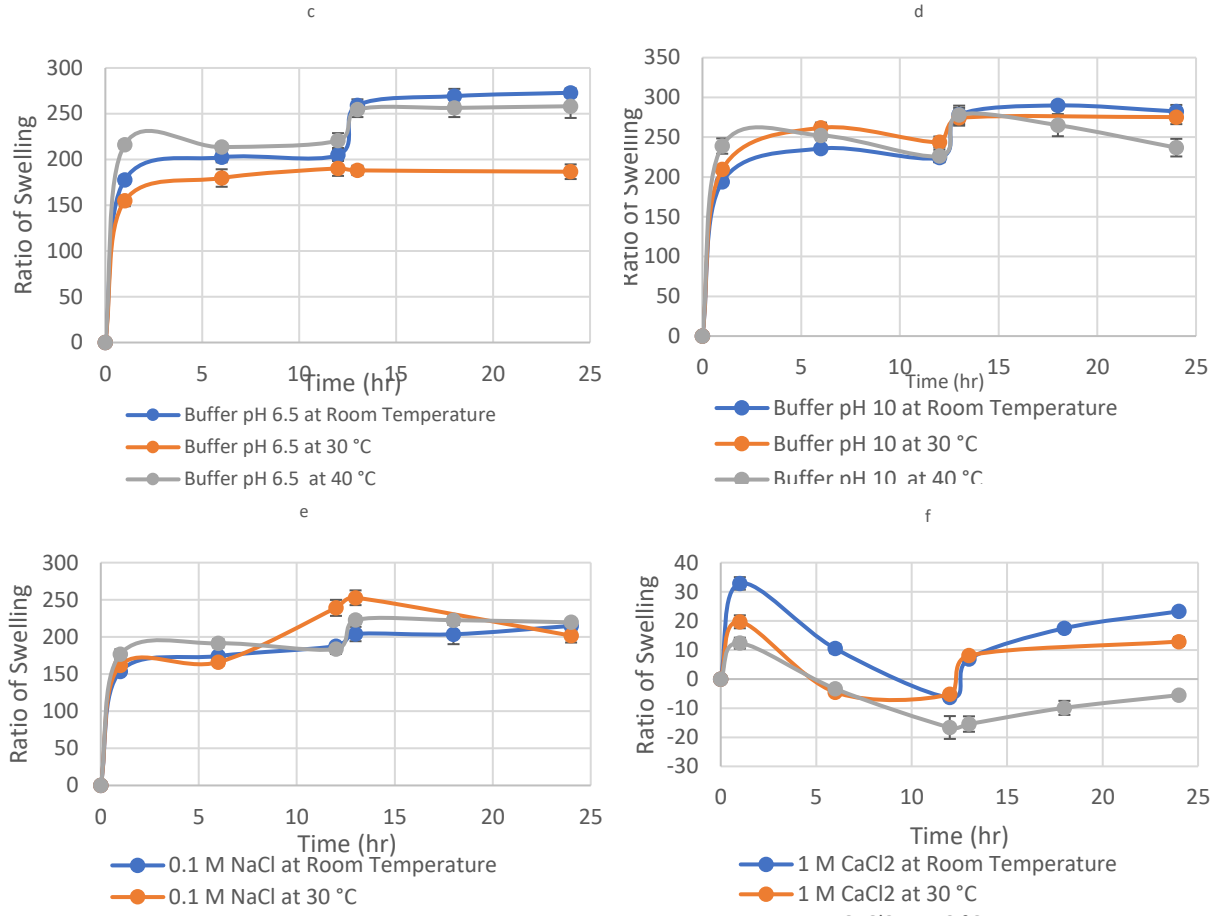

Figure 2-X: Swelling ratio of PMEOP in (a) pH 1.5 buffer, (b) Type 1 ultrapure water, (c) pH 6.5 buffer, (d) pH 10 buffer, (e) 0.1M NaCl and (f) 1M $CaCl_2$.

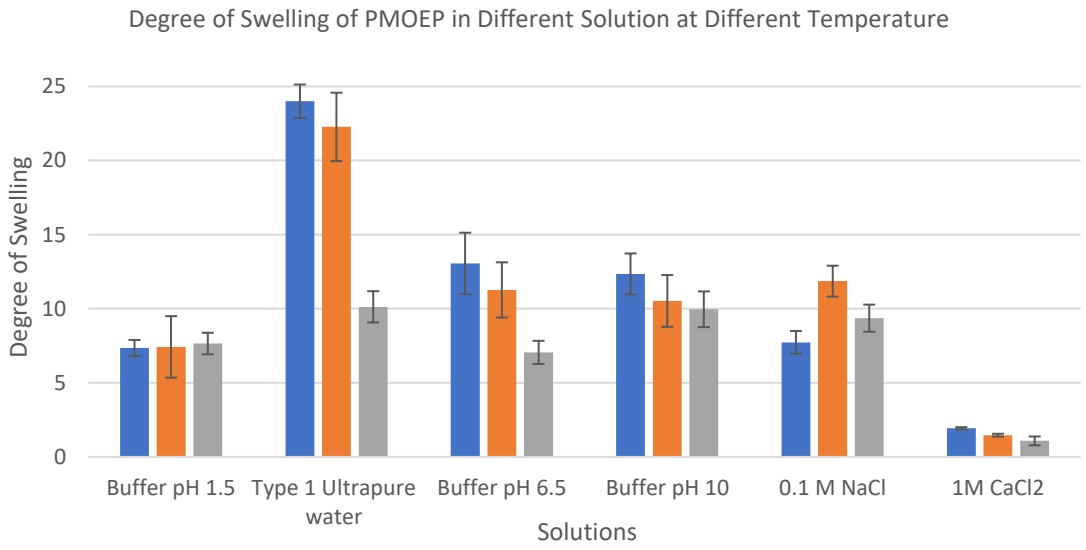

Figure 2-XI: Degree of swelling of PMOEP in different solution at different temperature.

Figure 2-X and Figure 2-XI shows the swelling behavior and degree of swelling of PMEOP

respectively in different solutions at different temperatures. temperature, 30 °C and 40 °C. PMOEP falls into category (2). In general, an increase in temperature resulted in a decrease in swelling ratio. However, this does not affect as much between room temperature and 30 °C. Type 1 water and Buffer pH 6.5 shows otherwise. The swelling ratio decreased significantly for Buffer solution pH 1.5. However, the degree of swelling was not affected. The lower swelling ratio could result from lower mass of the hydrogel in general, which allow the hydrogel to absorb less water. Type 1 Ultrapure water and Buffer pH 6.5 shows a large decrease in swelling ratio at 30 °C as well. However, the degree of swelling overall follows the same trend. An increase in temperature will result in the decrease in degree of swelling. Low critical swelling temperature (LCST) of the polymer chains could affect the volume change of hydrogel that is thermosensitive [26]. The crystallizations of monomer could happen at temperature above its LCST [27]. This results in shrinking behavior at temperatures above the LCST of the polymer. However, PMOEP did not show this characteristic in 0.1M NaCl. The degree of swelling was highest at 30 °C and dropped at 40 °C. Noticeably, PMOEP cracked when swelling in water at 40 °C as shown below while the no fractures observed in other solutions.

Figure 2-XII: PMOEP Hydrogel after Swelling in water at 40 °C (left) showing some fractures comparing to PMOEP swelled in PBS pH 10 (center) and 0.1 NaCl solution (right).

2.4.6. DSC Analysis of PMOEP

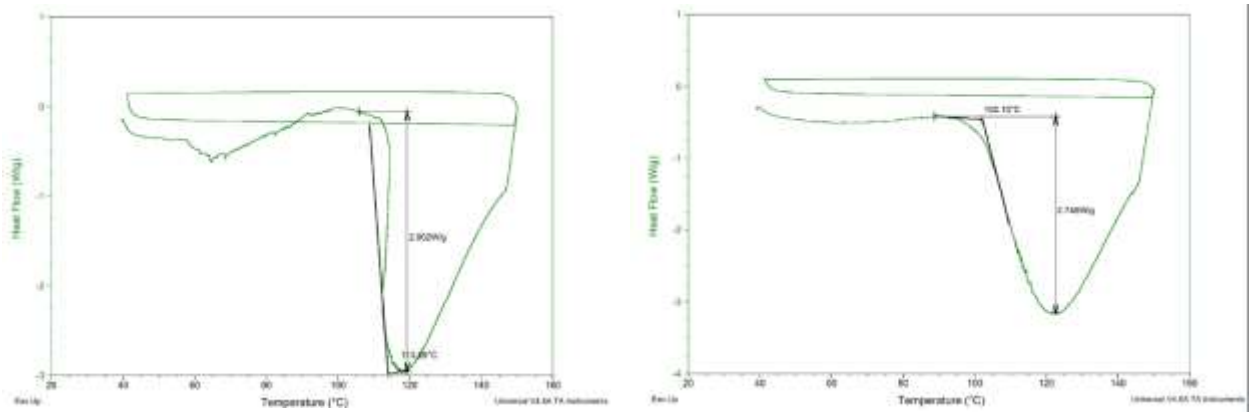

Figure 2-XIII: DSC analysis showing an endothermic peak for PMOEP at high temperature with left samples prepared without additional water, right samples taken with water in the DSC cell.

DSC were used to observe the thermal behavior of PMOEP hydrogel. Figure 2-XII showed the endothermic peak at 113.89 °C for samples prepared without water and 122 °C for samples prepared with water. These endothermic transition peaks are most likely due to the loss of water in the hydrogel network as water evaporates at around 100 °C [28]. DSC also showed that the hydrogel is more stable in water rather than by itself at higher temperature showing the effect of water interacting with the hydrogel. The hydrogel started to absorb the energy at 102.10 °C and continued the absorption up to 123 °C.

2.5. Conclusions

BMOEP impurity provides the crosslinker needed to form the hydrogel network in ARGET-ATRP. The resulted hydrogel showed great response to a wide range of salt, temperature, and pH. The swollen PMOEP hydrogels shrank when exposed to different salt solutions. Monovalent cations (Na^+ and K^+) showed lower ratio of deswelling comparing to divalent cations such as Ca^{2+} and Mg^{2+}. This is due to a stronger interaction between divalent cations and anions of the hydrogel network. A change in salt solutions allowed the hydrogel to deswell further. When swelling in salt solutions, the ratio and degree of swelling were found to be much lower than they

were for water. Water can form hydrogen bond which allows more water molecules to diffuse into the hydrogel network. Comparing to the swelling ratio at 1 hour, a drastic decrease in ratio of swelling was observed at 6 hours, when PMOEP was swelled in high salt concentrations (1M). PMOEP hydrogel collapsed, pushing initial solvent of MOEP out of the hydrogel in calcium chloride solutions resulting in a negative ratio of swelling at 12 hours. A change in salt concentration allows the hydrogel to swell a bit more. SEM and SEM-EDS showed the presence of cations on the dried hydrogel. Potassium chloride salts were observed on the sample swelled in 0.1M, 0.5M and 1M of potassium chloride solutions. PMOEP shows very little response at low (acidic) pH and high (basic) pH. However, the degree of swelling was affected greatly around the neutral pH. When increase the temperature of the environment, a decreased in degree of swelling and ratio of swelling was observed for PMOEP hydrogel network. DSC shows endothermic peaks at 113.89 °C and 123 °C for samples prepared with water and without water respectively. This is due to the evaporation of water out of the samples, resulting in only PMOEP experiencing the heat flow.

Future works could include the study of the effect of different solvent of MOEP solution (e.g using methanol instead of water) on the degree of swelling and its responsiveness in different salt solutions and pH. Moreover, the study of properties of PMOEP hydrogel including glass transitions, melting temperatures and more is needed to better understand PMOEP hydrogel network. Using PMOEP in pharmaceutical applications such as drug delivery could be conducted to further investigate PMOEP applications.

Chapter 3 PMOEP: The Potential Hydrogel for Expansion Microscopy

3.1. Abstract

Expansion microscopy has been proven to be very powerful in biological and medical imaging. It takes advantage of the isotropic expansion of a hydrogel that linked to cells to expand cells, and therefore providing better image of cell structures, mainly nucleus. Since the method was developed, is has shown to be able to expand the cells by 4, 10 and 20 folds. However, the process to get such high resolutions is very time consuming and requires a lot of work. Here, PMOEP is introduced to expansion microscopy by polymerize MOEP via aqueous ARGET-ATRP on a coverslip seeded with T41 mouse breast cancer cells. Cells attached to the hydrogel and expanded with the hydrogel. The initial data showed that cells can be expand up to 2 folds, however the image was not up to expectations. Further investigation focuses on how to better digest the cells to get better image.

3.2. Introduction

At microscopic level, many questions still do not have answers. Despite its diffraction limitation, diffraction-limited microscopy has helped to investigate the structures and processes of biological specimens at the microscopic level of a few hundred nanometers [29, 30]. While light microscopy is a solution to investigate how neural circuits and molecules work, in neuroscience, it is still unclear how different nerve systems are formed and how they affect our behaviors with such complexity of neurons due to its insufficient characterization of nanoscopic level organizations of the synapse molecules and other critical signals [31]. Other imaging techniques such as near-field imaging, far-field super resolution microscopy technique, optical microscopy technique provide great understanding of single molecules and their nanoscale structures [32]. Similar techniques have been used to characterize and analyze cancer cells. Light microscopy has

been used to observe breast carcinomas [33] while scanning near-field optical microscopy and confocal laser microspectrofluorometer were used to analyze P-glycoprotein of H69/VP small-cell lung cancer lines [34]. However, these techniques usually take long time to produce images including 3D super-resolution imaging, and most importantly require expensive equipment.

Recent studies have found that using hydrogel networks help to expand microstructures to a larger volume in a method called Expansion Microscopy (ExM). ExM overcomes the resolution limitation of light microscopy by using the hydrogel to physically expand the samples when swelling [35]. This shows that beside optical magnifications, physical magnifications can also help in imaging and analyzing the structures in fixed cells and tissues. This process takes the advantage of hydrogel network isotropic expansion, thus expanding the samples that crosslinked or chemically bonded with the hydrogel network. The expanded system then can be imaged by conventional diffraction-limited microscopes with nanoscale resolution and aberration-free microscopy [36]. Previous studies shows that superabsorbent monomer sodium acrylate combined with acrylamide and N,N'-methylenebisacrylamide shows great cell expansions up to 4.5-fold linear expansion [35, 36]. This process includes free radical polymerization with ammonium persulfate (APS) initiator and tetramethylethylenediamine (TEMED) accelerator, proteolysis with protease and dialysis in water. Other hydrogel such as poly(N-(2-acetamidoethyl)acrylamide supramolecular hydrogel could expand mouse brain tissues with linear expansion factor up to 1.75 times [37] Some versions for ExM include protein retention expansion microscopy (proExM) and expansion fluorescence insitu hybridization (ExFISH) [36]. This process takes sometimes and require a lot of work. Additionally, all these methods use sodium acrylate, and the purity of sodium acrylate determines the expansion factor of the hydrogel. However, the purity of commercially available sodium acrylate has little consistency between batches which caused inconsistent result.

In this studies, phosphate pendant hydrogel, poly(methacryloyloxyethyl phosphate) (PMOEP), were used in an attempt to expand breast cancer cells. Although the dimensional expansion of PMOEP is yet to explore, but PMOEP previously showed great degree of swelling, up to 6000% of its dried weight when swelling in phosphate buffer solution (PBS-pH 7.4) and water. Moreover, the procedure to form PMOEP hydrogel are rather quick, simple and require minimal amount of work comparing to the initial method. This method will avoid using sodium acrylate which could result in a more consistent expansion in ExM experiments. Most importantly, this will show another application for aqueous activators regenerated by electron transfer – atom transfer radical polymerization (aqueous ARGET-ATRP).

3.3. Materials and Methods

3.3.1. Materials

Phosphoric acid 2-hydroxyethyl methacrylate ester (CAS 52628-03-2; 90%), potassium bromide (CAS 7758-02-3, 99%), α-bromophenylacetic acid (BPAA, CAS 4870-65-9; 98%), potassium dihydrogen phosphate, 99% (ACS) (CAS 7778-77-0), potassium chloride (CAS 7447-40-7), hexane, mixture of isomers (CAS 107-83-5; 98.5%), magnesium chloride (CAS 7786-30-3), calcium chloride (CAS 10043-52-4), sodium hydroxide (CAS 1310-73-2), and ascorbic acid (CAS 50-81-7), Proteinase K (cat. No. P4850), gelatin from bovine skin (cat. No. 341635-1MG), were purchased from Sigma-Aldrich. Sodium chloride (CAS 7647-14-5, 98%), hydrochloric acid (CAS 7647-01-0; 36.5%-38%), tris(2-pyridylmethyl)amine (TPMA, CAS 16858-01-8, 98%), 18 mm round coverslips (cat. No. 16004-300) were purchased from VWR. Type 1 ultrapure water was used directly from Millipore Synergy UV Water Purification System.

3.3.2. Purification of MOEP

Commercialized MOEP has BMOEP impurity which makes up to about 25% on the molar basis. To reduce this crosslinker density, a 500 mL round bottom flask was used to extract BMOEP using hexane. 25 mL of MOEP, 25 mL of Type I ultrapure water and 100 mL of hexanes were added into the flask and rigorously stirred for an hour on a magnetic stir plate. This mixture was then separated using separation funnel. Aqueous MOEP/H2O went to the bottom of the funnel and then was transferred to a new clean 500 mL round bottom flask. This MOEP/H2O solution was further purified to extract hexane using reduced pressure Rotavap. The volume of purified solution was measured and transferred to a closed container and stored in the freezer until needed for synthesis.

3.3.3. Preparation of Coverslips for Aqueous ARGET-ATRP

Coverslips were cleaned with piranha solution and submerge into a nano pure water to wash out the piranha solution before seeding the cells. 2 mg/ml of gelatin solutions were made and treated with UV light along with 12 well plate for 10 minutes. Coverslips were then added to the 12 well plate and 1 ml of 2mg/mL of gelatin solution was added to the wells with coverslips for 2 hours. The prepared 4T1 mouse breast cancer epithelial cells were then seeded onto the coverslip to the desire density and were allowed to grow for 24 to 48 hours before using the coverslip in the polymerizations of PMOEP.

3.3.4. Synthesis of PMOEP via Aqueous ARGET-ATRP

An effort to determine the most stable PMOEP hydrogel was previously done. The degree of polymerization of 300 showed the highest degree of swelling with fewest fractures of the gel. The target degree of polymerization of 300 is used to examine the swelling behavior of PMOEP hydrogel. To obtain 300 degree of polymerization, 9.40 mg of αBPAA, 1.30 mg of TPMA, 1.00 g

of $CuBr_2$, 59.5 mg of KBr, and 61.5 mg of Ascorbic acid were added to a clean and dry 20 mL scintillation vial. 5 mL of 50:50 by volume of purified MOEP solution was then added to the vial and was gently twirled to dissolve the ingredients. For each coverslip, one glass slide was cut into smaller pieces and washed with ethanol along with other two glass slides. The coverslip was then placed on top of the glass slide while cut-glass slides were placed at the edge. The second glass slide was then placed on top of the cut-glass slides. The gap created by cut-glass slide between these two glass slides provides enough space for the coverslip. The homogenized MOEP solution was then added in between the two glass slides and placed in a sealed vessel covered by aluminum foil. This vessel was placed in an oven at 30 °C for 8 hours with under nitrogen rich environment.

3.3.5. Cell Digestion, Swelling and Equilibration of Hydrogels

After the polymerization was finished, the glass slides were removed. The coverslips were then transferred into a well plate. A digestion buffer containing 8U/ml proteinase K, 1 mM EDTA, 50 mM Tris-Cl, 46.7 mg/mL sodium chloride, and 50 mg/mL Triton X-100 was then added to the well and placed on a 55 °C hot plate for 6 hours to digest. The hydrogel was then removed from the glass slide and allowed to swell in PBS and Type 1 ultrapure water. PBS was made following Dulbecco's pH 7.4 phosphate buffer solution (PBS). Briefly, 8.0 g of NaCl, 1.15g of Na_2HPO_4 anhydrous, 0.2g KCl and 0.2 g of KH_2PO_4 were placed in a 1 L beaker and Type 1 ultrapure water was added to 800 mL on a magnetic stir plate and let to stir with a stirring rod for at least 10 minutes. When everything is dissolved, Type 1 ultrapure water was then added to obtain 1 L of pH 7.4 PBS solution with a pH meter attached to observe the final pH. Keyence BZX microscope and Zeiss LSM 880 laser scanning confocal microscope were used to picture the cells before and after expansion.

3.4. Results and Discussions

An attempt to use PMEOP hydrogel for expansion microscopy was done with 50/50 percent volume of MOEP monomer and water with the targeted degree of polymerization of 300 via aqueous ARGET-ATRP. The unsaturated carbon in the lipid bilayer has the ability to crosslink with some proteins which allows the PMOEP hydrogel network to crosslink with cell membrane. This means that PMOEP network can integrate cell into its network, therefore expand with the expansion of the hydrogel network during swelling.

3.4.1. Initial Result for Expansion Microscopy Using PMOEP

The initial attempt to use PMOEP in such system shows some expansion of the cell with very limited view of the cell. Figure 3-I shows an increase in diameter of 4T1 cells after expansion. The exact diameter of 4T1 cells were impossible to accurately measure due to the excessive background signals and autofluorescence on the post-expansion cell. The reduction in image brightness could cause by 3 main reasons: i. the polymerization could damage fluorophores, ii. the loss of dye after digestion and iii. the dilution of dyes during expansions [38]. For this sample, PMOEP did not go through digestion. Therefore, one reason that could cause this is due to the overlapping of DAPI signal and WGA AF488 signals preventing the microscope to distinguish between nuclei and membrane and other components. One other possible reason is that the image only showed autofluorescence from high laser power rather than the DAPI signal. However, based on the image in Figure 3-I, it was estimated that PMOEP could expand 4T1 cells by 2 folds.

Beside light scattering, another limitation of ExM is its visibility after expansion especially if the image is taken far away from the coverslip. One this reason this happened is due to the

refractive index (RI) mismatch between water in the hydrogel network (RI ~ 1.33) and coverslips (usually RI ~1.58) which results in spherical aberration [39].

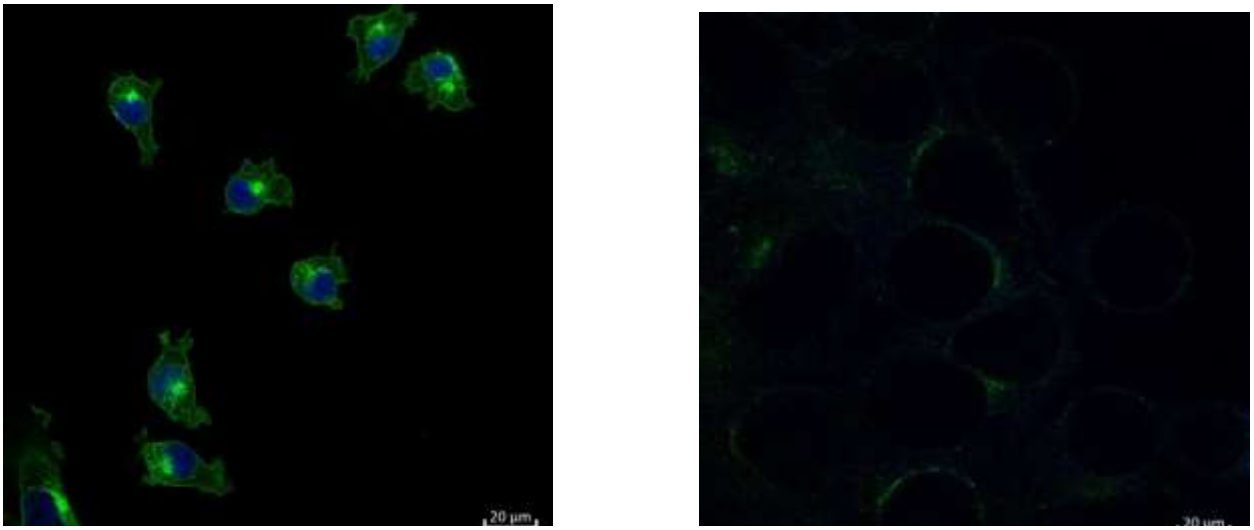

Figure 3-I: Images from Zeiss LSM 880 laser scanning confocal microscope using 40X water objective (NA=1.2) showing pre-expansion of 4T1 cells (left) and post-expansion of 4T1 cells (right).

3.4.2. Adjustment for Better Fluorescence

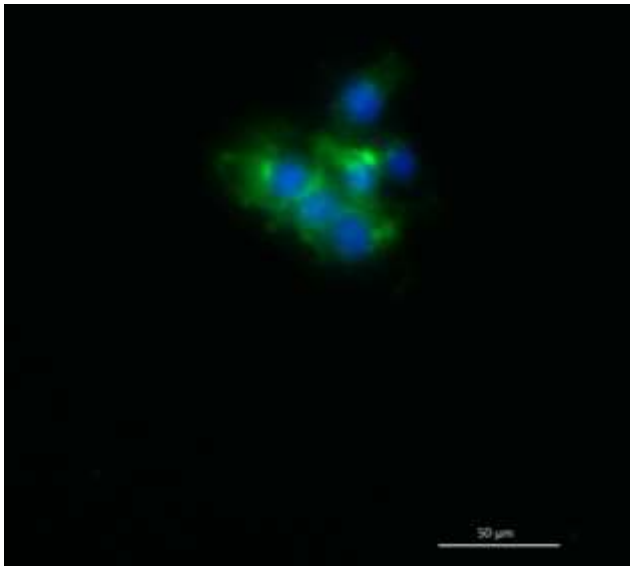

Figure 3-II: Images from Keyence BZX microscope using 40X air objective showing post-expansion of 4T1 cells with digestion.

An attempt to improve the image was done by letting the hydrogel and cell to digest in proteinase K solution for 6 hours on a 55 °C hotplate. The result showed significant improvement

of the image quality, but reduced the expansion completely as shown in Figure 3-II. The digestion step could have damaged the bond between the cell and hydrogel network, resulting in no expansion on the cell when the gel expanded.

3.5. Conclusions

PMOEP hydrogel was synthesized via aqueous ARGET-ATRP on a coverslip with seeded 4T1 mouse breast cancer cells on it. The preliminary data showed that PMOEP has a potential to be used in expansion microscopy and could help expand the cell up to 2 times its original size. However, obtaining a good image with the right color was an issue due most likely due to the mismatch of refractive index of water and cover glass, which result in spherical aberration. Some other possible reasons include the loss of fluorophores during polymerization, loss of dye during swelling and expansion and the overlapping of the signals from the microscope. An attempt to fix the quality of the image was done by digesting PMOEP in digestion solution after polymerization. However, this might release the cell from PMOEP network and result in no expansion of the cells observed.

Further investigation is needed to ensure the applicability of PMOEP in expansion microscopy. Future works should focus on adjusting the refractive index of cover glass and the hydrogel system which mainly consists of water. An addition of oil might solve this problem. Furthermore, an investigation for higher PMOEP expansion should be done to maximize the expansion ability of PMOEP, and therefore further expanding the cells.

Chapter 4 The Effects of pH and Temperature on Degree of Swelling, Mechanical Properties and Cytotoxicity of Phosphate-pendant Hydrogels

4.1. Abstract

Different conditions of PMOEP polymerization via aqueous ARGET-ATRP was introduced to study the effect of these conditions on the degree of swelling, mechanical properties and cytotoxicity of the hydrogel. Polymerizations were conducted at 30, 40 and 50 ℃ with the native pH of MOEP, pH 1 and pH 1.5. pH's were adjusted using sodium hydroxide. The composition of MOEP includes 40%, 50% and 60% by volume of MOEP in water. The increase in temperature resulted in a decrease in degree of swelling, as well as an increase in pH. The decrease in MOEP content resulted in higher degree of swelling when polymerized at its native pH and 30 °C. Hydrogel formed with 50% MOEP was found to be the most stable during swelling showing some fractured at 50 °C. PMEOP formed with 40% and 60% at 50 ℃ showed severe fractures after swelling. PMOEP formed with 50% MOEP, native pH at 40 °C showed to have the highest strain and could handle the force multiple times without any change in mechanical properties. Leaching test showed great cytotoxicity for PMOEP as very dead cells observed after exposing them to PMOEP for 24 hours.

4.2. Introduction

Hydrogels have found its place in many applications depending on their properties. Some hydrogels such as calcium alginate microcapsules, collagen, 2-hydroxyethl methacrylate are highly favored and studied for biomedical applications [40]. Their abilities to be produced in such small volume at any shape at dried state which make it easy to deliver to the body, either by injection or other way of delivery [41]. Atomic Transfer Radical Polymerization (ATRP) has been used to design several materials for biomedical application including tissue engineering, drug

deliver and imaging due to is ability to control the structure, functionality and order of the polymer [42]. On top of conventional ATRP, other types of ATRP such as activators generated by electron transfer (AGET) ATRP, surface initiated (SI) ATRP, supplemental activators and reducing agent (SARA) ATRP and photo-ATRP have also been used extensively for polymerizing new materials for different applications [43, 44, 45].

Activators regenerated by electron transfer (ARGET) ATRP was developed to reduce the amount of catalyst needed as the reducing agent is used to generate the catalyst from its high oxidation state (e.g. Cu^{II} to Cu^{I}) [46]. Some other advantages of ARGET-ATRP include its low side reactions, applicability to be done in the atmospheric environment and aqueous phase which make it easy to adjust the shape of the product and more compatible to biological system as well. ARGET-ATRP was previously used to polymerize poly(methacrylic acid-co-N,N-dietylaminoethyl methacrylate) polyampholyte brushes at a wide range of solution pH based on the copolymer composition to shift the equilibrium of solution [47]. This shows that ARGET-ATRP could be applied to a range of pH. Moreover, ARGET-ATRP was also applied to the polymerization of methacrylates and acrylates polymers at temperature up to 110 °C with great controlled over the reaction using anisole, benzonitrile and toluene as solvents [48].

2-methacryloyloxyethyl phosphate (MOEP) has been very attractive for biomedical applications. MOEP helps reduce the shape changes of a structure containing cations in a drug by using its anion groups to counteract the expansion of cations [11, 12]. PMOEP has been polymerized via reversible addition-fragmentation chain transfer resulting in molecular weight up to 20 K or below [20]. ATRP has shown to be viable for polymerization hydrophilic acid monomers and improved the control over side reactions and molecular weight [49].

In this study, aqueous ARGET-ATRP was applied to the polymerization of 2-methacryloyloxyethyl phosphate (MOEP) using bis(2-methacryloyloxyethyl) phosphate as cross linkers. The study includes the adjustment of polymerization temperature, pH and MOEP content which further affect the pH MOEP solutions. The change in temperature or pH or MOEP content could affect the polymerization rate which then affect the degree of swelling. Mechanical properties and cytotoxicity were investigated to further understand the effect of each change on the degree of swelling. Using ascorbic acid as reducing agent helps copper from oxidizing from Cu^{I} to Cu^{II} which therefore reduce the side reaction between copper and ligand and improve the rate of reaction of PMOEP in general. Cytotoxicity will show the applicability of PMOEP in tissue engineering, drug delivery and other biological system.

4.3. Materials and Methods

4.3.1. Materials

Phosphoric acid 2-hydroxyethyl methacrylate ester (CAS 52628-03-2; 90%), potassium bromide (CAS 7758-02-3, 99%), α-bromophenylacetic acid (BPAA, CAS 4870-65-9; 98%), potassium dihydrogen phosphate, 99% (ACS) (CAS 7778-77-0), potassium chloride (CAS 7447-40-7), hexane, mixture of isomers (CAS 107-83-5; 98.5%), magnesium chloride (CAS 7786-30-3), calcium chloride (CAS 10043-52-4), sodium hydroxide (CAS 1310-73-2), and ascorbic acid (CAS 50-81-7), tris base (cat no. 648311-1kg), bovine serum albumin (BSA, cat. no. A9647-100G), phosphate buffered saline (PBS, cat. no. P3813-5X10PAK), Corning costar transwell cell culture inserts (TC treated, PET membrane, diam. 6.5 mm, pore size 8.0 µm, sterile, cat. no. CLS3464) were purchased from Sigma-Aldrich. Sodium chloride (CAS 7647-14-5, 98%), hydrochloric acid (CAS 7647-01-0; 36.5%-38%), tris(2-pyridylmethyl)amine (TPMA, CAS

16858-01-8, 98%), Sterile syringe filters (0.2 µm, 25 mm diameter) (cat. no. 28143-310) were purchased from VWR.

Type 1 ultrapure water was used directly from Millipore Synergy UV Water Purification System. Cell freezing medium (cat. no. 12648010), cryovials (cat. no. 12-565-171N), Trypsin (cat. no. 25200072), 10% FBS (cat. no. 16000044), 1% Penicillin/Streptomycin (P/S, cat. no. 15140122), α- MEM (cat. no. 12561072), calcein, AM (MW: 994.87, LOT: 2326049, cat. no. L3224) and ethidium homodimer-1 (LOT: 1976809, cat. no. L3224) were purchased from Thermo Fisher Scientific. 2 ng/ml Fibroblast Growth Factor-2 (FGF-2, cat. no. 100-18B) was purchased from Peprotech.

4.3.2. Purification of MOEP

Commercialized MOEP is has BMOEP impurity which makes up to about 25% on the molar basis. To reduce this crosslinker density, a 500 mL round bottom flask was used to extract BMOEP using hexane. 60 mL of MOEP, 40 mL of Type I ultrapure water and 200 mL of hexanes were added into the flask and rigorously stirred for an hour on a magnetic stir plate to form 60%/40% by volume of MOEP/H_2O. This mixture was then separated using separation funnel. Aqueous MOEP/H2O went to the bottom of the funnel and then was transferred to a new clean 500 mL round bottom flask. This MOEP/H2O solution was further purified to extract hexane using reduced pressure Rotavap. The volume of purified solution was measured and transferred to a closed container and stored in the freezer until needed for synthesis.

4.3.3. Volume Compositions, pH and Temperature Adjustments for PMOEP Synthesis

6 mL of 60/40 by volume of MOEP/H_2O was transferred into a 20 mL scintillation vial and pH of this solution was recorded. To adjust the pH, sodium hydroxide pellets were grinded by mortar and pestle to small pieces and then added to scintillation vial containing 60/40 by volume

of MOEP/H_2O until the pH 1 is measured by the pH meter. Similarly, grinded sodium hydroxide was added to another vial until pH 1.5 is obtained.

60/40 by volume of MOEP/H2O was diluted to 50/50 by volume of MOEP/H_2O and 40/60 by volume of MOEP/H_2O. An appropriate amount of 60/40 by volume of MOEP/H2O was placed in a scintillation vial and Type I ultrapure water was then added to receive the targeted percent volume of MOEP. The pH of these diluted solutions was recorded and separated into three vials for pH adjustment described above. The polymerization happens in the oven setting to the certain temperature. The temperatures were adjusted and let to stabilize for at least an hour before the polymerization began.

4.3.4. Synthesis of PMOEP via Aqueous ARGET ATRP

An effort to determine the most stable PMOEP hydrogel was previously done. The degree of polymerization of 300 showed the highest degree of swelling with fewest fractures of the gel. The target degree of polymerization of 300 is used to examine the swelling behavior of PMOEP hydrogel. To obtain 300 degree of polymerization, 9.40 mg of αBPAA, 1.30 mg of TPMA, 1.00 g of $CuBr_2$, 59.5 mg of KBr, and 61.5 mg of Ascorbic acid were added to a clean and dry 20 mL scintillation vial. 5 mL of 50:50 by volume of purified MOEP solution was then added to the vial and was gently twirl to dissolve the ingredients. The homogenized solution was then transferred to a preformed mold and covered with a glass slide. This mold was then placed in a sealed vessel filled with nitrogen gas. The vessel is then transferred into an oven at 30 °C with continuous nitrogen flow for 8 hours to complete the polymerization. The glass cover is then carefully removed from the mold and the cylindrical-shaped hydrogels can be removed from the mold for swelling. Attenuated Total Reflection Fourier Transform Infrared Spectroscopy (ATR-FTIR) was used to study the structures of the hydrogel after swelling.

4.3.5. Swelling and Equilibration of Hydrogels

These hydrogels were then put on pre-weighed metal mesh weigh boats to obtain the initial mass of the hydrogel before swelling. The boats were then dipped into a dish filled with homemade Dulbecco's pH 7.4 phosphate buffer solution (PBS). Briefly, 8.0 g of NaCl, 1.15g of Na_2HPO_4 anhydrous, 0.2g KCl and 0.2 g of KH_2PO_4 were placed in a 1 L beaker and Type 1 ultrapure water was added to 800 mL on a magnetic stir plate and let to stir with a stirring rod for at least 10 minutes. When everything is dissolved, Type 1 ultrapure water was then added to obtain 1 L of pH 7.4 PBS solution with a pH meter attached to observe the final pH.

The degree of swelling is calculated using the swollen weight and dried weight as followed:

$$S = \frac{W_W - W_D}{W_D}$$

where:

- S is the swelling ratio;
- W_W is the swollen weight (in grams); and
- W_D is the swollen weight in grams.

4.3.6. Preparation of Rat Bone Marrow-Mesenchymal Stem Cells (rBMSC) and Poly(2-Methacryloyloxyethyl Phosphate) (PMOEP) Hydrogel for Cytotoxicity Study

Rat bone marrow-mesenchymal stem cell (rBMSC) was removed from T-150 flask and transferred to a well plate with α-MEM media and FGF-2. This well plate was then left in the incubator for 24 hours to let the cell grow. The swollen hydrogels were placed on a glass slide. A 2 mm biopsy punch was used to cut the hydrogel to the desire diameter and later adjusted the height with a sharp blade, appropriate for the transwell. The hydrogel was cured under UV-light

for at least 15 minutes. The prepared hydrogel was then added to the transwell plate and placed on the well with cells at the bottom. α-MEM media was added to cover the hydrogel. rBMSCs were exposed to the hydrogel for at least 24 hours in the incubator.

To kill the cells, a 70% methanol was made in a 20 mL vial by adding 700 µL of methanol in 300 µL of PBS. This solution was added to the dead controlled well to kill cells for 30 minutes in the incubator. All wells were then washed with PBS. A Live/Dead (L/D) assay solution was made with 6 mL of methanol, 3 µL for calcein, AM, and 18 µL of ethidium homodimer-1 in a 15 mL tube. 0.5 mL of L/D assay solution was then added to each well and let it sit in the incubator for 20 minutes. L/D solutions was then removed from the well plate and PBS was added for imaging using EVOS M7000 Imaging System microscope by Thermo Fisher Scientific to image live and dead cells in each well.

4.4. Results and Discussions

The polymerization of PMOEP hydrogel via aqueous ARGET-ATRP was previously studied and showed an increase in mass by more than 6000% comparing to its dried weight [50]. This showed possibilities of using aqueous ARGET-ATRP with acidic monomers which previously found difficult. The conversion was studied, and the polymerization reached 100% conversion of the monomer within 6 hours at 40 °C. This showed great reduction of time to create such hydrogel. It also resulted in better shape retention comparing to polymerization of PMOEP via ATRP using copper wire, both before and after swelling. Moreover, aqueous ARGET-ATRP made the polymerization easier to obtain the sample in different shape since it could be easily transferred to a mold. The purification process of MOEP in hexane when preparing MOEP solution showed a reduction of BMOPE from 25% to 14%. This gives the final ratio of MOEP:BMOEP of 84:16 on the molar basis.

4.4.1. pH Adjustments for MOEP Solutions

50/50 by volume of MOEP/water solution usually has a very low pH, at around 0.7. This is due to the contribution of phosphoric acid inherited from commercial MOEP. Sodium hydroxide was used to increase the pH of MOEP solutions up to 1 and 1.5. It was noticed that the pH of MOEP solution dropped with an addition of a small amount of NaOH, contradicting to what usually happen when such a strong base is added to a solution.

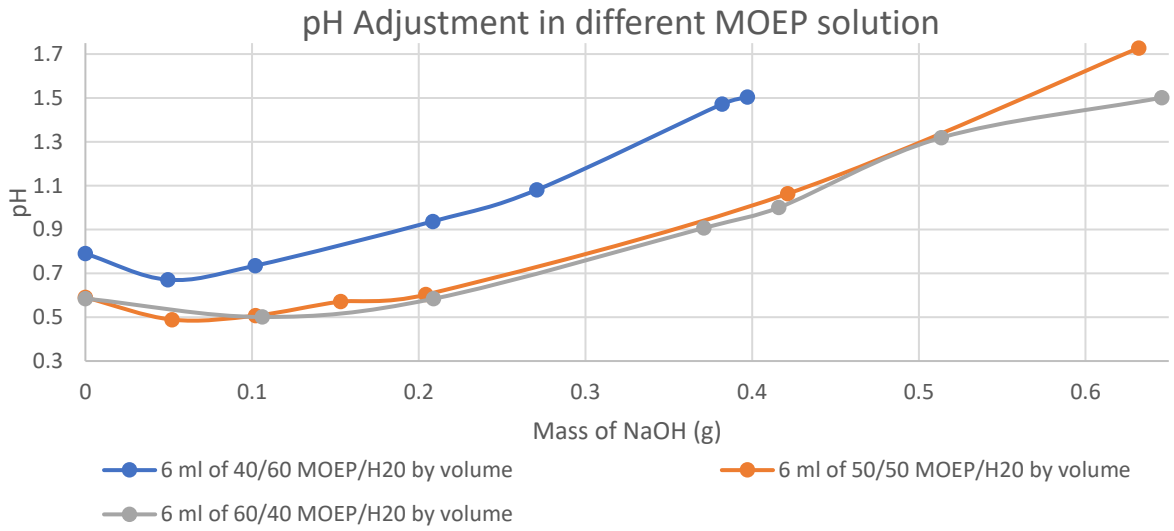

Figure 4-I: pH adjustment of MOEP solutions showing mass of NaOH needed to reach a certain pH value.

Figure 4-I shows that regardless of concentration, adding a small amount of NaOH into MOEP solution resulted in a drop in pH. This could result from the hydrolysis process which allow extra hydrogen to from hydronium ions and resulting in a drop in pH. 50/50 MOEP/water solution showed the most decrease in pH when adding a very small amount of sodium hydroxide while 40/60 MOEP/water shows a small drop in pH when adding NaOH. Besides having different native pH between each solution, it was observed that the amount of NaOH needed to achieve pH 0.7 and pH 1 for 50/50 and 60/40 MOEP/water solutions were quite close to each other. However, the pH significantly increased for 50/50 MOEP/water when similar mass of NaOH was added.

4.4.2. Degree of Swelling of PMOEP at different pH and Temperature of Polymerization

The addition of sodium hydroxide resulted in the increase in pH of MOEP solution prior to polymerizations. It appeared that the addition of sodium hydroxide did not affect the polymerization time since the polymerization went to completion within 8 hours as previously studied. However, the resulted hydrogel appeared to have additional hydroxide group presented in their structure as shown in ATR-FTIR below.

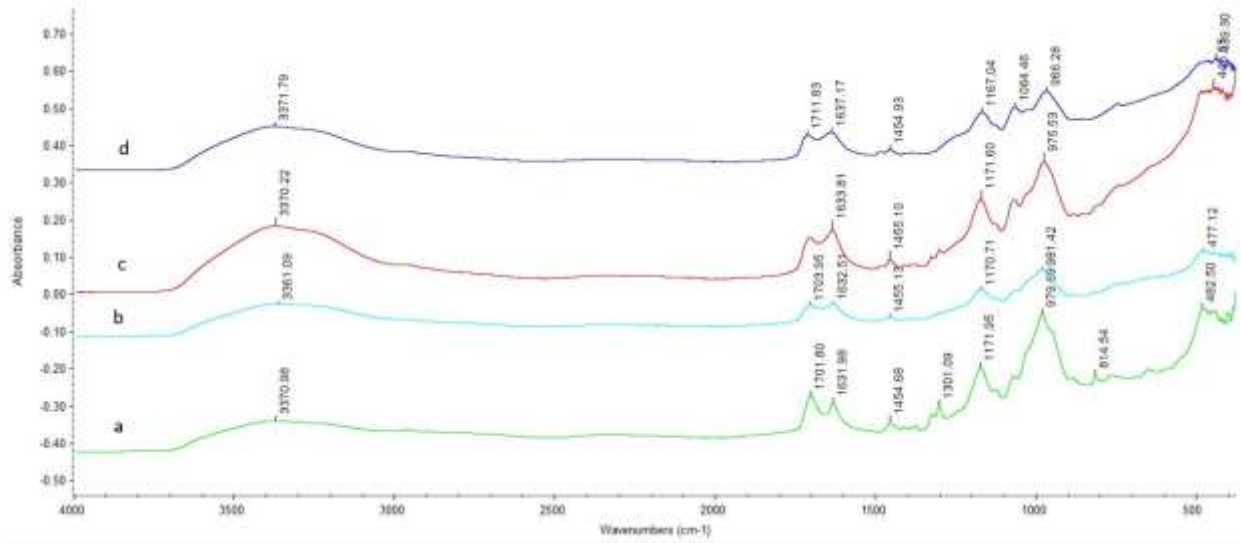

Figure 4-II: ATR-FTIR of (a) 50/50 v/v of MOEP, and the development of hydroxide groups as pH increases from its native pH of (b) 40/60 v/v MOEP to pH values of (c) 1 and (d) 1.5.

Figure 4-I shows the FTIR spectra of MOEP monomer and PMOEP after polymerization with different starting pH. The peak at around 3370 cm^{-1}, 1700 cm^{-1} and 1630 cm^{-1} are assigned to hydroxyl group, carbonyl of the carboxylic group and alkene C=C group respectively. The peak at ~1064 cm^{-1} and 970 cm^{-1} were assigned to the P-O-C stretching and P-O-H stretching respectively. The C-H bending peak was observed at around 1455 cm^{-1}. The increase in signal at around 1064

cm^{-1} correspond to the vibration of phosphate group, mainly for P-O stretching as more NaOH was added to the solution. The resulted hydrogels were let to swell in PBS and water for 24 hours.

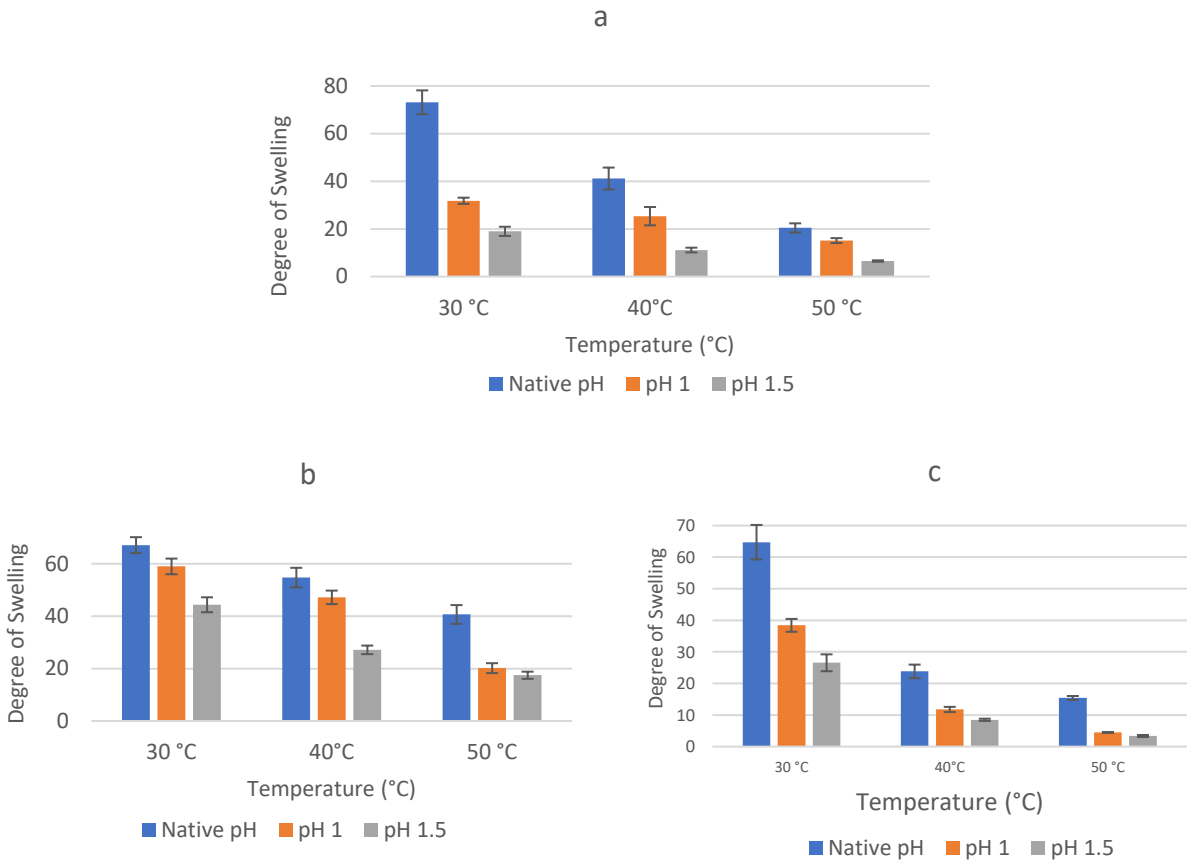

Figure 4-III: Degree of swelling of PMOEP at (a) 40% MOEP, (b) 50% MOEP and (c) 60% MOEP by volume at 30, 40 and 50 °C when pH is increased to 1 and 1.5.

The overall trend shows that an increase in pH (ca. sodium hydroxide) decreased the degree of swelling mainly when pH is changed from native pH to pH 1. Figure 4-II-a shows that at low MOEP content, the degree of swelling significantly dropped when the pH increased from its native pH to pH 1 when polymerized at 30 °C. Degree of swelling dropped from ~73 to ~32, more than half of DS of MOEP polymerized with its native pH. This could result from the interaction between Na^+ cations and anion groups of PMOEP which then increase the pressure within PMOEP network, and therefore reduce the ability of water to diffuse into the network (i.e., reduce osmotic pressure). Moreover, the present of Na^+ could result in ionic crosslinking which then reduce the ability of

water to swell into PMOEP. However, Figure 4-II-b shows that at 50/50 by volume of MOPE/water, the change in pH slightly decreased the degree of swelling when polymerized at 40 and 30 °C. At 30 °C, the 50/50 of MOEP/water at native pH result in the degree of swelling of ~67 and dropped to ~58 when increase the pH to 1.

The increase in temperature result in a drop in the degree of swelling as shown in Figure 4-II-a to c. While the degree of swelling dropped very significantly for 40/60 MOPE/Water and 60/40 MOEP/Water, the degree of swelling did not decrease as much between for 50/50 MOEP/water gel. It dropped form ~67 at 30 °C to ~55 at 40 °C and 44 at 50 °C. The increase in temperature means that the reaction rate went up, resulting in less organized system of hydrogel. Moreover, the increase in temperature could also affect the properties of the polymer itself. It was also noted that at high MOEP concentration (60/40 MOEP/Water) and 50 °C, the resulted hydrogel gave a light brown color, which could result from the oxidation of copper at such temperature. Similar color was also observed for 50/50 MOEP/Water solution.

Figure 4-IV: Images showing the coloring of PMOEP after polymerization at 50 °C with native pH (left), pH 1 (center) and pH 1.5 (right).

After swelling, the hydrogels became clear similar to other hydrogels made at lower temperature. This change in color could result from the expansion which a high volume of water was absorbed, therefore no color was observed. It is also possible that oxidized copper is released during swelling, turning the hydrogel to its usual color.

The increase in MOEP content decrease the degree of swelling. Figure 4-II-a to c shows that the degree of swelling increases from 65 to 67 to 73 when increasing the percent volume of MOEP from 40 to 50 to 60% respectively when polymerization happened at 30 °C in native pH. However, a more general trend was observed. The degree of swelling increased as MOEP volume is increased up to 50% MOEP and dropped when MOEP content was further increased up to 60%. The decrease in degree of swelling at higher monomer content was also previously reported for methacrylic acid and poly(methacrylic acid) [51, 52]. The increase in monomer content provided more crosslinkers embedded in the solution since MOEP contained 14% of BMOEP crosslinker. The result hydrogel could be more crosslinked than the hydrogel with lower monomer content.

The addition of sodium hydroxide to MOEP solution can also change the mechanism of the polymerization. Hydroxide ions (OH^-) were introduced to the system along with sodium cation (Na^+). This could also affect the ability of the monomer to polymerize. Furthermore, these hydroxide and sodium ions could result in petition between polymer and sodium cations vs. polymer and hydroxide ions. This could further affect the swelling ratio and degree of swelling. The properties of the monomers and crosslinker could also be changed due to these interactions. Similarly, the change in temperature could also affect the reactivity of the polymerization process, noticeably on the copper catalyst. As shown in Figure 4-IV, the hydrogel color was different at higher temperature. This could indicate the change in mechanism and reactivity of the catalyst, as well as how the catalyst act in the reaction. Additionally, the effect could result in an increase inside reaction that allows monomer to self-polymerize. This could also introduce more entanglement and/or polymer chains that do not include in the hydrogel network. It is also possible that there were unreacted monomers due to the change in the mechanism with respect to the change

in temperature. This could result in the increase in degree of crosslinking of the hydrogel network, therefore, decrease the degree of swelling.

4.4.3. Fractures of Hydrogel During Swelling

Figure 4-V: PMOEP polymerized at 50 °C with its native pH (left), pH 1 (center) and pH 1.5 (right) showing fracturing became more severe as pH increased.

The fracturing of PMOEP hydrogel during swelling was previously reported for lower degree of polymerization. This study showed that fracturing also occurred when the polymerization happened at different temperature, different pH and different MOEP content. At 50 °C, the swollen hydrogel showed from minimal fracture to significantly fractured for 60/40 MOEP/water. As shown in figure 4-V, PMOEP synthesized at pH 1.5 and 50 °C is nearly completely fractured after swelling while at lower pH, the shape remained with some minor fractures. Fracturing also occurred to PMOEP synthesized at 50 °C with 50/50 MOEP/Water. However, the fracturing decreased as shown below. In fact, these were the only sample set from 50 °C that could be repeated and result in a fairly cylindrical shape for mechanical testing.

4.4.4. Mechanical Properties of PMOEP Hydrogel

As mentioned previously, only 50/50 MOEP/water solutions formed hydrogel good enough for mechanical testing. Therefore, the PMOEP hydrogel made from 50/50 by volume of MOEP/Water were chosen to further studied their mechanical properties and cytotoxicity.

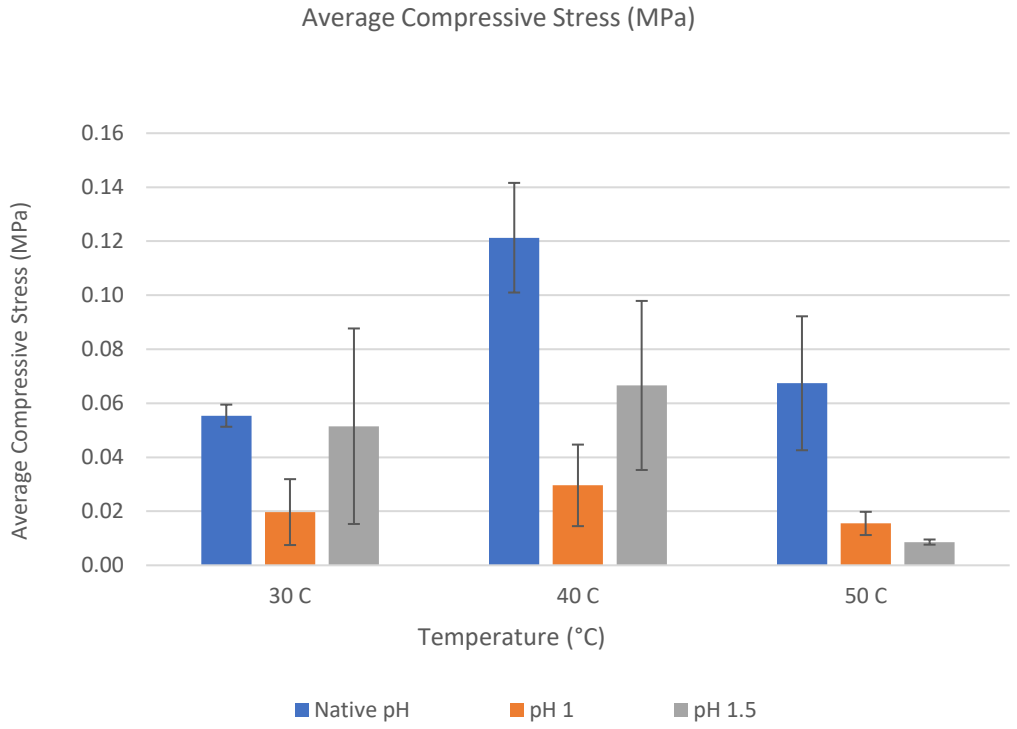

Figure 4-VII: Average stress of PMOPE polymerized at different temperature and pH.

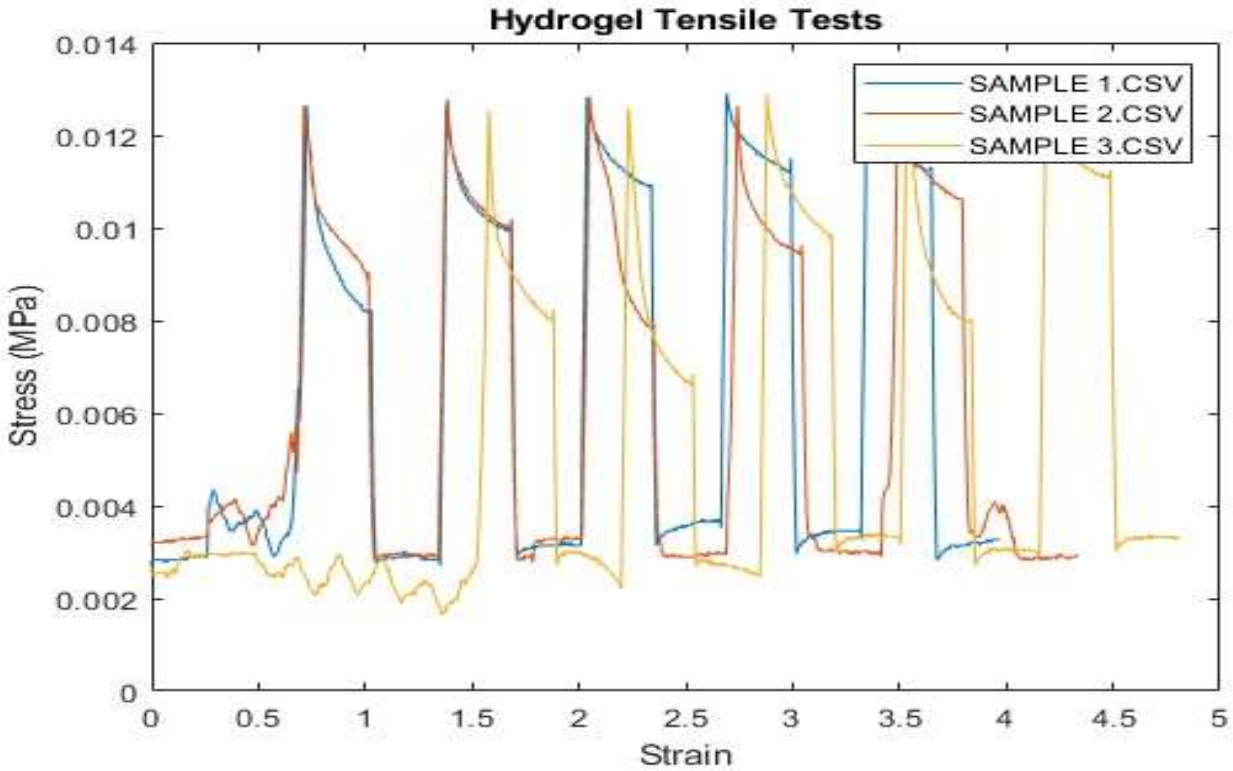

Figure 4-VI: Cyclic test result for PMOEP – 40C- pH 0.5.

The data showed that an increase in pH to a certain level decreased the overall compressive

stress. As shown in Figure 4-VII, the compressive stress was significantly reduced when increasing the pH to 1 and increased to a certain point at pH 1.5 for 30 and 40 °C. For 50 °C, the compressive stress rapidly decreased when increased pH to 1, and slightly decreased when increased the pH further to 1.5. On the other hand, for each pH, the compressive stress showed its maximum at 40 °C. For example, when polymerized at 30 °C at its native pH, the compressive stress was 0.0554 MPa and increased to 0.1213 MPa at 40 °C. The compressive stress dropped to 0.0674 MPa when the temperature is increased to 50 °C.

PMOEP hydrogel polymerized at pH 1.5 and 40 °C has the ability to receive the same force multiple times if the force is not strong enough to break the hydrogel. Figure 4-VIII shows that the hydrogel could at least stayed under the stress of 0.01 MPa for 5 times without showing any fracture or deformation.

4.4.5. Cytotoxicity of PMOEP Hydrogel

The same set of samples were used to study the cytotoxicity of PMOEP with rBMSCs via leaching test. The cells were exposed to PMOEP hydrogels for 24 hours in the incubator and let to grow as usual. The exposure to hydrogel resulted in a decrease in pH of the media (more acidic) as observed by the color changed of the media from pink to lighter pink. The could be due to the Type 1 ultrapure water used to swell the hydrogel which usually has the pH around 5.6. The result shows that very few cells were killed, and cells continued to grow as usual. This means that PMOEP could be in contact with cells at least for 24 hours which could allow PMOEP to be used in a wide range of biomedical application from drug release to contact lens and more.

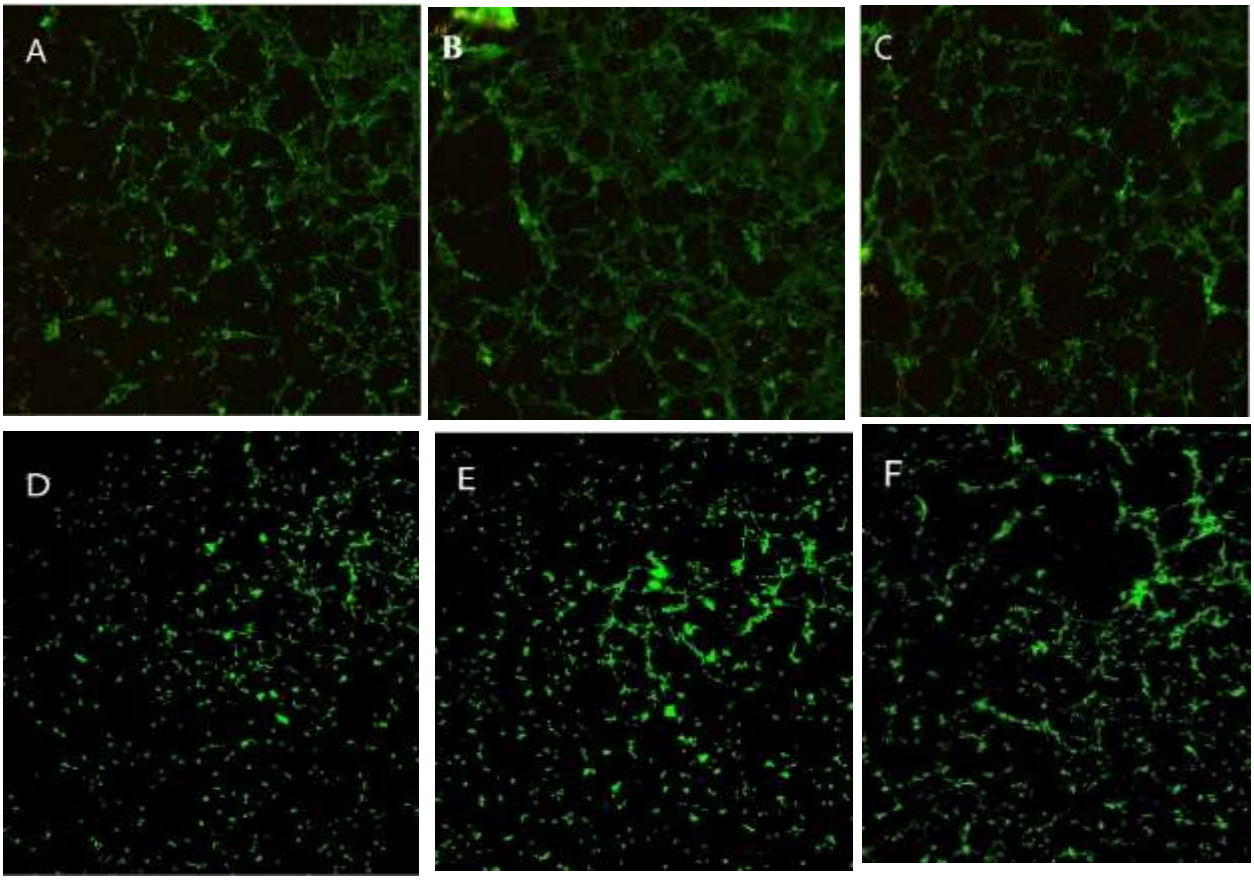

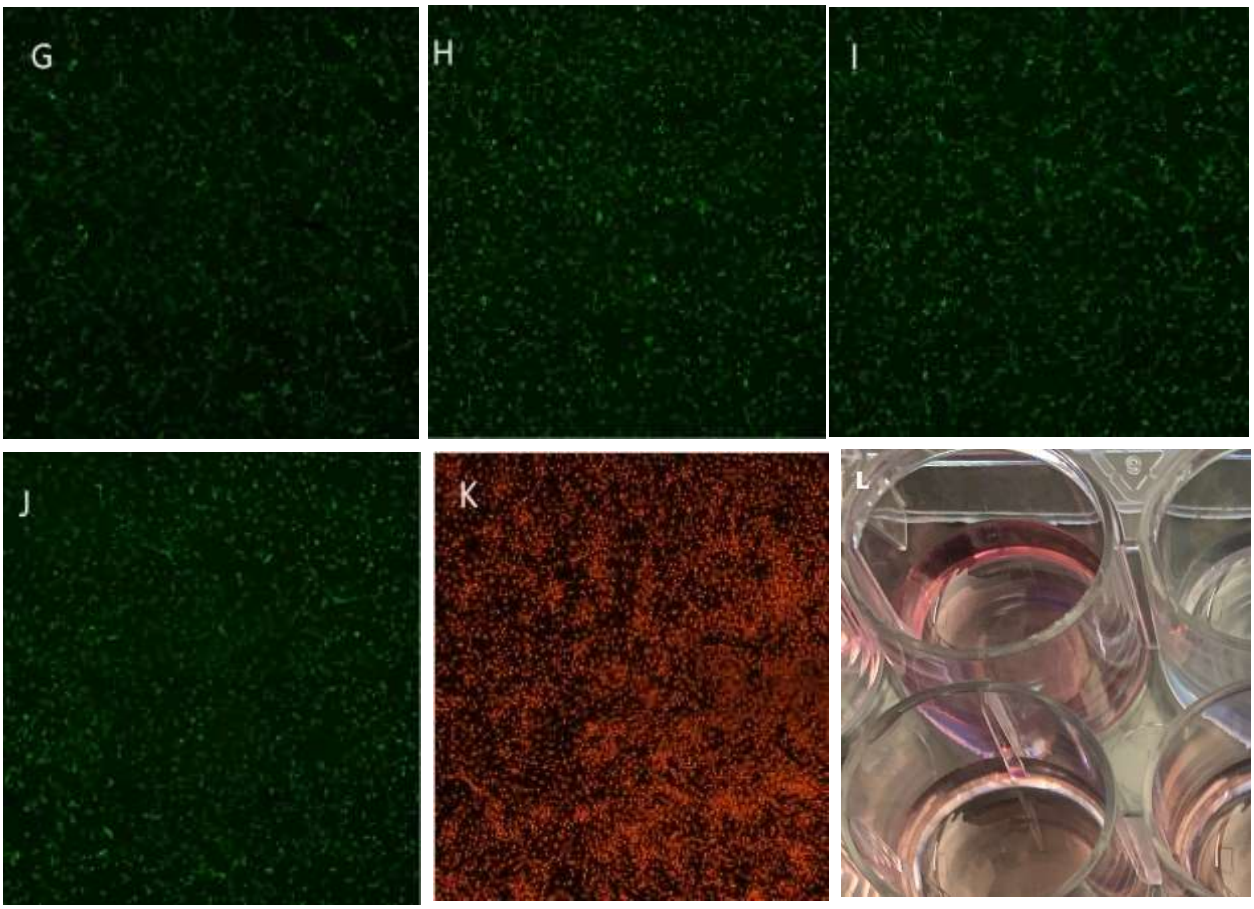

Figure 4-VIII: Images showing live and dead rBMSCs after exposing to hydrogel polymerized at (A) 30 °C pH 0.5, (B) 30 °C pH 1, (C) 30 °C pH 1.5, (D) 40 °C pH 0.5, (E) 40 °C pH 1, (F) 40 °C pH 1.5, (G) 50 °C pH 0.5, (H) 50 °C pH 1, (I) 50 °C pH 1.5, (J) Live Controlled rBMSCs, (K) Dead Controlled rBMSCs killed by 70% Methanol in PBS, and (L) Changed in Colors of the media with the top well is the controlled well and bottom well is the well exposed to hydrogel.

4.5. Conclusions

PMOEP was synthesized at different conditions: composition of MOEP including 40%, 50% and 60% by volume of MOEP, polymerization temperature at 30, 40 and 50 °C in an oven and pH of MOEP solution at its native pH, pH 1 and pH 1.5. The result shows that an increase in MOEP content, temperature and pH would result in a decrease in swelling. The addition of sodium hydroxide could alter the reaction mechanism, especially at higher temperature. It is hypothesized that high temperature will affect the copper bromide catalyst, and could result in different mechanism that was previously studied. Moreover, some monomers may not have reacted due to

the change in temperature as well. However, 50% MOEP solutions showed the best shape retention after swelling with minimal fracture when polymerized at 50 °C. The composition of 50% MOEP was then used to investigate the mechanical properties and cytotoxicity of the hydrogel. The result showed that 50% MOEP polymerized at 40 °C in its native pH has the highest strain and could return to its original strength after experiencing a certain force below its maximum strain. Evidently, the exposure of rBMSCs to PMOEP hydrogels did not affect the ability of cells to live in the incubator although PMOEP hydrogel turned the media more acidic then its originally was. Further investigations should include the ability of cells to adhere to the hydrogel and grow on the hydrogel. Moreover, the increase in pH of MOEP solution could affect aqueous ARGET-ATRP mechanism. A study of the formation and degree of swelling of PMOEP polymerized at higher pH should be conducted to observe the effect of pH on ARGET-ATRP.

Chapter 5 Conclusions and Recommendations

5.1. Overall Conclusions

In this study, PMOEP hydrogel was observed in different solvents including sodium chloride, potassium chloride, magnesium chloride and calcium chloride solutions at 0.1 M, 0.5 M and 1M. Interestingly, when swelling in slat solutions, PMOEP increased its weight within the first hours and significantly decreased within 6 hours. In fact, PMOEP collapsed and pushing out its initial water from the hydrogel network when swelling in high concentration of calcium chloride (0.5M). When swelling in 0.5M of $MgCl_2$ solution, a drastic decreased in mass was also observed between 1 and 6 hours. The increase in temperature during swelling showed further decrease in PMOEP mass in 0.5M calcium chloride solution. The general degree of swelling trend followed $Na^+ > K^+ > Mg^{2+} > Ca^{2+}$. Due to the intermolecular interaction between cations of salt and anion groups of PMOEP, a decrease in mass was observed when swollen PMEOP hydrogels were exposed to salt solutions. A new equilibrium between solvent and hydrogel network was established as induced swelling occurred. The final degree of swelling followed the same trend as the ratio of swelling in salt solution.

Water showed to result the highest degree of swelling due to the formation of hydrogen bond which further allowed more water molecules to diffuse into the hydrogel network. PBS solutions at different pH was also observed and the result showed very little to no impact from pH to the degree of swelling at low or high pH. However, the degree of swelling increased significantly at neutral pH, mainly between 6.5 to 7.4. An increase in temperature did not affect the degree of swelling as much as it did when swelling in salt solutions. However, a small decrease in ratio of swelling were observed when the temperature was increased from 30 °C to 40 °C.

PMOEP showed that it could be used in expansion microscopy as cells could be attached to the hydrogel network. Current result showed around 2 folds expansion of the cells. However, the final image resolution was significantly reduced maybe due to the mismatch of the refractive index of water and glass cover, light distribution, or loss of dye on the process of swelling. A digestion step was included to improve the quality of the image, however it showed very little to no expansion of the cells.

The temperature, MOEP composition, and pH were altered to study the effect of these conditions toward aqueous ARGET-ATRP of PMOEP. The data showed that an increase in MOEP content, pH or temperature resulted in a decrease in degree of swelling. PMOEP hydrogel showed its highest degree of swelling when 40% MOEP solution is polymerized with its native pH at 30 °C. Fractures were observed across the samples polymerized at 50°C showing the lower stability of hydrogel. This could result from the bad arrangement of the hydrogel network as polymerization happened faster at higher temperature. Entanglement and dangling could also affect the stability of hydrogel during selling as well. PMOEP polymerized from 50% MOEP at 40 °C in its native pH could maintain its formation up to the highest force, which result in the highest strain. Cyclic test also showed no deformation to this sample when a force lower than its maximum force is applied multiple times.

5.2. Recommendations for Future Work

The study showed great progress to understand the properties of PMOEP, especially its degree of swelling at different solvent. However, further investigation of PMEOP properties and aqueous ARGET-ATRP should be done. The solvent used for swelling PMOEP could be a mix solution (e.g. water and methanol). MOEP has been copolymerized with many other monomers such as HEMA. The addition of HEMA into MOEP solutions may improve the properties of the

hydrogel, therefore, using aqueous ARGET-ATRP to copolymerize HEMA and MOEP could introduce MOEP to new applications. Furthermore, a change in solvent of MOEP solution (e.g. change from water to methanol) may result in different properties of PMOEP as well. A study of trivalent cations such as iron (III) chloride could further prove the effect of cations on the induced selling and collapsing of PMOEP hydrogel.

From chapter 3, future work should focus on the adjustment of dye to obtain better quality of the image. A good cross linker between hydrogel and cells might be needed to avoid any damage to the cells and hydrogel connection during digestion. This would be a new application of PMOEP that had never done before. Chapter 4 hypothesize the effect of temperature and the addition of sodium hydroxide to the monomer. Further investigation is needed to better understand the effect toward reaction mechanism and monomer in general. Moreover, PMOEP alone without copolymerization could be polymerize with different drug to observe the ability to release drug of such hydrogel. Further investigation of mechanical properties of PMOEP should be conducted as this study did not intensively look at all the mechanical properties of the hydrogel. The study of degree of crosslinking using different theories and calculations should be done for comparison to its initial crosslinking density which was found to be 84:16 of MOEP:BMOEP. Additionally, aqueous ARGET-ATRP should be extended to monomer with sulfonate group which could introduce ATRP to different monomer solutions, therefore new applications.

Appendix

Appendix A – EDS Data for Different Salts and Concentrations

I. Deswelling of PMOEP in 0.1 M Calcium Chloride

EDS 0.1 M Ca Top

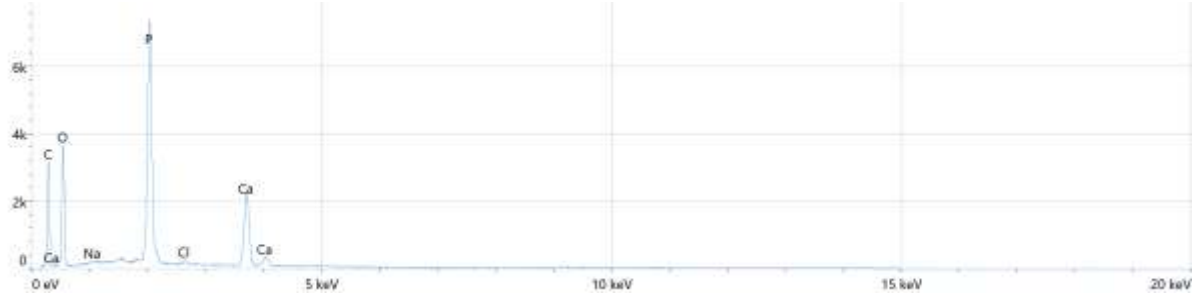

Element	Atomic %	Atomic % Error	Weight %	Weight % Error
C	32.6	0.2	20.3	0.1
O	42.2	0.2	35.0	0.2
Na	0.2	0.0	0.3	0.0
P	15.9	0.1	25.6	0.1
Cl	0.4	0.0	0.7	0.0
Ca	8.7	0.0	18.0	0.1

EDS 0.1 M Ca Center

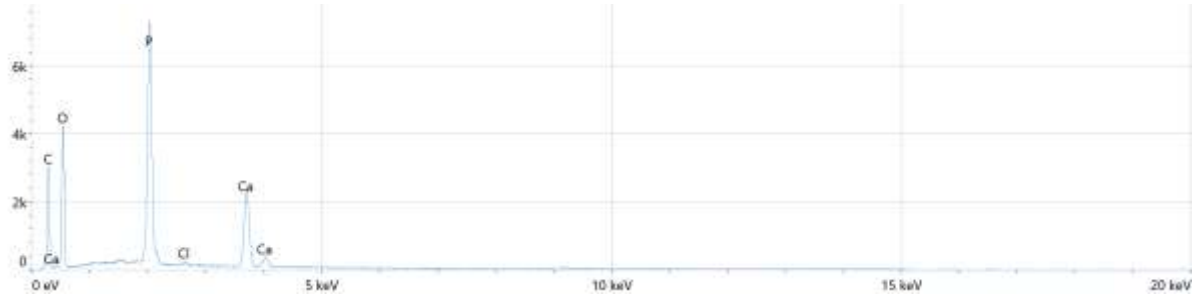

Element	Atomic %	Atomic % Error	Weight %	Weight % Error
C	29.4	0.2	18.3	0.1
O	46.3	0.2	38.4	0.2
P	15.4	0.1	24.7	0.1
Cl	0.3	0.0	0.5	0.0

Element	Atomic %	Atomic % Error	Weight %	Weight % Error
Ca	8.7	0.0	18.1	0.1

EDS 0.1 M Ca Bottom

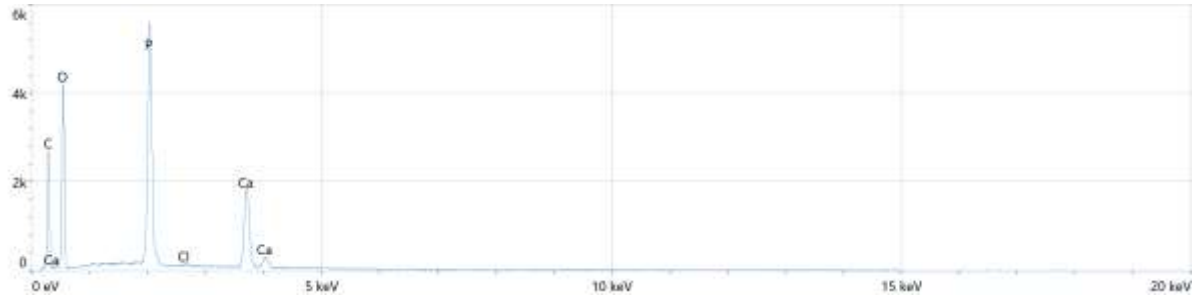

Element	Atomic %	Atomic % Error	Weight %	Weight % Error
C	27.7	0.1	17.3	0.1
O	48.9	0.2	40.8	0.2
Na	0.1	0.0	0.2	0.0
P	14.6	0.1	23.6	0.1
Cl	0.2	0.0	0.4	0.0
Ca	8.5	0.0	17.7	0.1

II. Dried PMOEP After Swelling in Different Salts and Concentrations

(A) 0.1M $CaCl_2$

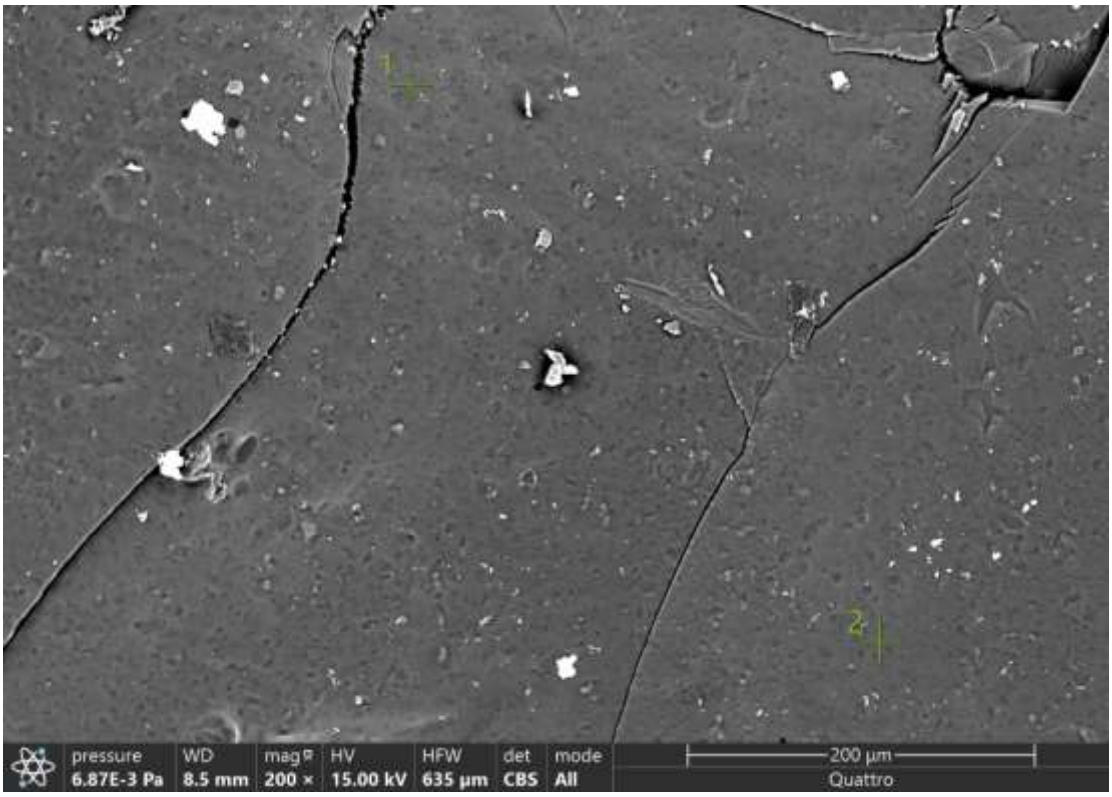

Point 1

Total Number of Counts: 284 208
Total Acquisition Time: 29 seconds
Average Count Rate: 9 800 cps
Acceleration Voltage: 15 kV

Element	Atomic %	Atomic % Error	Weight %	Weight % Error
C	29.9	0.1	18.8	0.1
O	48.0	0.2	40.3	0.2
P	14.8	0.1	24.0	0.2
Cl	0.4	0.0	0.8	0.0
Ca	6.8	0.0	14.4	0.1
Ir	0.2	0.1	1.7	0.6

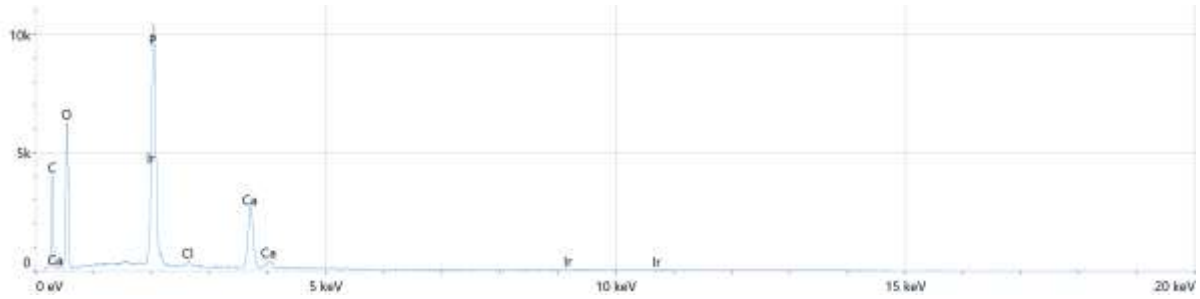

Point 2

Total Number of Counts: 170 308
Total Acquisition Time: 29 seconds
Average Count Rate: 5 873 cps
Acceleration Voltage: 15 kV

Element	Atomic %	Atomic % Error	Weight %	Weight % Error
C	24.4	0.1	14.6	0.1
O	47.8	0.2	38.0	0.2
P	17.4	0.1	26.8	0.1
Cl	0.5	0.0	0.8	0.0
Ca	10.0	0.1	19.9	0.1
Ir	0.0	0.0	0.0	0.0

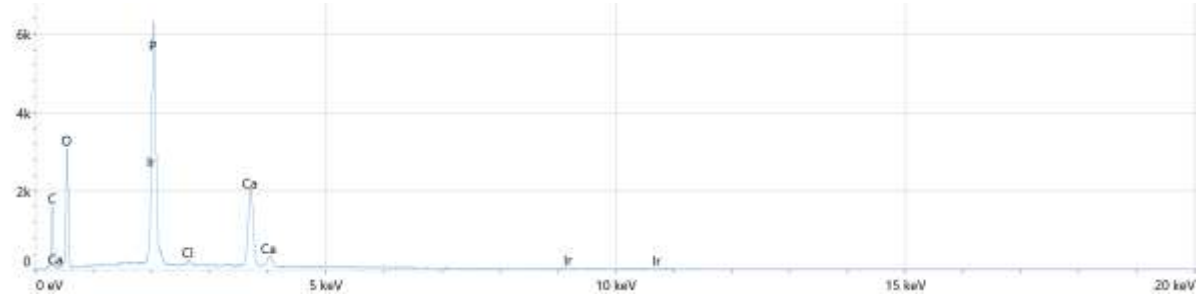

(B) 0.5 M $CaCl_2$

Point 1

Total Number of Counts: 197 074
Total Acquisition Time: 29 seconds
Average Count Rate: 6 796 cps
Acceleration Voltage: 15 kV

Element	Atomic %	Atomic % Error	Weight %	Weight % Error
C	23.1	0.2	14.1	0.1
O	52.2	0.2	42.4	0.2
P	14.2	0.2	22.3	0.2
Cl	1.7	0.0	3.1	0.0
Ca	8.7	0.0	17.6	0.1
Ir	0.1	0.0	0.5	0.3

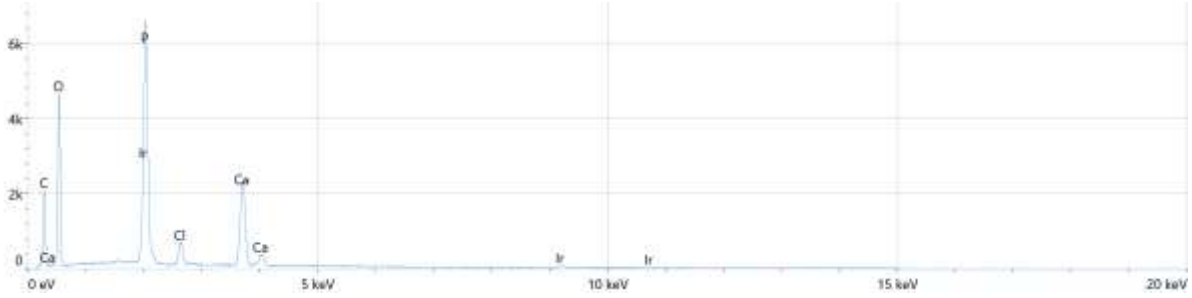

Point 2

Total Number of Counts: 134 238
Total Acquisition Time: 29 seconds
Average Count Rate: 4 629 cps
Acceleration Voltage: 15 kV

Element	Atomic %	Atomic % Error	Weight %	Weight % Error
C	18.5	0.1	10.2	0.1
O	46.8	0.3	34.3	0.2
P	18.6	0.1	26.5	0.1

Element	Atomic %	Atomic % Error	Weight %	Weight % Error
Cl	2.0	0.0	3.2	0.0
Ca	14.0	0.1	25.8	0.1
Ir	0.0	0.0	0.0	0.0

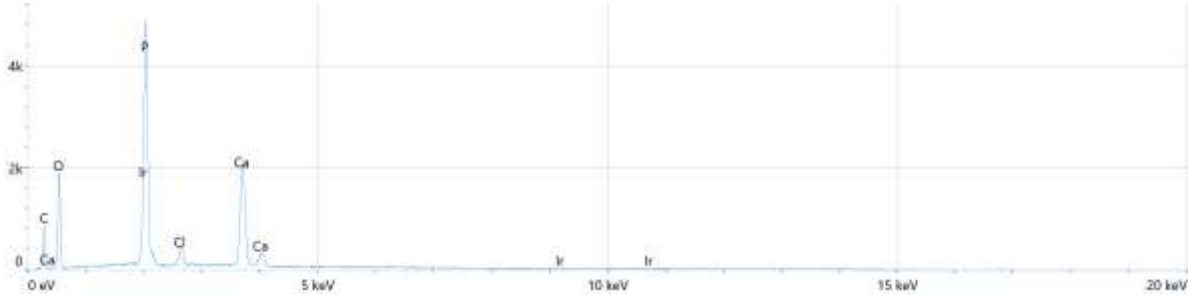

(C) 1 M $CaCl_2$

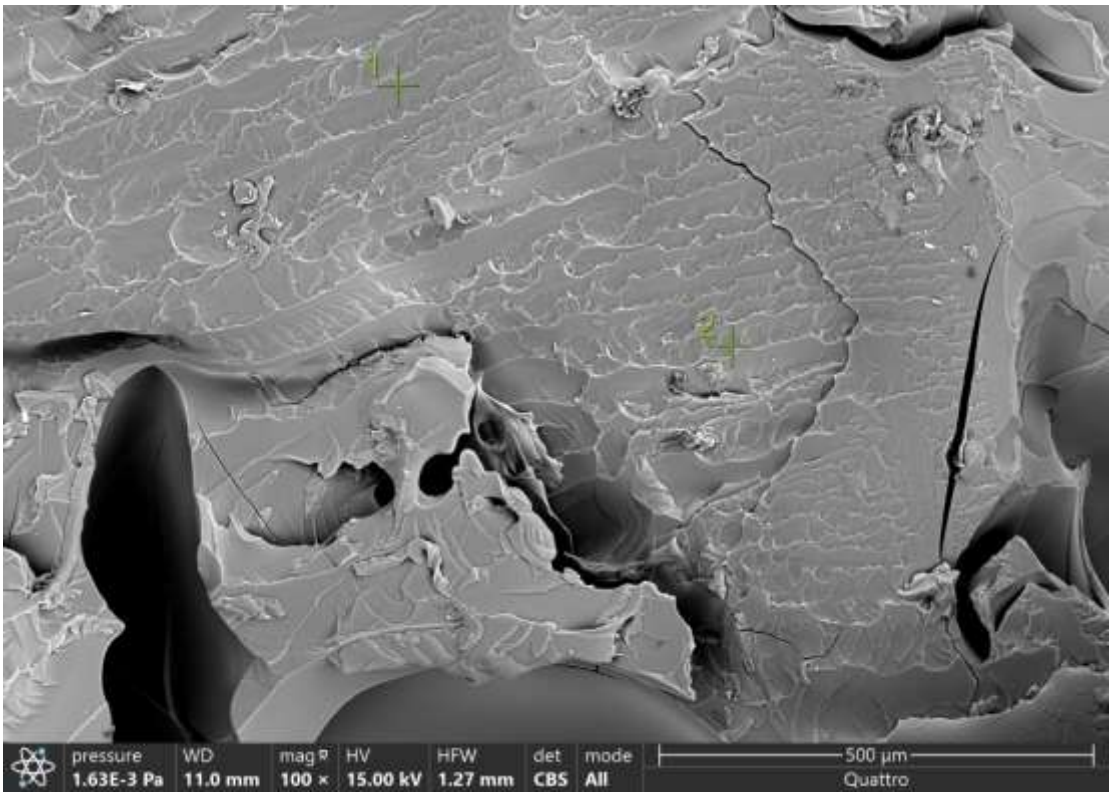

Point 1

Total Number of Counts: 245 439
Total Acquisition Time: 29 seconds
Average Count Rate: 8 463 cps
Acceleration Voltage: 15 kV

Element	Atomic %	Atomic % Error	Weight %	Weight % Error
C	26.6	0.1	16.4	0.1
O	49.0	0.2	40.3	0.2
P	14.0	0.1	22.2	0.1
Cl	2.1	0.0	3.8	0.0
Ca	8.4	0.0	17.3	0.1
Ir	0.0	0.0	0.0	0.0

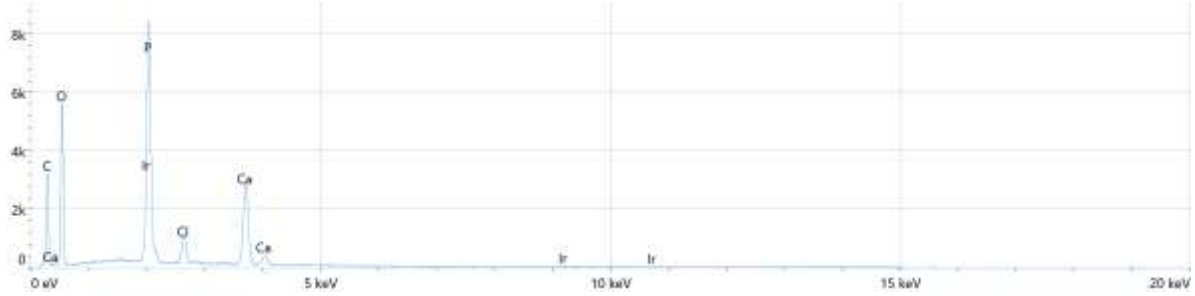

Point 2

Total Number of Counts: 152 051
Total Acquisition Time: 29 seconds
Average Count Rate: 5 243 cps
Acceleration Voltage: 15 kV

Element	Atomic %	Atomic % Error	Weight %	Weight % Error
C	20.7	0.1	12.5	0.1
O	54.7	0.2	44.1	0.2
P	12.6	0.0	19.6	0.1
Cl	2.4	0.0	4.3	0.0
Ca	9.6	0.0	19.4	0.1
Ir	0.0	0.0	0.0	0.0

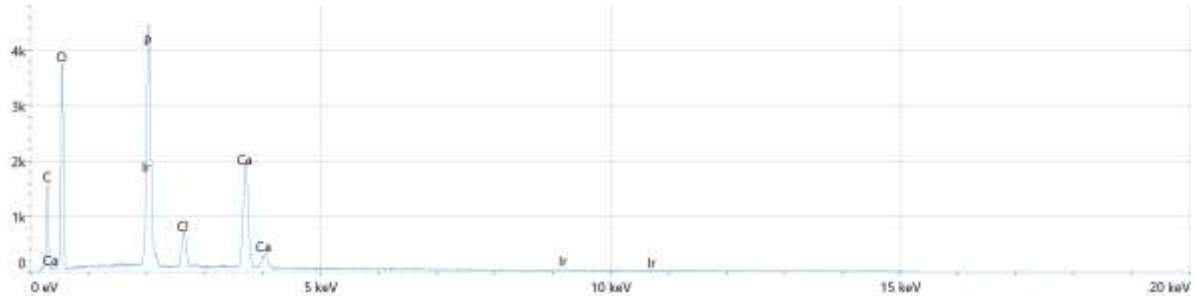

(D) 0.1M KCl

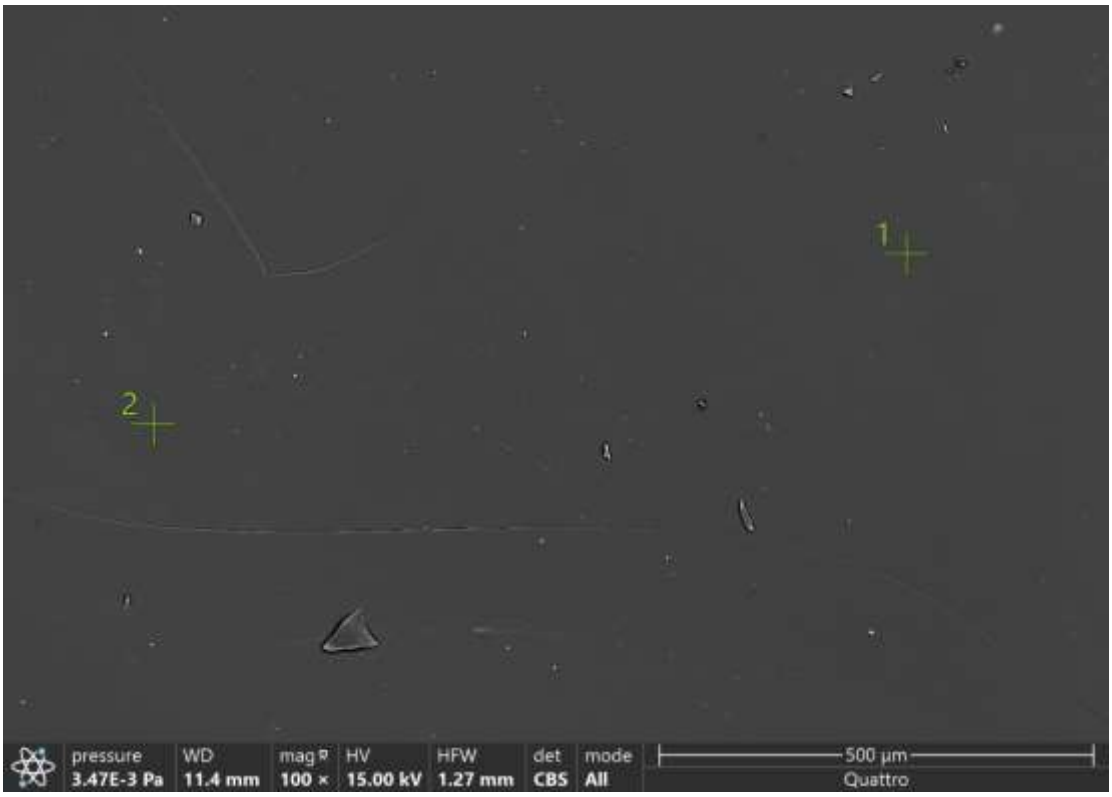

Point 1

Total Number of Counts: 218 125
Total Acquisition Time: 29 seconds
Average Count Rate: 7 522 cps
Acceleration Voltage: 15 kV

Element	Atomic %	Atomic % Error	Weight %	Weight % Error
C	28.0	0.2	16.9	0.1
O	43.8	0.2	35.1	0.2
Na	0.2	0.0	0.3	0.0
Mg	0.1	0.0	0.1	0.0
P	16.9	0.1	26.3	0.1
Cl	0.9	0.0	1.6	0.0
K	8.3	0.0	16.2	0.1
Ca	1.8	0.0	3.6	0.1

Element	Atomic %	Atomic % Error	Weight %	Weight % Error
Ir	0.0	0.0	0.0	0.0

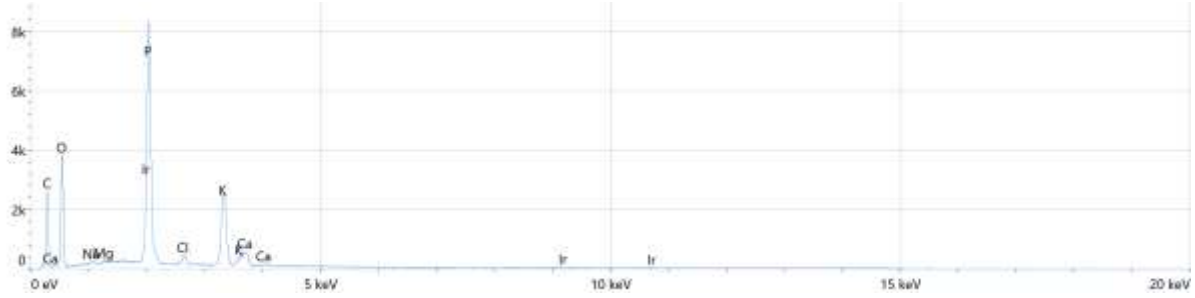

Point 2

Total Number of Counts: 293 586
Total Acquisition Time: 29 seconds
Average Count Rate: 10 124 cps
Acceleration Voltage: 15 kV

Element	Atomic %	Atomic % Error	Weight %	Weight % Error
C	32.1	0.1	20.7	0.1
O	46.4	0.2	40.0	0.2
Na	0.2	0.0	0.3	0.0
Mg	0.2	0.0	0.2	0.0
P	13.0	0.1	21.7	0.2
Cl	0.7	0.0	1.3	0.0
K	6.1	0.0	12.8	0.1
Ca	1.2	0.0	2.7	0.1
Ir	0.0	0.0	0.3	0.3

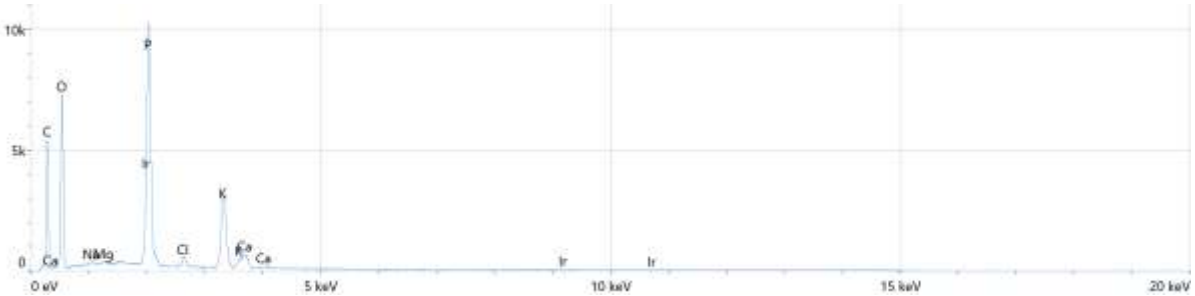

(E) 0.5M KCl

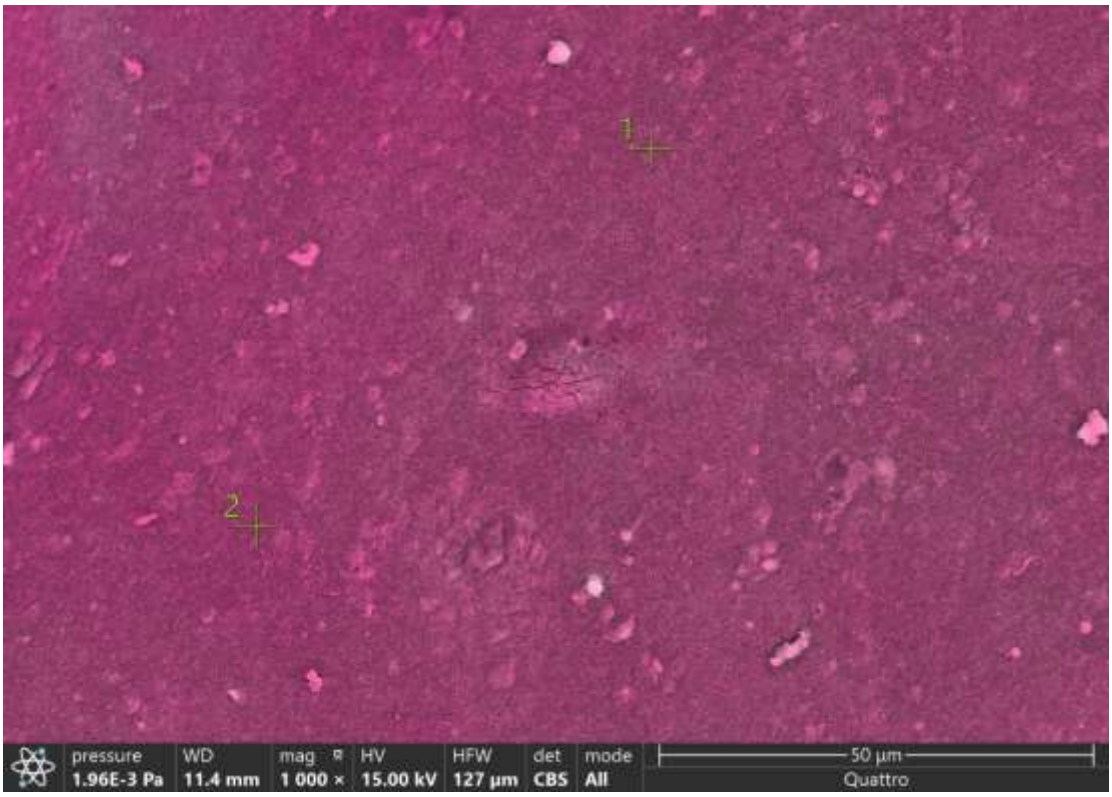

Point 1

Total Number of Counts: 128 648
Total Acquisition Time: 29 seconds
Average Count Rate: 4 436 cps
Acceleration Voltage: 15 kV

Element	Atomic %	Atomic % Error	Weight %	Weight % Error
C	18.9	0.3	8.1	0.1
O	22.3	0.3	12.7	0.2
Na	0.4	0.0	0.4	0.0
P	29.2	0.4	32.3	0.5
Cl	2.6	0.0	3.2	0.0
K	25.4	0.1	35.4	0.2
Ir	1.2	0.2	7.9	1.5

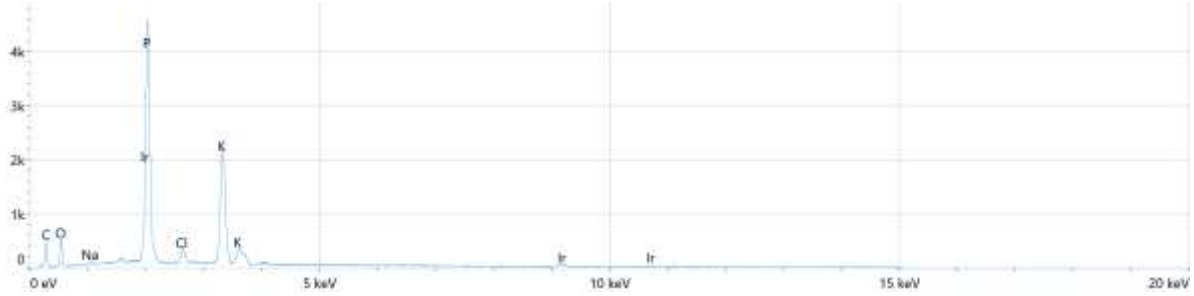

Point 2

Total Number of Counts: 106 058
Total Acquisition Time: 29 seconds
Average Count Rate: 3 657 cps
Acceleration Voltage: 15 kV

Element	Atomic %	Atomic % Error	Weight %	Weight % Error
C	18.4	0.2	7.5	0.1
O	21.0	0.4	11.4	0.2
Na	0.3	0.0	0.2	0.0
P	27.2	0.5	28.5	0.5
Cl	3.5	0.0	4.2	0.0
K	27.8	0.1	36.8	0.2
Ir	1.8	0.2	11.5	1.6

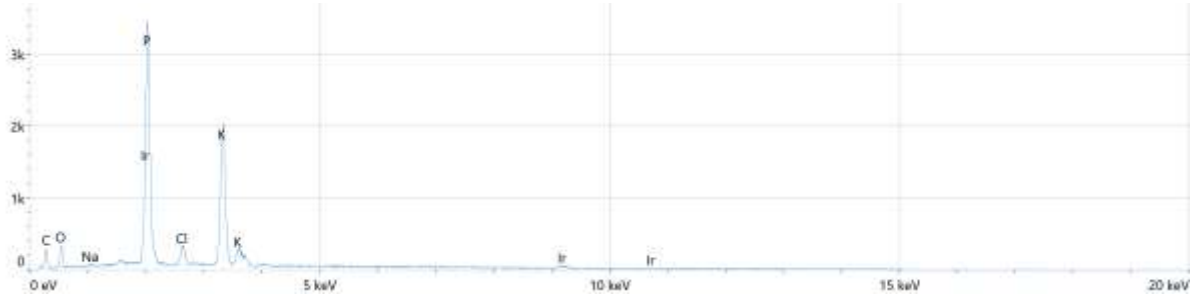

(F) 1M KCl

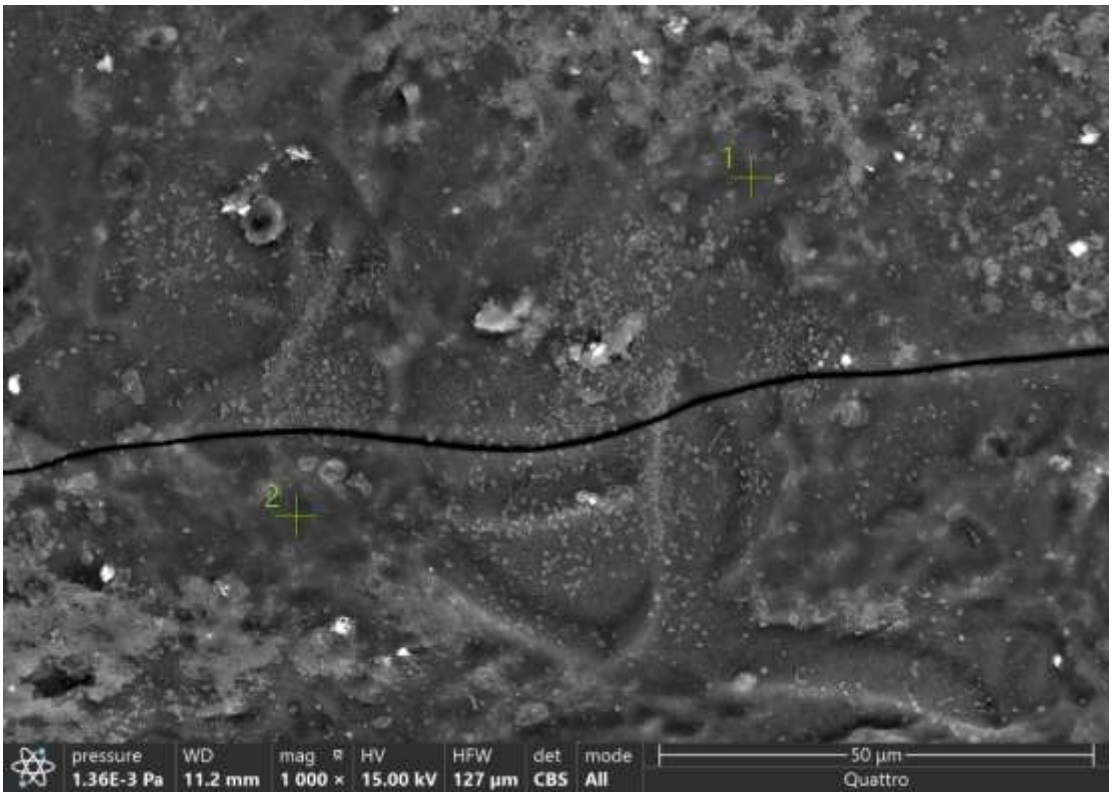

Point 1

Total Number of Counts: 187 004
Total Acquisition Time: 29 seconds
Average Count Rate: 6 448 cps
Acceleration Voltage: 15 kV

Element	Atomic %	Atomic % Error	Weight %	Weight % Error
C	26.1	0.1	13.8	0.1
O	34.1	0.2	24.0	0.2
Na	0.6	0.0	0.7	0.0
Mg	0.2	0.0	0.2	0.0
P	21.3	0.3	29.0	0.3
Cl	0.7	0.0	1.1	0.0
K	14.6	0.1	25.1	0.1
Ca	2.2	0.1	3.8	0.1

Element	Atomic %	Atomic % Error	Weight %	Weight % Error
Ir	0.3	0.1	2.3	0.8

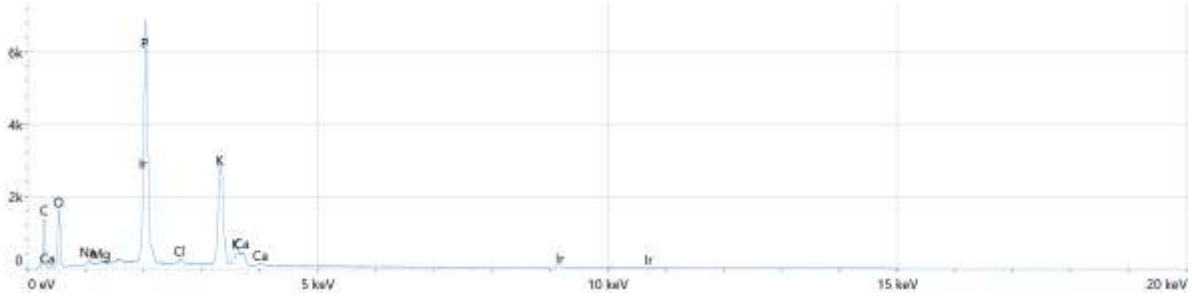

Point 2

Total Number of Counts: 145 453
Total Acquisition Time: 29 seconds
Average Count Rate: 5 016 cps
Acceleration Voltage: 15 kV

Element	Atomic %	Atomic % Error	Weight %	Weight % Error
C	20.8	0.3	9.7	0.1
O	27.6	0.3	17.1	0.2
Na	0.3	0.0	0.2	0.0
P	25.9	0.3	31.1	0.4
Cl	1.1	0.0	1.6	0.0
K	20.2	0.1	30.5	0.2
Ca	3.6	0.1	5.6	0.1
Ir	0.6	0.2	4.3	1.3

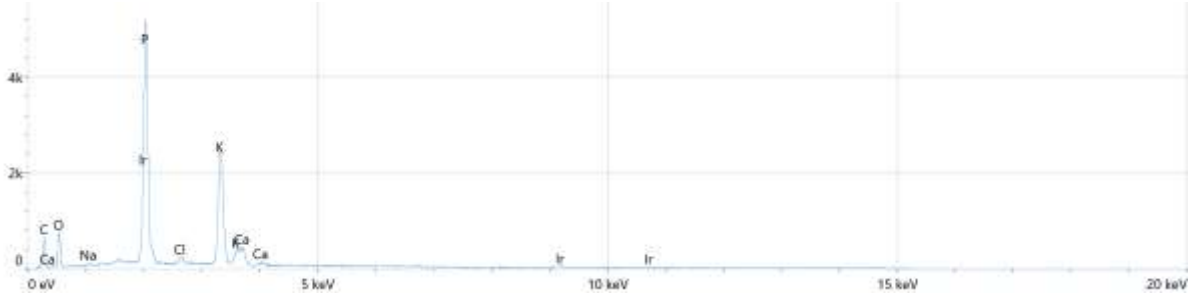

(G) 0.1M $MgCl_2$

Point 1

Total Number of Counts: 102 289
Total Acquisition Time: 29 seconds
Average Count Rate: 3 527 cps
Acceleration Voltage: 15 kV

Element	Atomic %	Atomic % Error	Weight %	Weight % Error
C	27.0	0.2	16.1	0.1
O	36.7	0.3	29.1	0.2
Mg	6.1	0.0	7.4	0.1
P	26.3	0.1	40.5	0.2
Cl	3.9	0.0	6.9	0.0
Ir	0.0	0.0	0.0	0.0

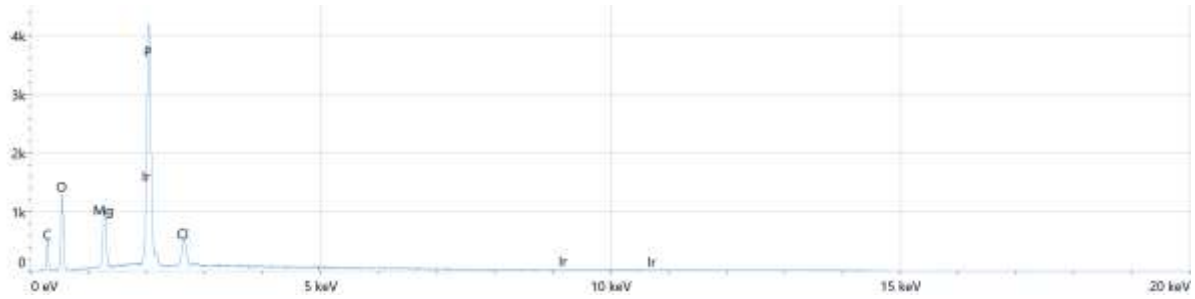

Point 2

Total Number of Counts: 137 001
Total Acquisition Time: 29 seconds
Average Count Rate: 4 724 cps
Acceleration Voltage: 15 kV

Element	Atomic %	Atomic % Error	Weight %	Weight % Error
C	27.3	0.2	16.4	0.1
O	37.5	0.2	30.1	0.2
Mg	6.7	0.0	8.1	0.0
P	24.5	0.1	38.1	0.1
Cl	4.1	0.0	7.2	0.0
Ir	0.0	0.0	0.0	0.0

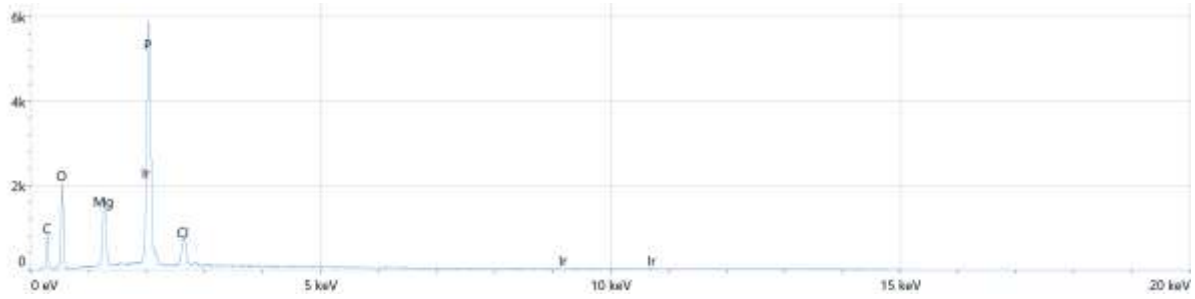

Point 3

Total Number of Counts: 116 840
Total Acquisition Time: 29 seconds
Average Count Rate: 4 029 cps
Acceleration Voltage: 15 kV

Element	Atomic %	Atomic % Error	Weight %	Weight % Error
C	26.1	0.4	15.3	0.2
O	35.7	0.2	28.0	0.2
Mg	6.8	0.0	8.1	0.0
P	26.1	0.1	39.5	0.2
Cl	5.3	0.0	9.1	0.0
Ir	0.0	0.0	0.0	0.0

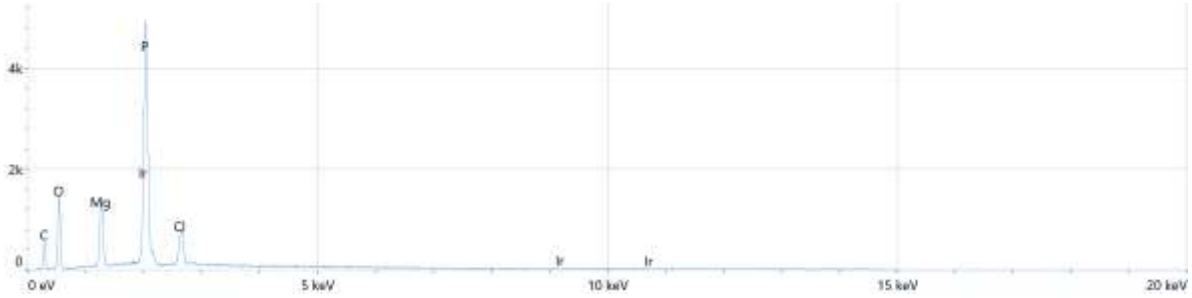

(H) 0.5M $MgCl_2$

Point 1

Total Number of Counts: 307 509
Total Acquisition Time: 29 seconds
Average Count Rate: 10 604 cps
Acceleration Voltage: 15 kV

Element	Atomic %	Atomic % Error	Weight %	Weight % Error
C	19.7	0.1	12.7	0.1
O	55.3	0.2	47.6	0.1
Mg	8.1	0.0	10.6	0.0
P	13.1	0.0	21.8	0.1
Cl	3.8	0.0	7.3	0.0
Ir	0.0	0.0	0.0	0.0

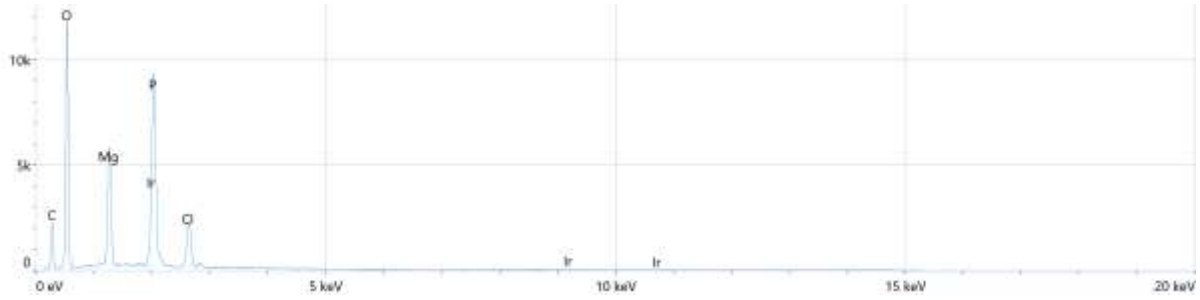

Point 2

Total Number of Counts: 306 027
Total Acquisition Time: 29 seconds
Average Count Rate: 10 553 cps
Acceleration Voltage: 15 kV

Element	Atomic %	Atomic % Error	Weight %	Weight % Error
C	20.9	0.1	13.6	0.1
O	54.7	0.2	47.4	0.1
Mg	7.7	0.0	10.1	0.0

Element	Atomic %	Atomic % Error	Weight %	Weight % Error
P	13.4	0.1	22.5	0.1
Cl	3.4	0.0	6.4	0.0
Ir	0.0	0.0	0.0	0.0

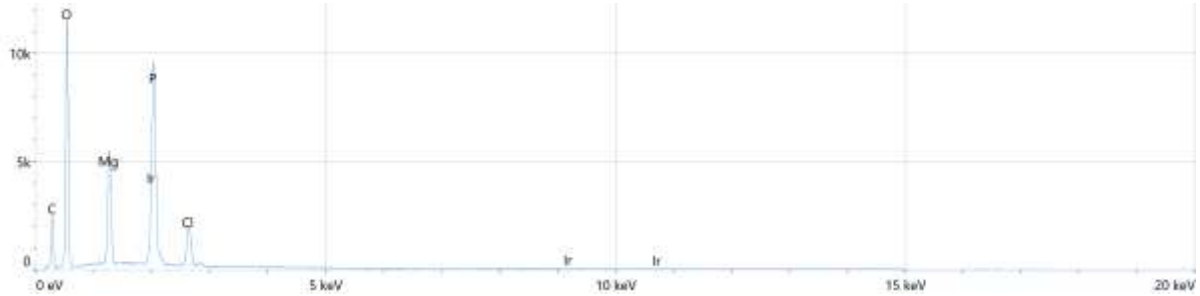

(I) 1M $MgCl_2$

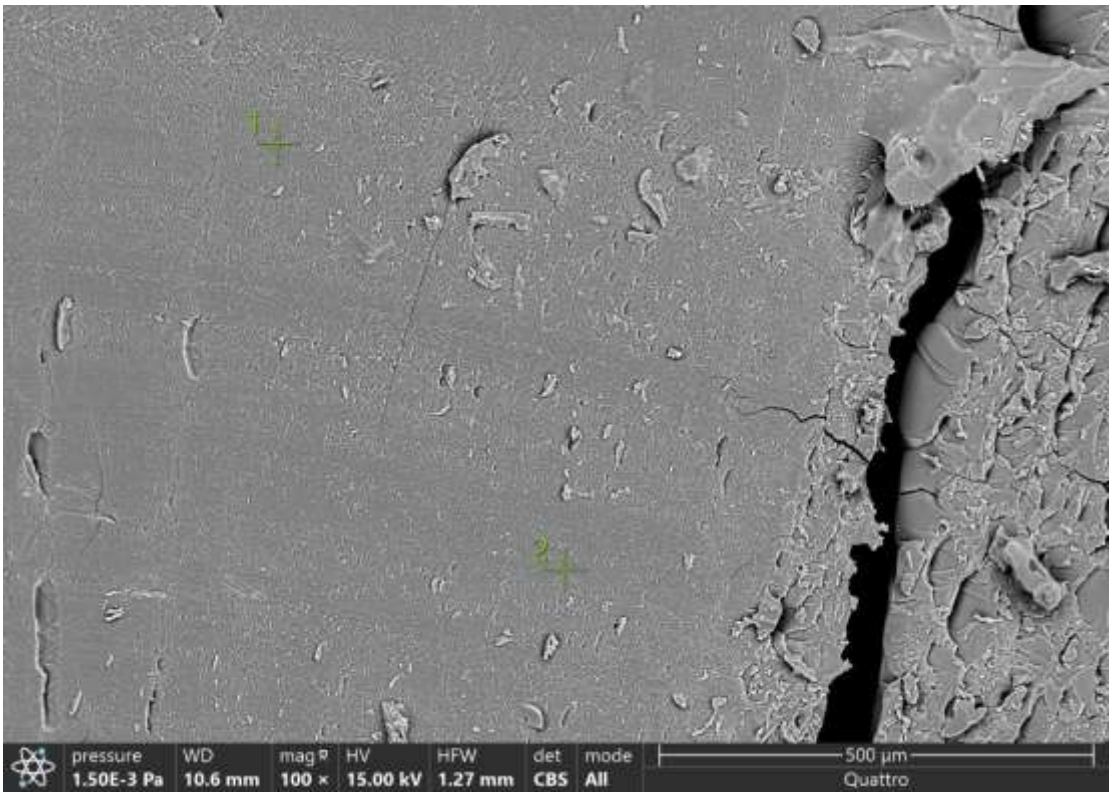

Point 1

Total Number of Counts: 282 189
Total Acquisition Time: 29 seconds
Average Count Rate: 9 731 cps
Acceleration Voltage: 15 kV

Element	Atomic %	Atomic % Error	Weight %	Weight % Error
C	21.1	0.1	13.7	0.1
O	54.3	0.2	47.0	0.1
Mg	7.9	0.0	10.4	0.0
P	13.3	0.0	22.4	0.1
Cl	3.4	0.0	6.5	0.0
Ir	0.0	0.0	0.0	0.0

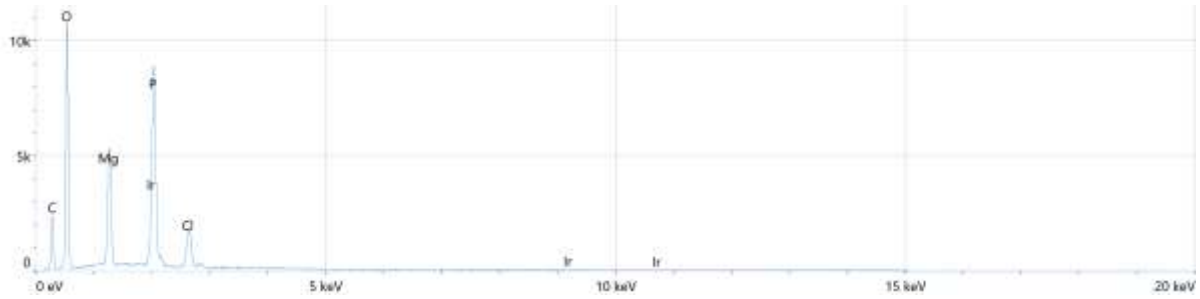

Point 2

Total Number of Counts: 201 139
Total Acquisition Time: 29 seconds
Average Count Rate: 6 936 cps
Acceleration Voltage: 15 kV

Element	Atomic %	Atomic % Error	Weight %	Weight % Error
C	22.4	0.1	13.8	0.1
O	46.1	0.2	37.8	0.1
Mg	8.0	0.0	10.0	0.0
P	17.8	0.1	28.3	0.1
Cl	5.6	0.0	10.1	0.0
Ir	0.0	0.0	0.0	0.0

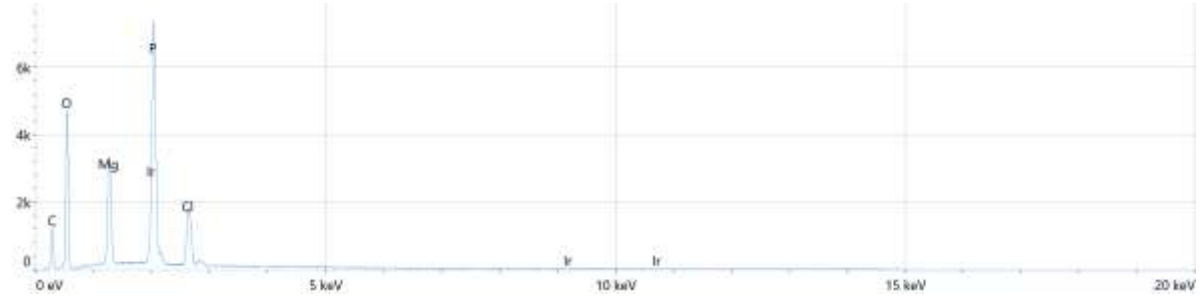

(J) 0.1M NaCl

Point 1

Total Number of Counts: 260 202
Total Acquisition Time: 29 seconds
Average Count Rate: 8 972 cps
Acceleration Voltage: 15 kV

Element	Atomic %	Atomic % Error	Weight %	Weight % Error
C	32.4	0.2	21.9	0.1
O	43.5	0.2	39.3	0.1
Na	7.8	0.0	10.1	0.0
P	15.4	0.1	26.9	0.1
Cl	0.9	0.0	1.8	0.0
Ir	0.0	0.0	0.0	0.0

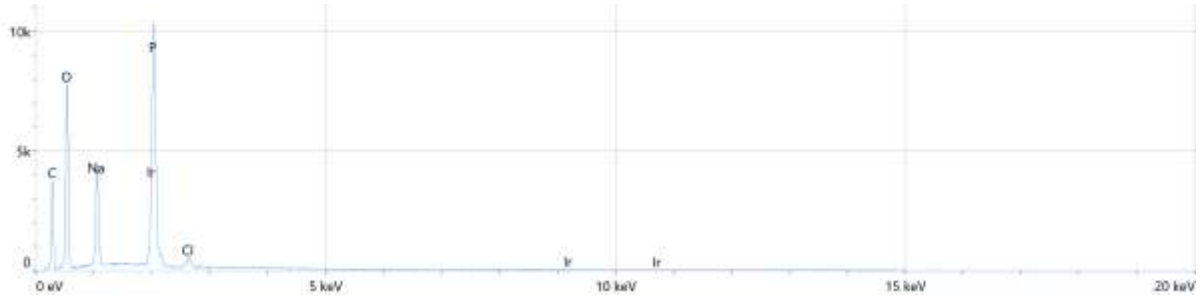

Point 2

Total Number of Counts: 182 074
Total Acquisition Time: 29 seconds
Average Count Rate: 6 278 cps
Acceleration Voltage: 15 kV

Element	Atomic %	Atomic % Error	Weight %	Weight % Error
C	29.0	0.2	18.3	0.1
O	39.2	0.2	32.9	0.1
Na	7.8	0.0	9.5	0.0

Element	Atomic %	Atomic % Error	Weight %	Weight % Error
P	23.1	0.1	37.6	0.1
Cl	0.9	0.0	1.7	0.0
Ir	0.0	0.0	0.0	0.0

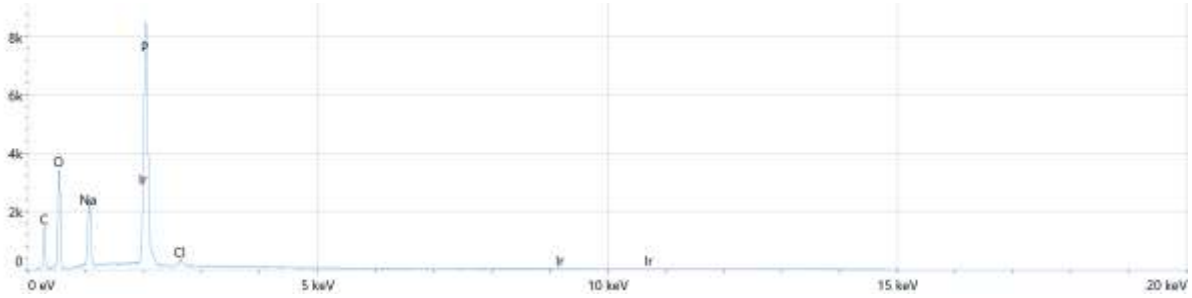

Point 3

Total Number of Counts: 174 425
Total Acquisition Time: 29 seconds
Average Count Rate: 6 015 cps
Acceleration Voltage: 15 kV

Element	Atomic %	Atomic % Error	Weight %	Weight % Error
C	28.5	0.2	17.9	0.2
O	38.9	0.2	32.4	0.2
Na	7.7	0.0	9.2	0.0
P	24.0	0.1	38.8	0.1
Cl	0.9	0.0	1.7	0.0
Ir	0.0	0.0	0.0	0.0

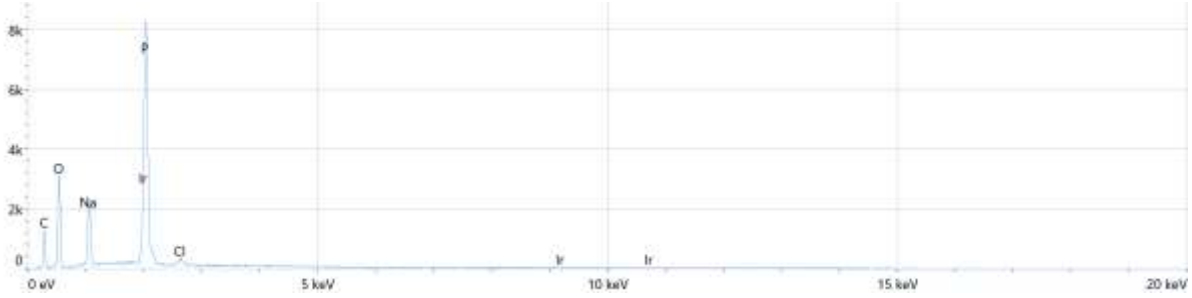

(K) 0.5M NaCl

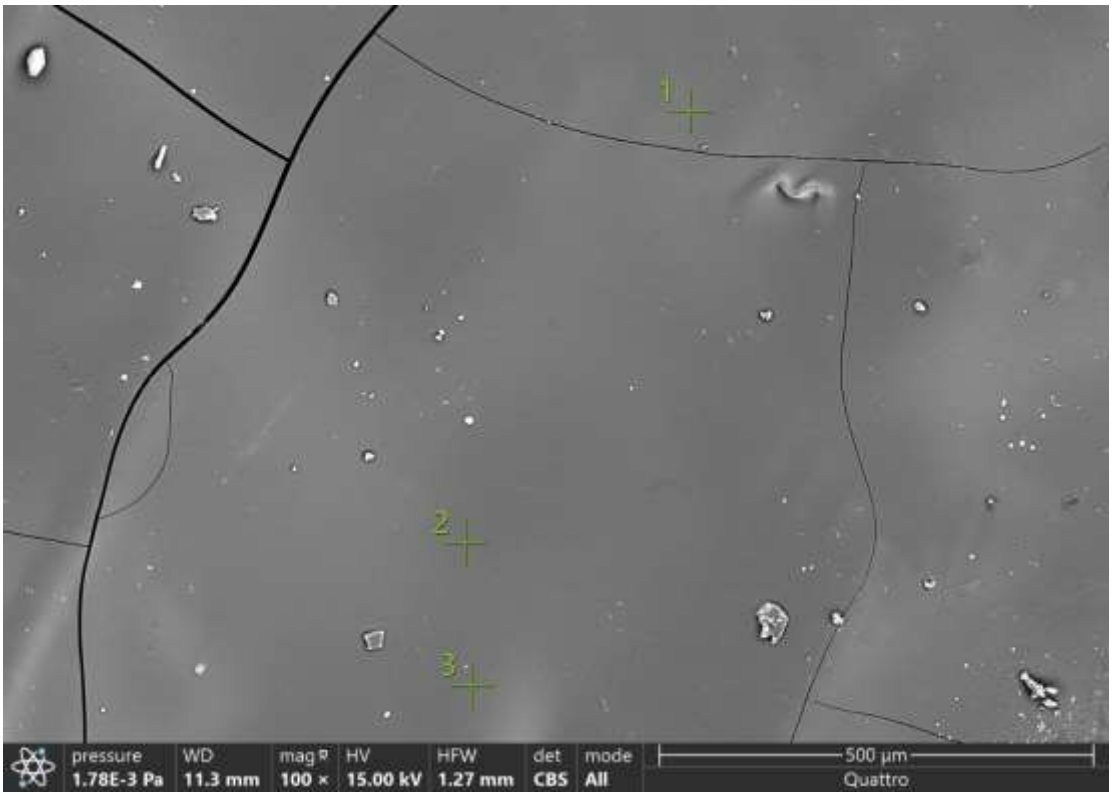

Point 1

Total Number of Counts: 180 678
Total Acquisition Time: 29 seconds
Average Count Rate: 6 230 cps
Acceleration Voltage: 15 kV

Element	Atomic %	Atomic % Error	Weight %	Weight % Error
C	31.1	0.2	20.2	0.1
O	40.2	0.2	34.9	0.2
Na	8.4	0.0	10.4	0.0
P	19.6	0.1	33.0	0.1
Cl	0.7	0.0	1.4	0.0
Ir	0.0	0.0	0.0	0.0

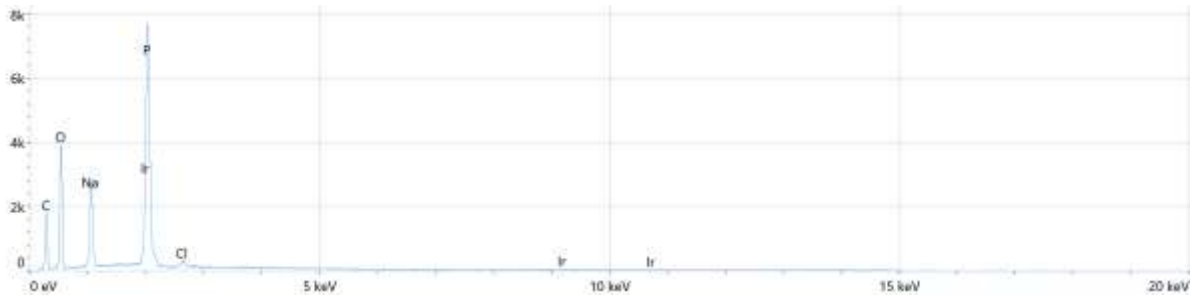

Point 2

Total Number of Counts: 172 860
Total Acquisition Time: 29 seconds
Average Count Rate: 5 961 cps
Acceleration Voltage: 15 kV

Element	Atomic %	Atomic % Error	Weight %	Weight % Error
C	29.8	0.2	18.9	0.1
O	38.5	0.2	32.5	0.2
Na	8.6	0.0	10.4	0.0
P	22.3	0.1	36.4	0.1
Cl	0.9	0.0	1.7	0.0
Ir	0.0	0.0	0.0	0.0

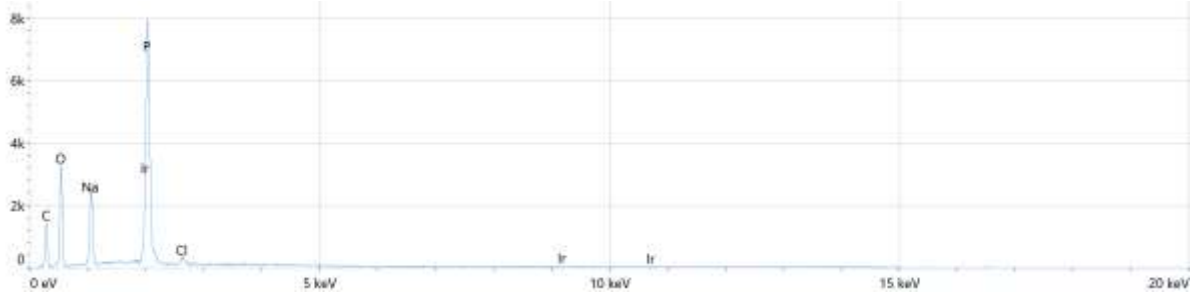

Point 3

Total Number of Counts: 250 693
Total Acquisition Time: 29 seconds
Average Count Rate: 8 645 cps
Acceleration Voltage: 15 kV

Element	Atomic %	Atomic % Error	Weight %	Weight % Error
C	29.3	0.2	19.6	0.1
O	45.3	0.2	40.4	0.1
Na	9.1	0.0	11.7	0.0
P	15.5	0.1	26.7	0.1
Cl	0.6	0.0	1.3	0.0
Ca	0.1	0.0	0.3	0.0
Ir	0.0	0.0	0.0	0.0

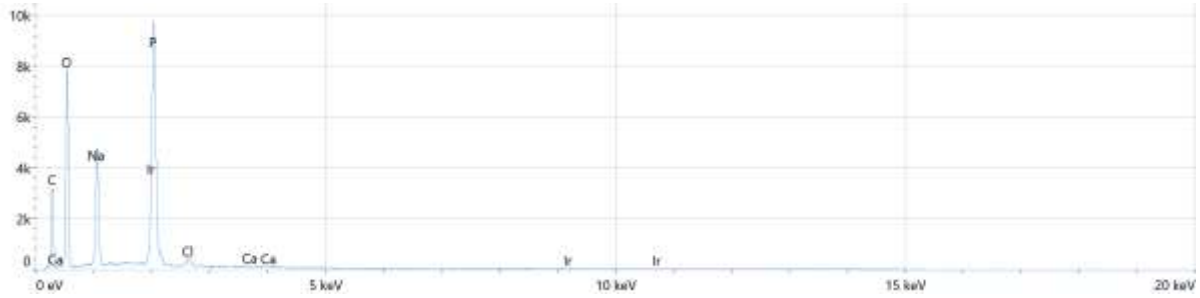

(L) 1M NaCl

Point 1

Total Number of Counts: 176 568
Total Acquisition Time: 29 seconds
Average Count Rate: 6 089 cps
Acceleration Voltage: 15 kV

Element	Atomic %	Atomic % Error	Weight %	Weight % Error
C	32.4	0.3	20.8	0.2
O	36.8	0.2	31.5	0.2
Na	9.1	0.0	11.2	0.0
P	20.1	0.1	33.2	0.1
Cl	1.5	0.0	2.7	0.0
K	0.3	0.0	0.6	0.0
Ir	0.0	0.0	0.0	0.0

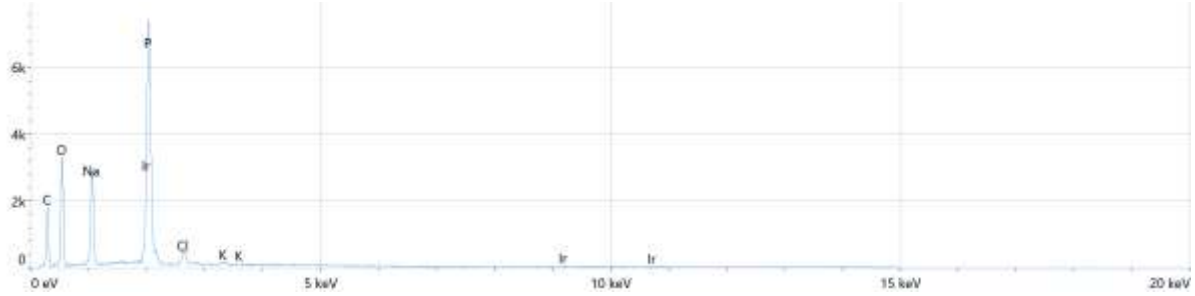

Point 2

Total Number of Counts: 211 847
Total Acquisition Time: 29 seconds
Average Count Rate: 7 305 cps
Acceleration Voltage: 15 kV

Element	Atomic %	Atomic % Error	Weight %	Weight % Error
C	27.7	0.1	17.7	0.1
O	40.8	0.2	34.7	0.1
Na	10.2	0.0	12.5	0.0
P	20.1	0.1	33.1	0.1
Cl	0.9	0.0	1.6	0.0
K	0.2	0.0	0.5	0.0
Ir	0.0	0.0	0.0	0.0

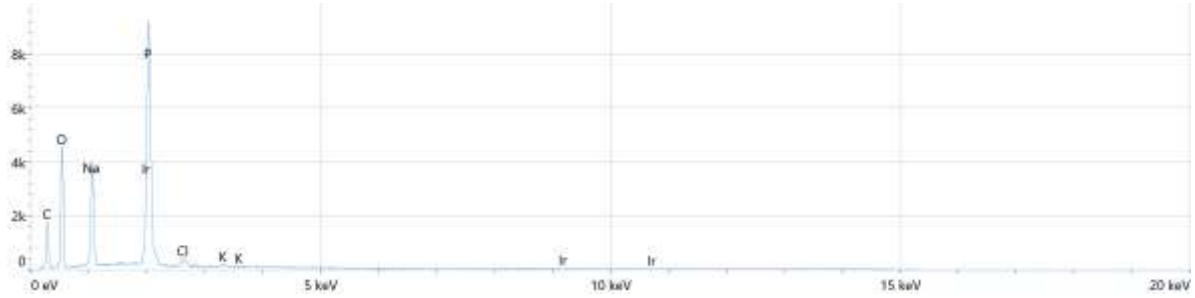

III. Structures and Compositions of Precipitated Potassium Chloride Salt on Dried PMOEP Hydrogel

1. SEM Images

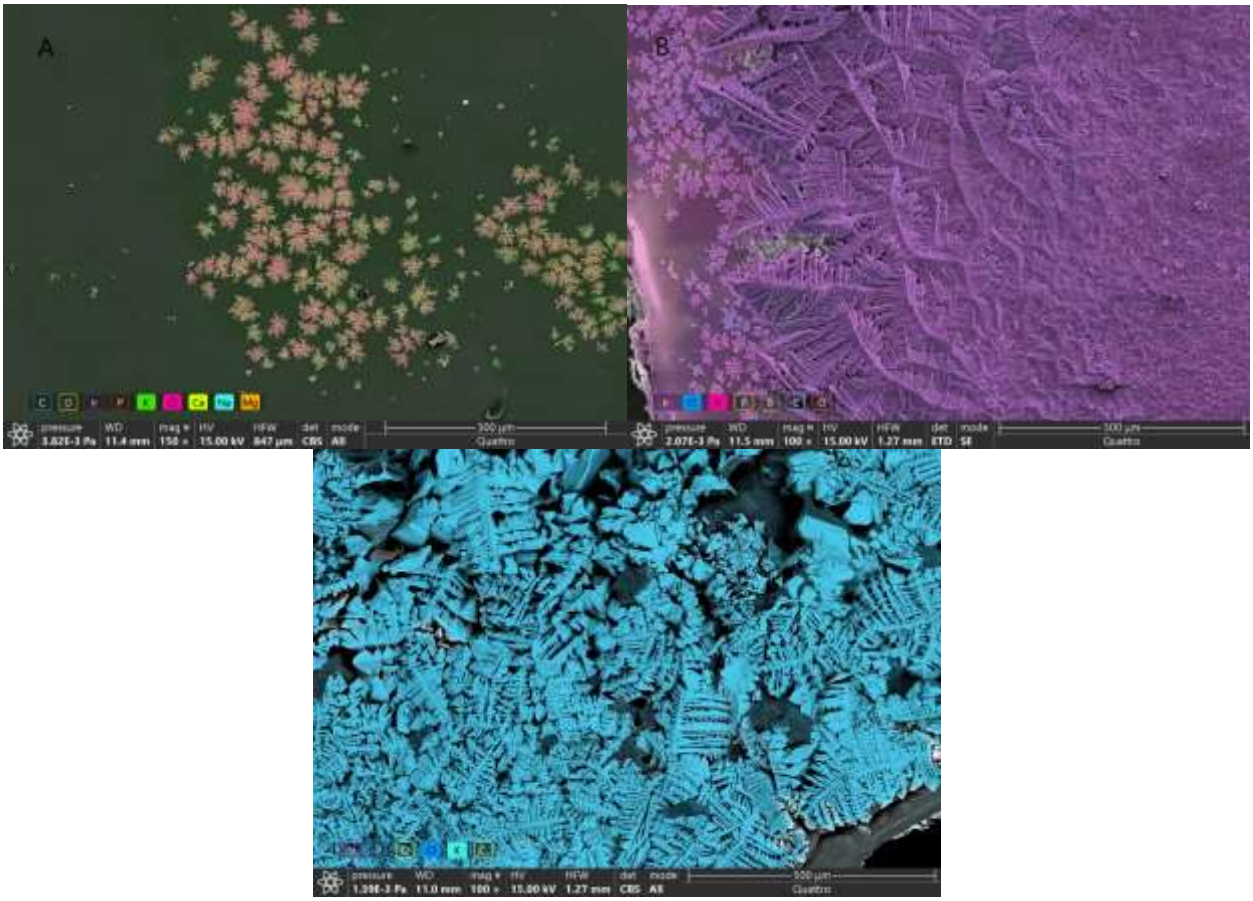

SEM Images Showing Potassium Salt Precipitation on Dried PMOEP Hydrogels after Swelling in (A). 0.1 M KCl, (B). 0.5M KCl, (C). 1M KCl

2. EDS Data

a. 0.1 M KCl

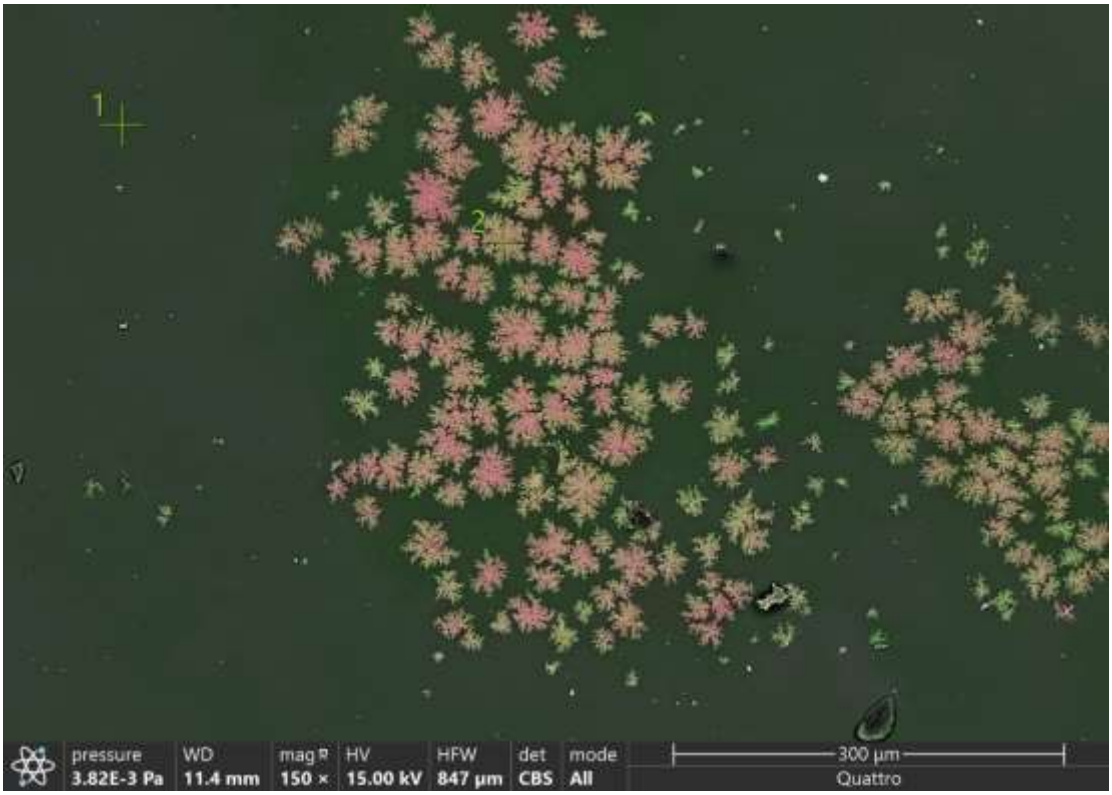

Point 1

Total Number of Counts: 168 084
Total Acquisition Time: 29 seconds
Average Count Rate: 5 796 cps
Acceleration Voltage: 15 kV

Element	Atomic %	Atomic % Error	Weight %	Weight % Error
C	25.4	0.1	14.2	0.1
O	39.0	0.2	29.0	0.2
Mg	0.1	0.0	0.1	0.0
P	19.7	0.1	28.3	0.1
Cl	1.3	0.0	2.1	0.0
K	11.8	0.1	21.3	0.1

Element	Atomic %	Atomic % Error	Weight %	Weight % Error
Ca	2.8	0.1	5.1	0.1
Ir	0.0	0.0	0.0	0.0

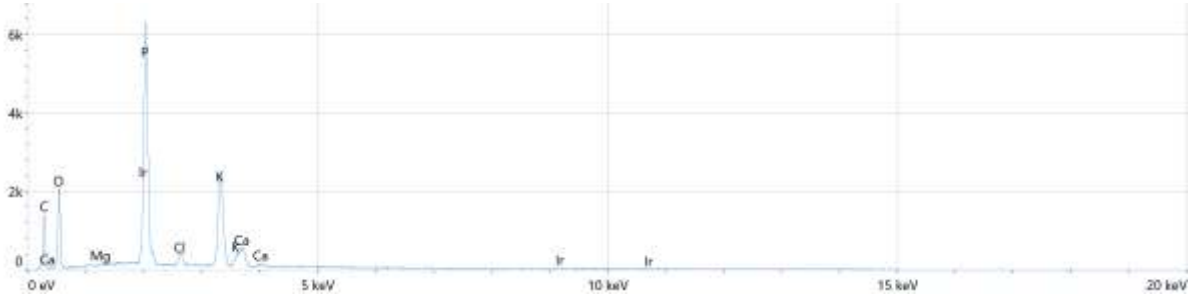

Point 2

Total Number of Counts: 242 065
Total Acquisition Time: 29 seconds
Average Count Rate: 8 347 cps
Acceleration Voltage: 15 kV

Element	Atomic %	Atomic % Error	Weight %	Weight % Error
B	3.1	0.1	1.0	0.0
C	13.4	0.2	4.9	0.1
O	3.0	0.1	1.5	0.1
P	17.5	0.3	16.7	0.3
Cl	26.0	0.1	28.2	0.1
K	36.2	0.1	43.4	0.1
Ir	0.7	0.2	4.3	1.3

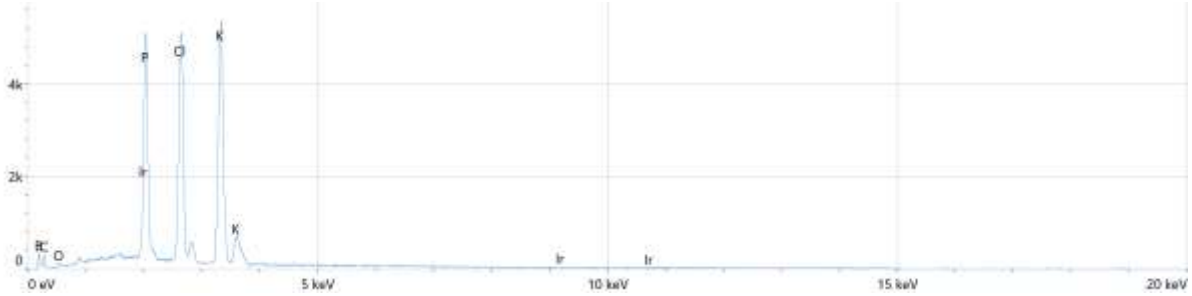

b. 0.5 M KCl

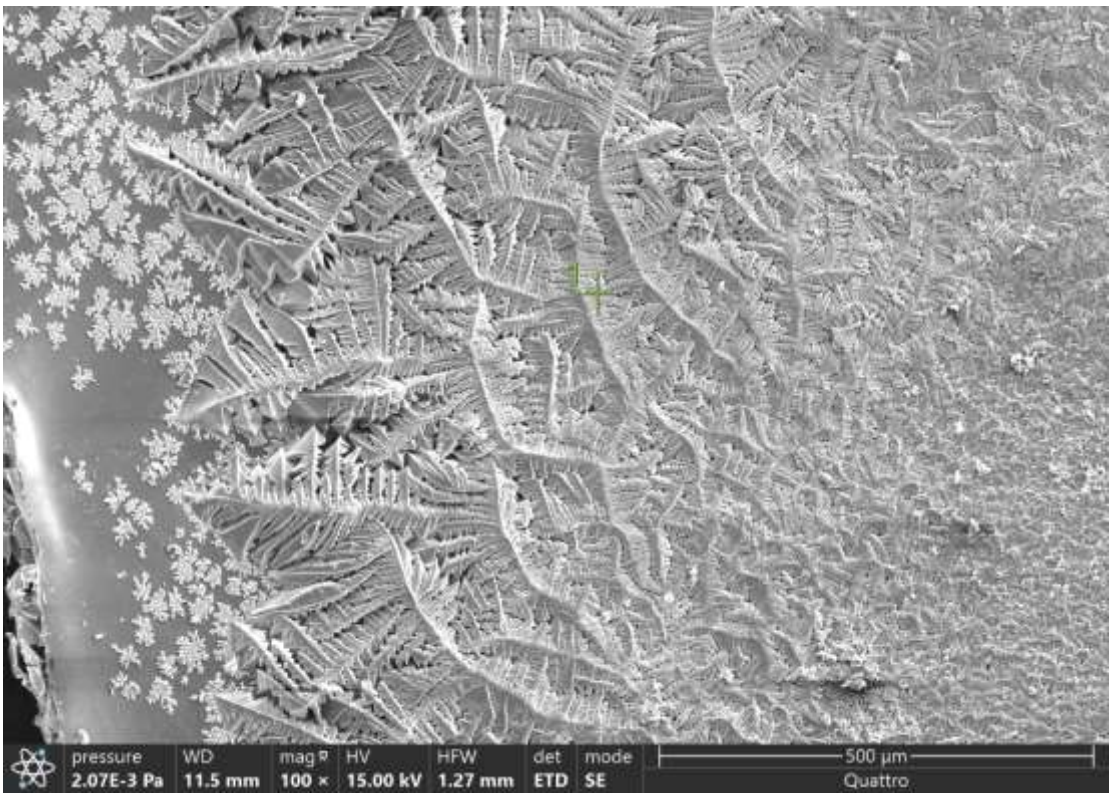

Point 1
Total Number of Counts: 693 677
Total Acquisition Time: 29 seconds
Average Count Rate: 23 920 cps
Acceleration Voltage: 15 kV

Element	Atomic %	Atomic % Error	Weight %	Weight % Error
C	6.6	0.3	2.2	0.1
P	0.0	---	0.0	---
Cl	47.1	0.0	46.3	0.0
K	46.0	0.1	49.9	0.1
Ir	0.3	0.0	1.6	0.1

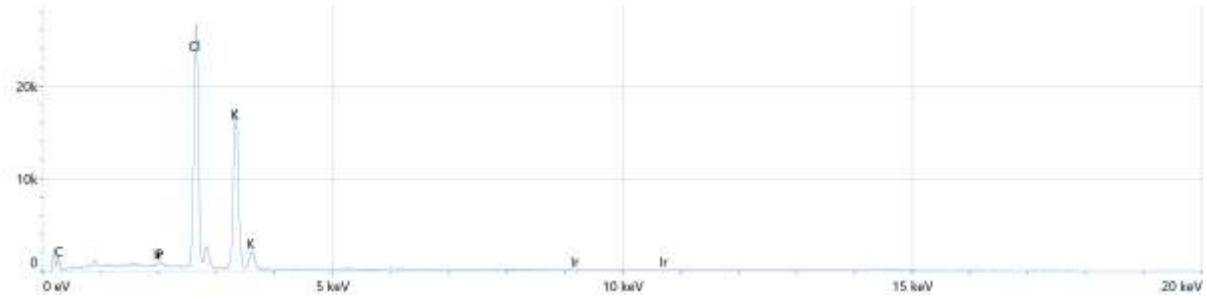

c. 1M KCl

Point 1

Total Number of Counts: 695 174
Total Acquisition Time: 29 seconds
Average Count Rate: 23 972 cps
Acceleration Voltage: 15 kV

Element	Atomic %	Atomic % Error	Weight %	Weight % Error
C	4.8	0.3	1.6	0.1
O	2.0	0.2	0.9	0.1
P	0.0	---	0.0	---
Cl	46.9	0.0	45.5	0.0
K	45.8	0.1	49.1	0.1
Ir	0.6	0.0	3.0	0.1

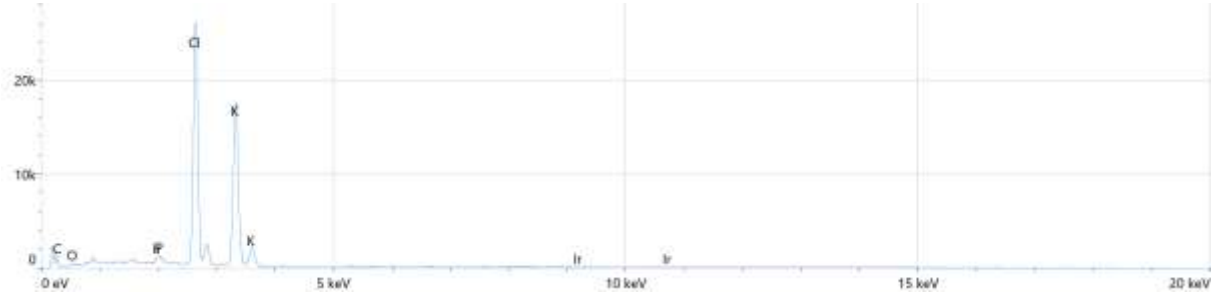

Appendix B: Compressive Test Data

1. PMOEP 30C pH 0.5

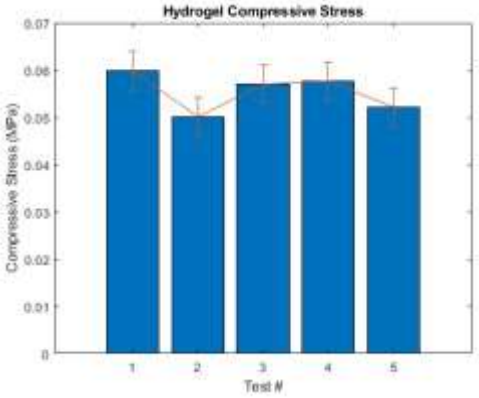

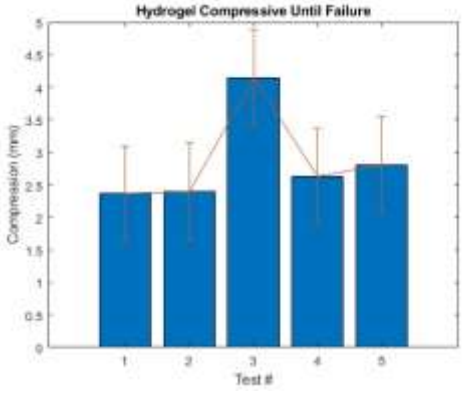

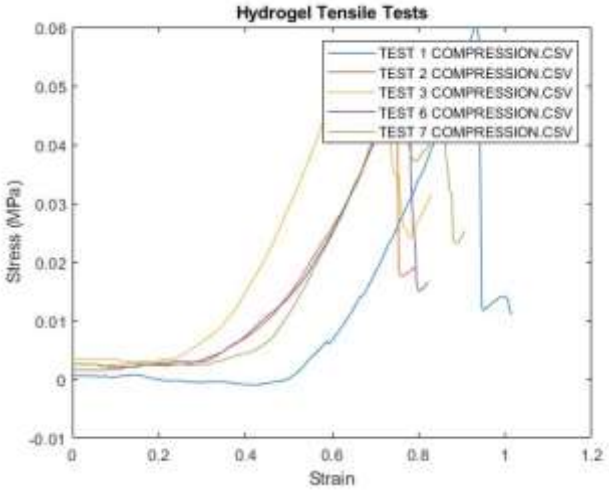

2. PMOEP 30C pH 1

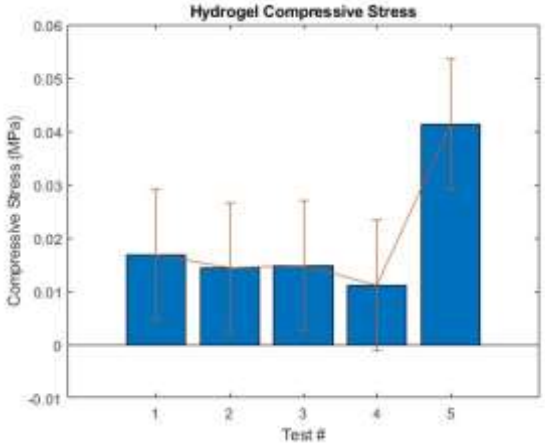

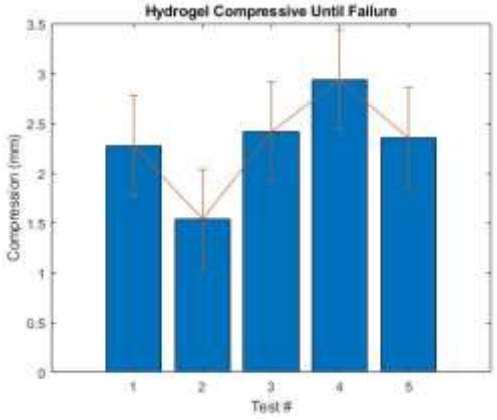

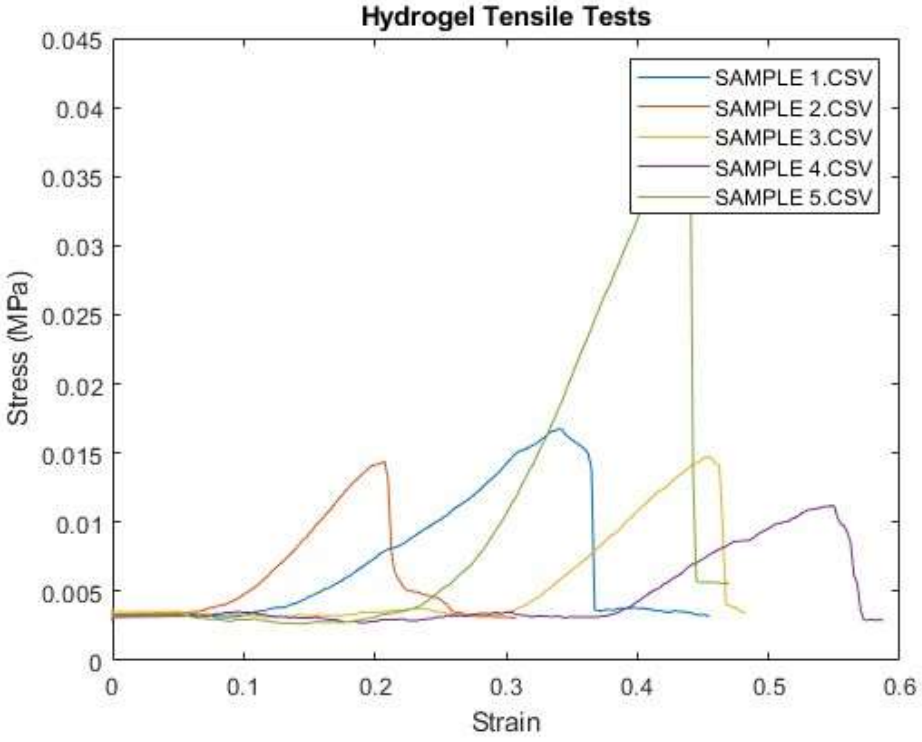

3. PMOEP 30C pH 1.5

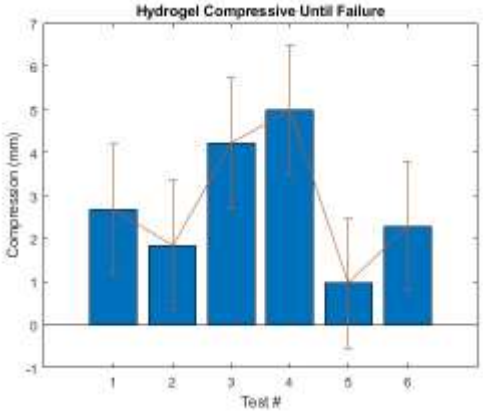

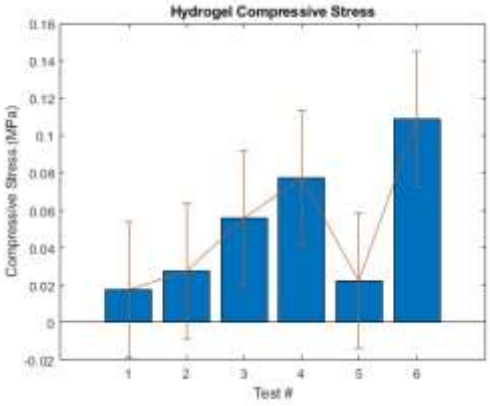

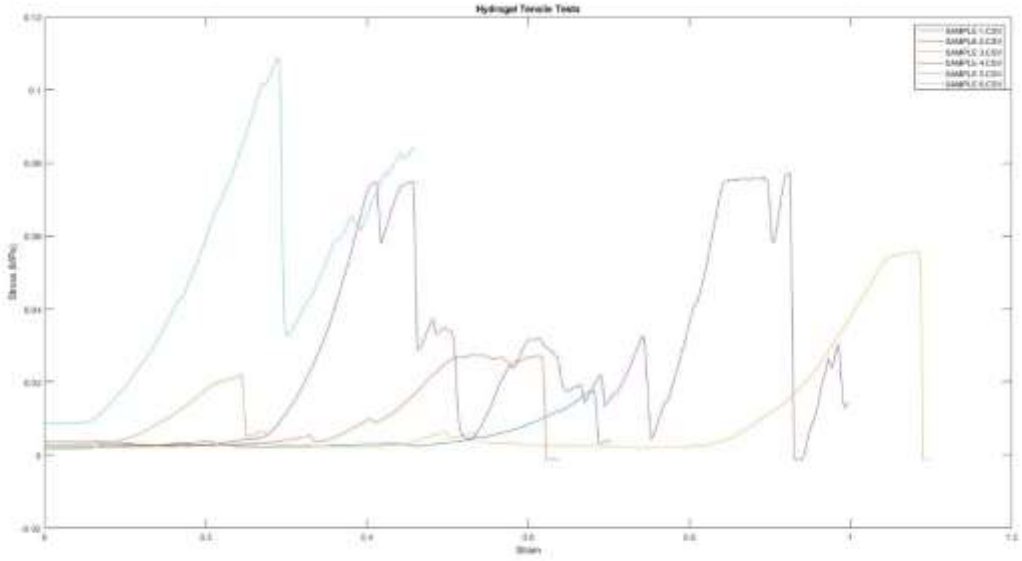

4. PMOEP 40C pH 0.5

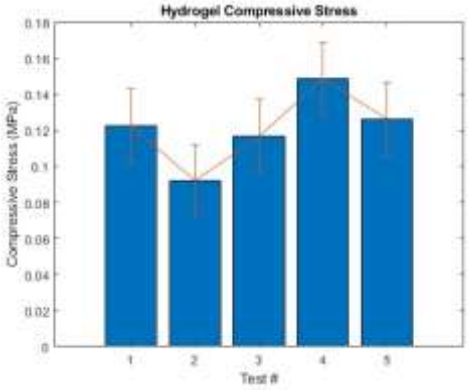

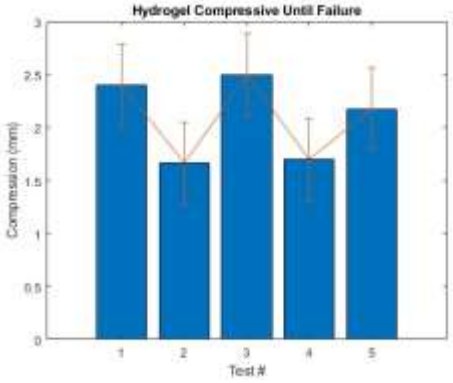

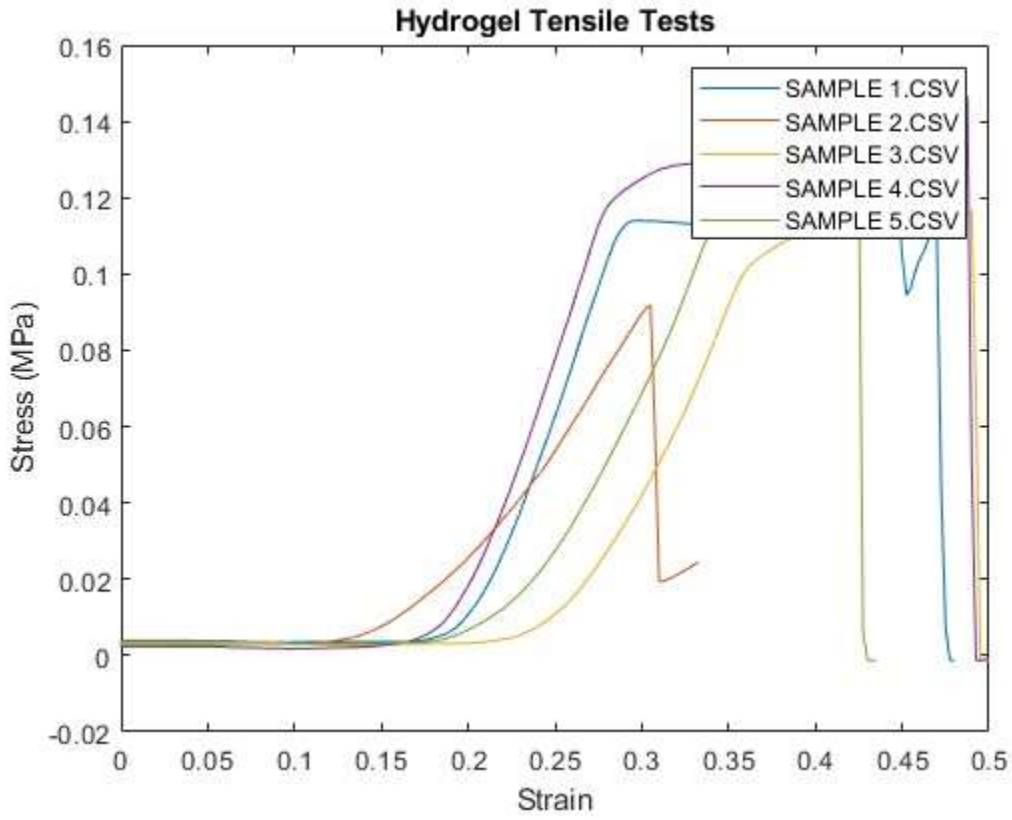

5. PMOEP 40C pH 1

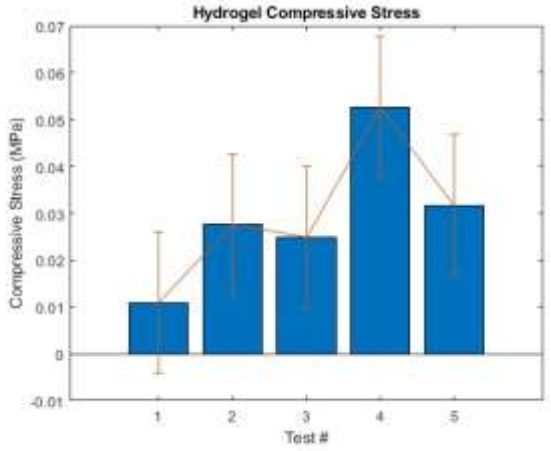

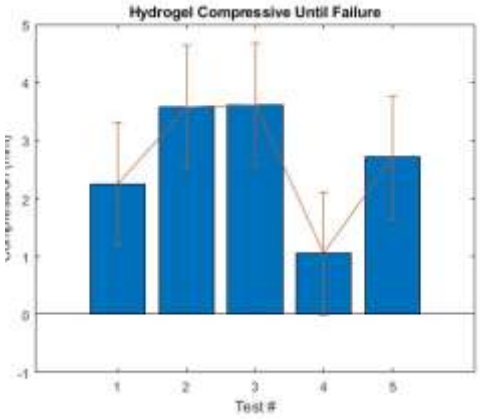

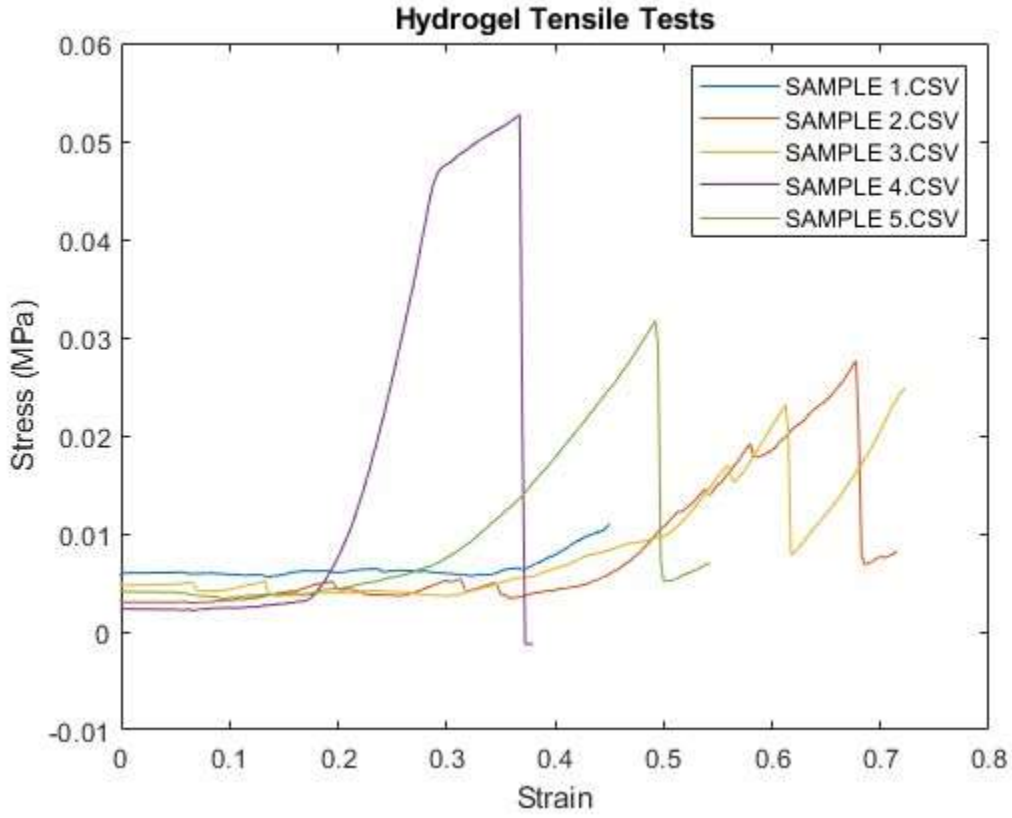

6. PMOEP 40C pH 1.5

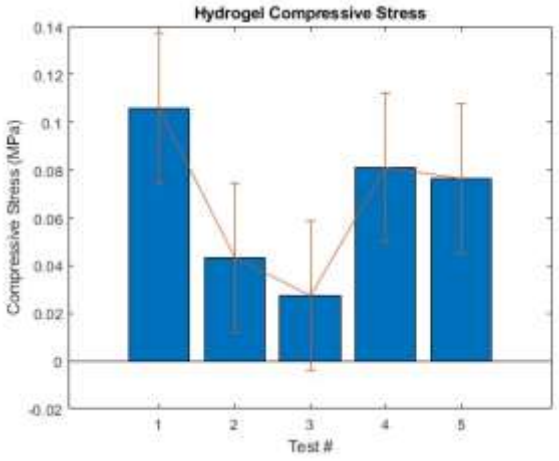

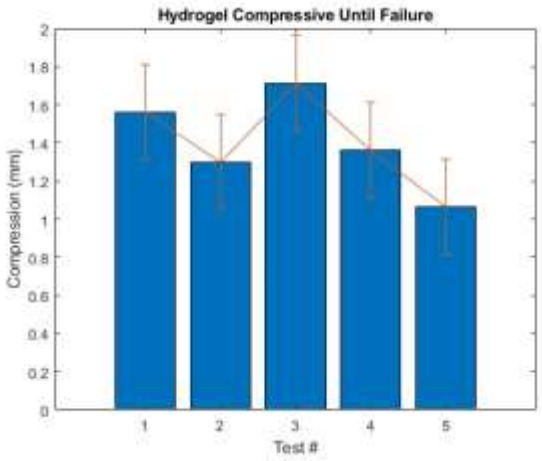

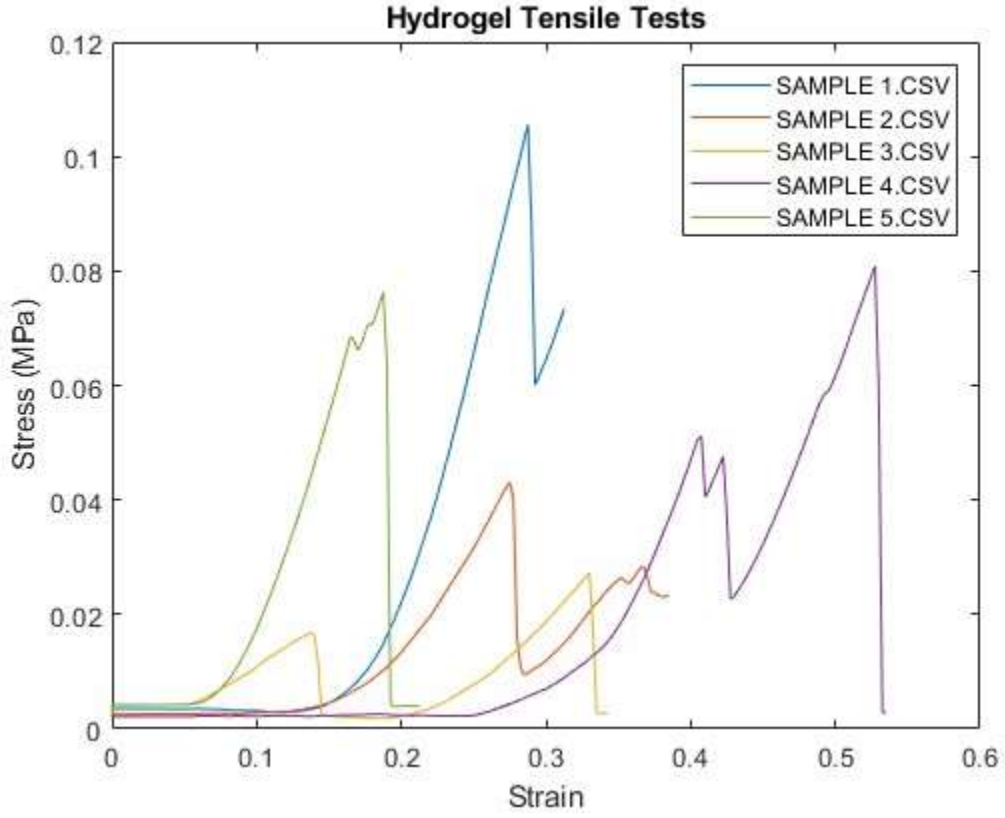

7. PMOEP 50C pH 0.5

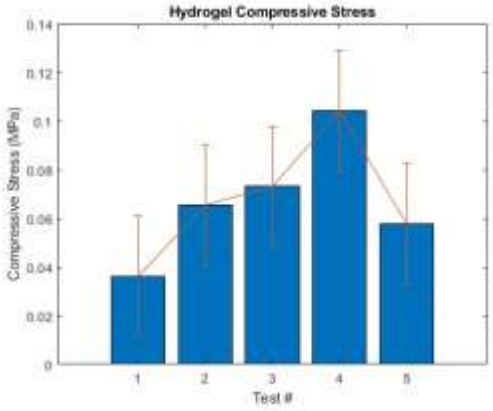

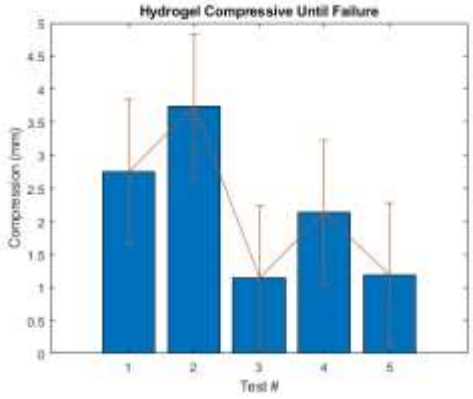

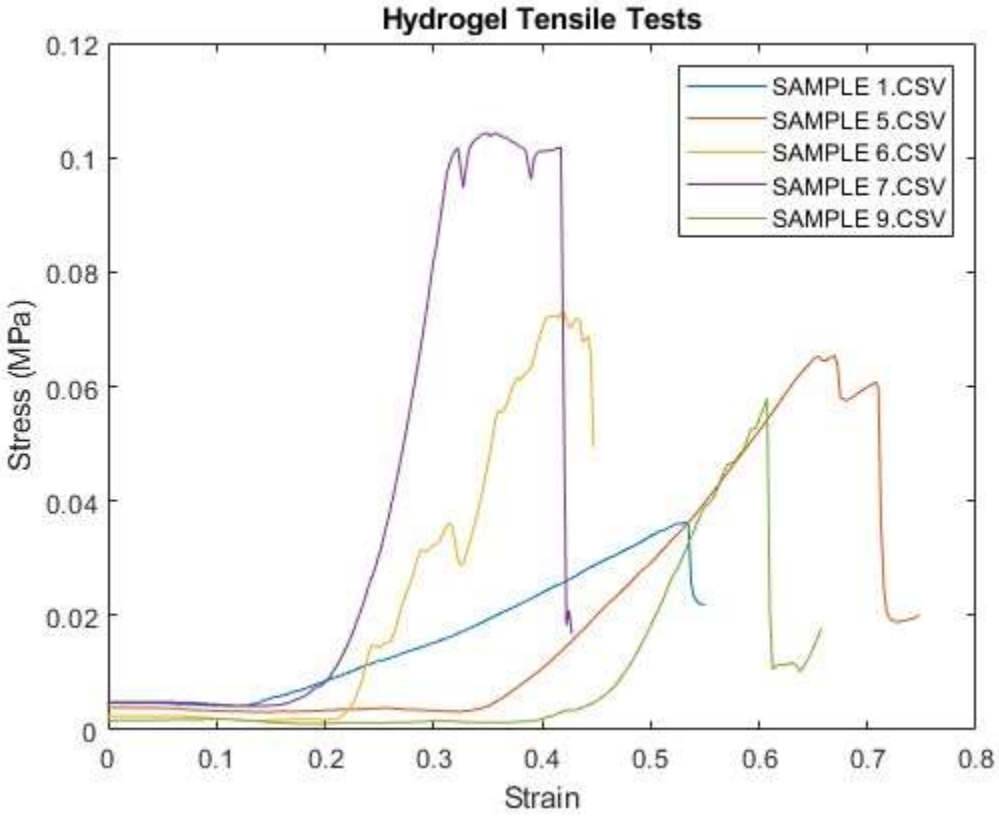

8. PMOEP 50C pH 1

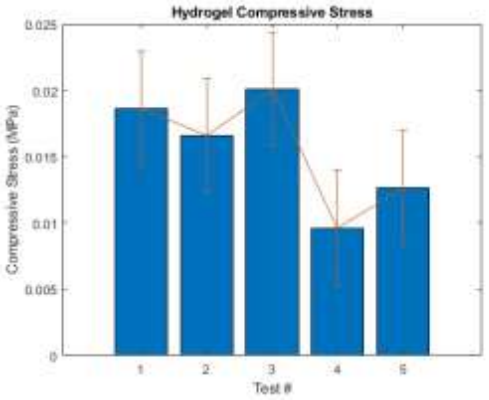

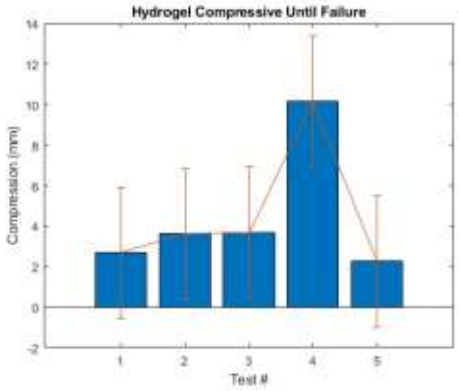

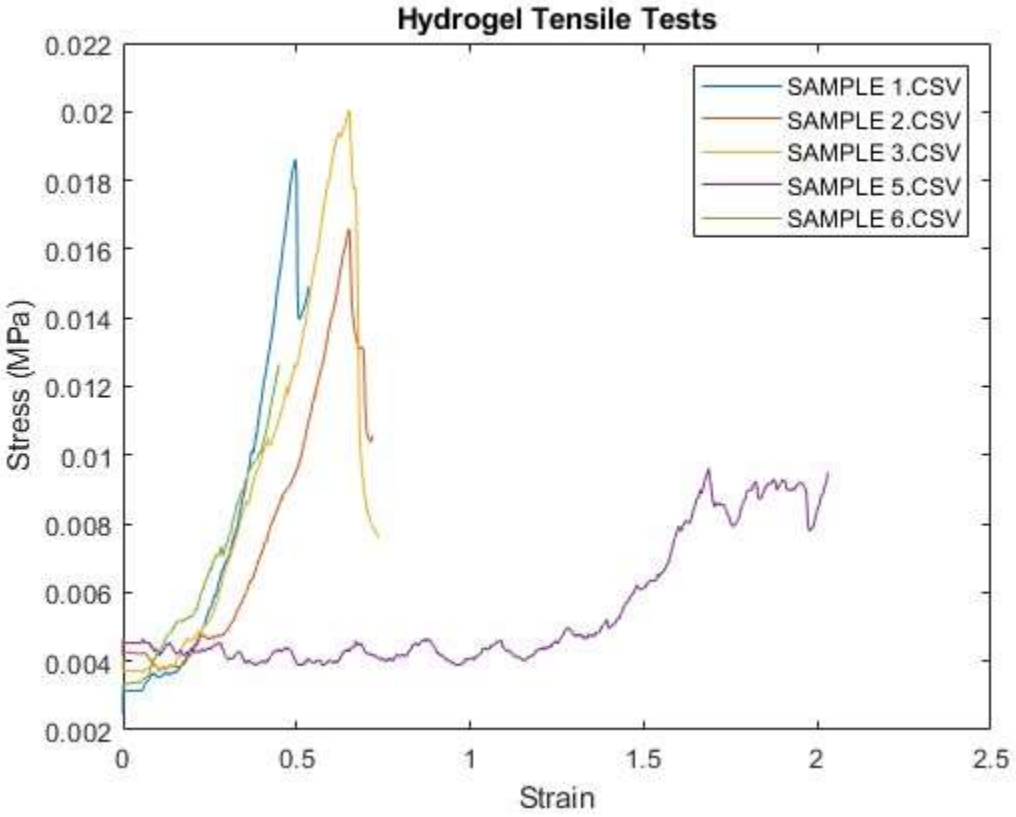

9. PMOEP 50C pH 1.5

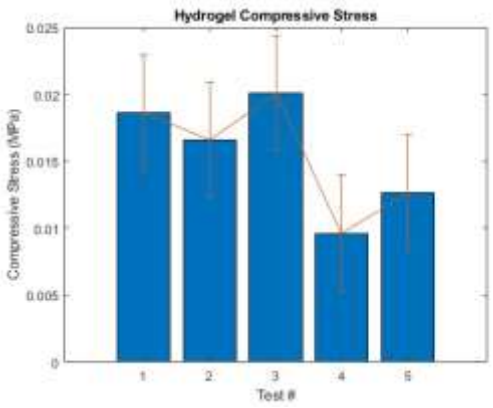

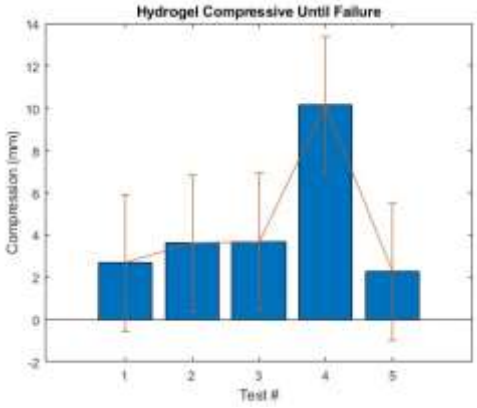

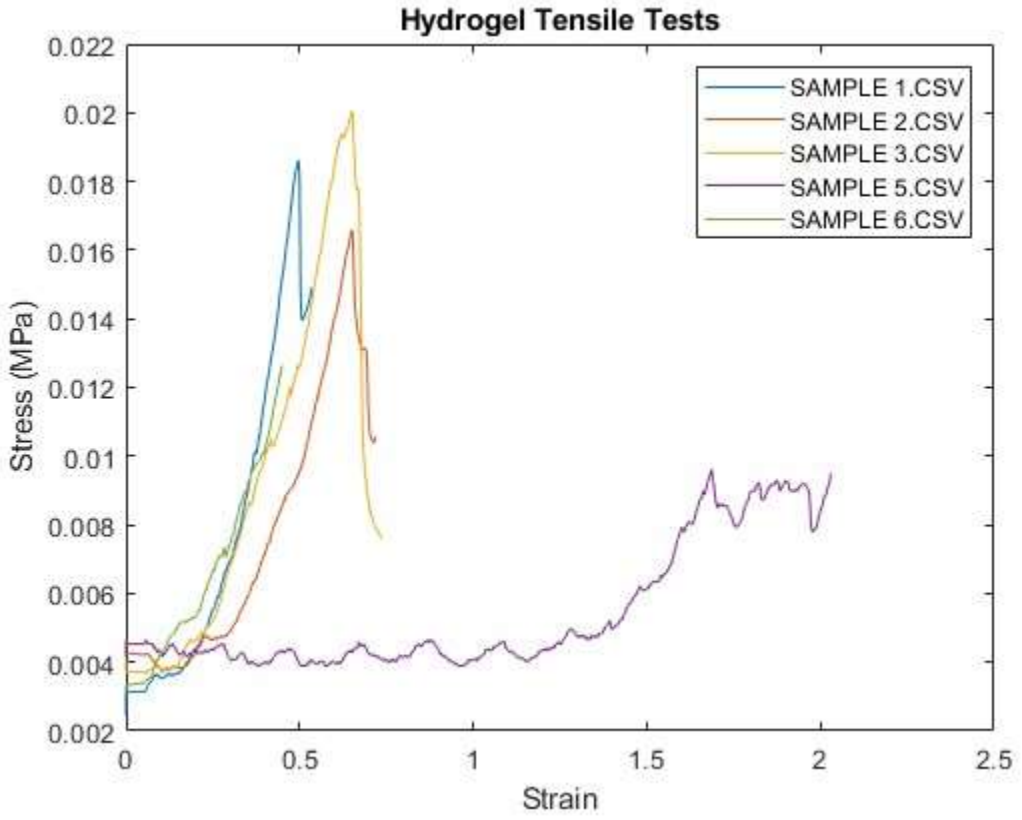

Appendix C: Photopolymerization of Pyrrole and Chitosan Using Titanium Dioxide as Initiator

Introduction:

By 2030, 40% of US adults is estimated to have cardiovascular-related problems including myocardial infarction (MI) [53]. Cardiac patch is used to support the infarcted area of heart muscle after myocardial infarction (MI). On top of comparable mechanical property to the heart muscle, a cardiac patch also requires biodegradable, biocompatible, bioactivity, conductive properties and more [54]. Polyurethane (PU), polycaprolactone (PCL), chitosan (CHI) and other polymers have been studied and used in cardiac patch in animal model. The current development of cardiac patch is to include the conductivity property to the patch which could help to participate in pumping and in synchronizing heart muscle and the patch. Polypyrrole (PPy) have been synthesized with PCL via film casting [55] and with chitosan in ferric chloride [56]. PPy is a organic and conductive polymer consists of multiple pyrroles. Chitosan is a biodegradable polymer with good mechanical properties suitable for cardiac patch. When pyrrole is in contact with titanium dioxide (TiO_2) under UV light at the wavelength of 365 nm, the photopolymerization happens and PPy is produced

The goal is to determine a photopolymerization method for polypyrrole and chitosan. Photoreactor releases photons from light source (e.g. LED, UV, …) to excite the photocatalyst in contact with reactants, which result in chemical products derived from physicochemical transformations [57]. Attenuated Total Reflectance Fourier Transform Infrared Spectroscopy (ATR-FTIR) is used to characterize materials and reaction product. Pyrrole is a conductive polymer that has the potential to be synthesized and used for cardiac patch material. Polypyrrole has been synthesized in acidic environment using $FeCl_3$ catalyst before [58]. Photopolymerization of polypyrrole using Mesoporous Titanium Dioxide photoinitiator has been accomplished in

sodium sulfate and methyl viologen dichloride under UV illumination at the wavelength of 365 nm [59]. However, this method has not been used to form polypyrrole and chitosan hydrogel yet. The photopolymerization of polypyrrole was done using Titanium Dioxide as a photo initiator in sulfuric acid and sodium chloride solution. In this study, polypyrrole is synthesized in the present of sulfuric acid and sodium chloride using Rayonet-500 photoreactor. ATR-FTIR spectroscopies is used to determine the present of PPy product after washing multiple times with water and ethanol and drying for 24 hours.

Materials and Methods:

Pyrrole (>98%) is purchased from Sigma Aldrich and stored the dark fridge until the reaction. Titanium Dioxide Anatase 99.8% is obtained from Alfa Aesar while sulfuric acid is obtained from EMD. The reaction happens at room temperature under UV light at the wavelength of 365 nm from Kayonet photoreactor. 0.5 g of TiO_2 is dissolved in 25 ml of water and 1 ml of sulfuric acid in a beaker and stirred continuously for 5 hours. After TiO_2 is dissolved, filtration is used to extract TiO_2 and washed with ethanol for 3 times and with water for 3 times to wash out sulfuric acid. This cleaned TiO_2 is dried in the vacuum for 24 hours. 40 µl of pyrrole is added into 5.5 ml of water in a test tube. A nitrogen gas line is used to mix water and pyrrole for 20 minutes. Then, 0.5 mg of the cleaned TiO_2 is added to the test tube and let to mix for another 20 minutes. 1 mL of sulfuric acid is added into the test tube and the photoreactor is turned on. The reaction happens for 3 hours. Then, filtration paper is used to filter out the unreacted pyrrole and liquid. Then, polypyrrole was cleaned with ethanol for 3 times and with water for 3 times. The cleaned polypyrrole is dried in the vacuum for 24 hours before taking the FTIR spectra.

An attempt to add chitosan to the system was done. 1 g of Chitosan (CAS: 9012-76-4) was dissolved in 10 mL of Type 1 Ultrapure water, 0.1 g of sodium chloride and 1 mL of acetic acid.

This solution was stirred with a magnetic stirrer for 1 hour. 5 mL of Type 1 Ultrapure water and 40 µL of pyrrole was added into a test tube and stirred with a magnetic stirrer for 20 minutes. Then, 0.5 mg of titanium dioxide (CAS: 13463-67-7) was added into the test tube and continued to stir for another 20 minutes. 1 mL of sulfuric acid and dissolved chitosan solution were added into the test tube. This test tube is then sealed with a needle feeding nitrogen into the test tube. Rayonet-500 photoreactor (365 nm wavelength) was then turned on and let to react for 4 hours.

Results and Discussion:

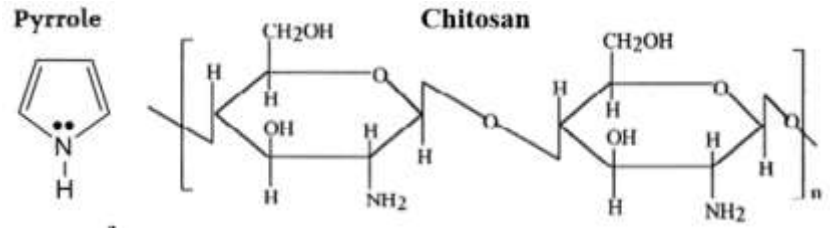

Figure C-1: Structure of pyrrole (left) and chitosan (right).

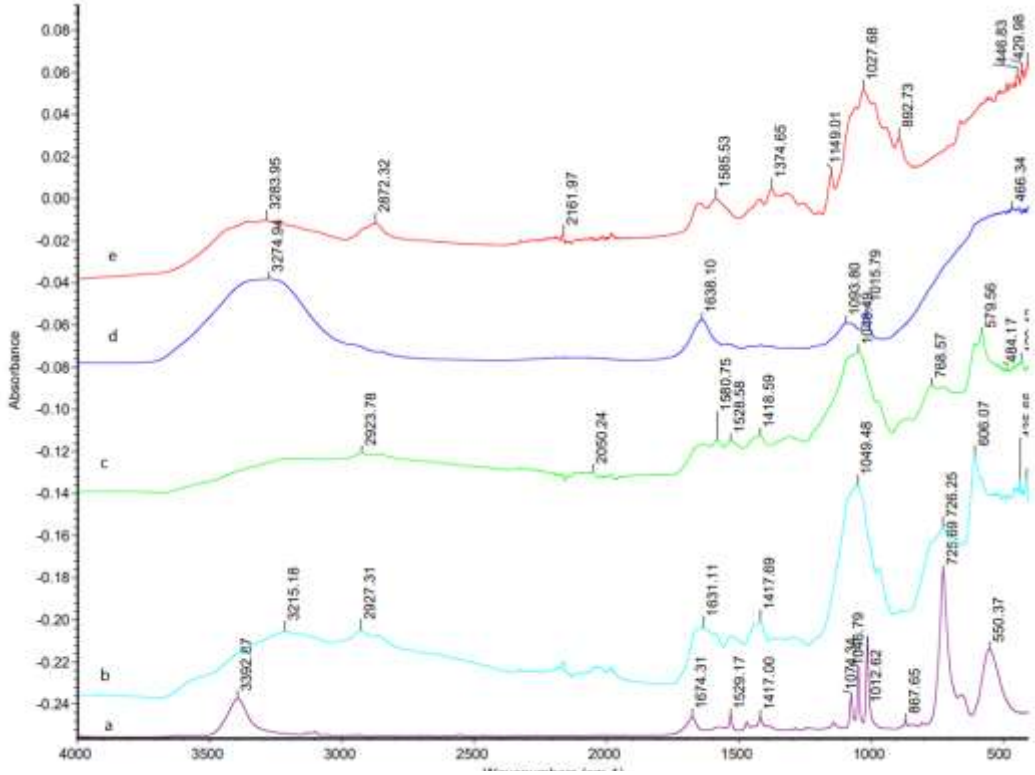

Figure C-2: FTIR spectra of (a) stock pyrrole, (b) synthesized polypyrrole, (c) dried synthesized polypyrrole-chitosan, (d) wet polypyrrole-chitosan after synthesis, and (e) stock chitosan.

Pyrrole molecules contain the bond between carbon and carbon double bond (C=C), carbon and hydrogen (=C-H), carbon and nitrogen bond (C-N) at around and nitrogen and hydrogen bond (N-H) as shown in Figure C-1. On top of that, in polypyrrole, one carbon of a pyrrole molecule next to nitrogen atom is connected to another carbon next to nitrogen atom of another pyrrole molecule creating the carbon and carbon single bond (C-C). Figure C-2 shows the FTIR result of the synthesis. The FTIR from Figure C-2.a shows a peak at 3392 cm^{-1} representing the N-H bonding in pyrrole which is observed between 3300 to 3500 cm^{-1} [60]. In PPy, this N-H symmetric stretching vibration is appeared as a large stretch at 3215 cm^{-1} as shown in Figure C-2.b. The peak at 2927 cm^{-1} is a C-H stretch which would be observed between 2850 to 2960 cm^{-1} [60]. The C=C peaks is expected to observe between 1500 to 1700 cm^{-1} [60]. These peaks are observed at 1674 cm^{-1} for Pyrrole and 1631 cm^{-1} for synthesized PPy. The peaks at 1529 and 1417 cm^{-1} for Pyrrole and for PPy are the stretching modes for the pyrrole rings which are anti-symmetric and symmetric [61]. The C-C out of phase bond is expected around 926 cm^{-1} [62]. The synthesized PPy shows a large peak stretching around 1049 cm^{-1} for C-C bond. The sharp peaks at around 1074, 1046 and 1012 cm^{-1} of pyrrole are peak of =C-H vibrating in the plane [62] while the peaks at 725 cm^{-1} for pyrrole is the =C-H wagging vibration mode stretch. Figure C-2.c and d showed very little to no evidence of chitosan presented in the final product. Figure C-2.c shows the peak at 1580 cm^{-1} for the dried product which is close to the peak at 1585 cm^{-1} appeared on the stock chitosan spectra in Figure C-2.e. Further investigation of the polypyrrole and chitosan synthesis is need to ensure the present of chitosan and pyrrole in the product after photopolymerization.

Conclusion:

Polypyrrole has been synthesized in the present of sulfuric acid, titanium dioxide under the UV light at 365 nm wavelength. The FTIR spectra show some similarity between pyrrole and the synthesized PPy. The C=C peaks, N-H peaks and symmetric and anti-symmetric stretching peaks are observed in both Pyrrole and PPy spectra. Some differences include the appearance of C-H peaks in PPy spectra and a large peak at 1040 cm^{-1} for C-C out of phase bond. Chitosan was integrated into the system and showed a small peak in the FTIR spectra. However, further investigation is needed to confirm the present of chitosan after the synthesis. Future work will focus on further characterization of PPy to confirm the formation of PPy, synthesizing PPy and Chitosan hydrogel, and properties of the product.

References

[1] T. G. Ribelli, L. Francesca, M. Fantin and K. Matyjaszewski, "Atom Transfer Radical Polymerization: Billion Times More Active Catalysts and New Initiation Systems," *Macomolecular Rapid Communications,* vol. 40, no. 1, 2019.

[2] G. Szczepaniak, L. Fu, H. Jafari, K. Kapil and K. Matyjaszewski, "Making ATRP More Practical: Oxygen Tolerance," *Accounts of Chemical Research,* vol. 54, pp. 1779-1790, 2021.

[3] K. Matyjaszewski, H. Dong, W. Jakubowski, J. Pietrasik and A. Kusumo, "Grafting from Surfaces for “Everyone”: ARGET ATRP in the," *Langmuir,* vol. 23, pp. 4528-4531, 2007.

[4] A. Simakova, S. E. Averick, D. Konkolewicz and K. Matyjaszewski, "Aqueous ARGET ATRP," *Macromolecules,* vol. 45, pp. 6371-6379, 2012.

[5] N. A. Peppas, B. V. Slaughter and M. A. Kanzelberger, "Hydrogels in Polymer Science: A Comprehensive Reference," *Polymer Science: A Comprehensive Reference,* vol. 10, no. Set 9, pp. 385-395, 2012.

[6] E. H. Schacht, "Polymer Chemistry and hydrogel systems," *Journal of Physics: Conference Series 3,* pp. 22-28, 2004.

[7] M. Bustamante-Torres, D. Romero-Fierro, B. Arcentales-Vera, K. Palomino, H. Magana and E. Bucio, "Hydrogels Classification According to the Physical or Chemical Interactions and as Stimuli-Sensitive Materials," *gels,* vol. 7, pp. 182-207, 2021.

[8] R. Shah, N. Saha and SahaPetr, "Influence of temperature, pH and simulated biological solutions," *Prog Biomater,* vol. 4, pp. 123-136, 2015.

[9] L. R. Shivakumara and T. Demappa, "Synthesis and Swelling Behavior of Sodium," *Turk J Pharm Sci,* vol. 16, no. 3, pp. 252-260, 2019.

[10] J. Liu, Y. Su, Q. Yue and B. Gao, "Characterization and swelling–deswelling properties of wheat straw," *Carbohydrate Polymers,* vol. 107, pp. 232-240, 2014.

[11] R. Uchida, T. Sato, H. Tanigawa and K. Uno, "Azulene incorporation and release by hydrogel containing methacrylamide propyltrimenthylammonium chloride, and its application to soft contact lens," *Journal of Controlled Release,* vol. 92, no. 3, pp. 259-264, 2003.

[12] T. Sato, R. Uchida, H. Tanigawa, Murakami and A. Murakami, "Application of Polymer Gels Containing Side-ChainPhosphate Groups to Drug-Delivery Contact Lenses," *Journal of Applied Polymer Science, ,* vol. 98, pp. 731-735, 2005.

[13] D. Aydinoglu, "Investigation of pH-dependent swelling behavior and kinetic parameters of novel poly(acrylamide-co-acrylic acid) hydrogels with spirulina," *e-Polymers,* vol. 15, no. 2, pp. 81-93, 2014.

[14] L. Popa, M. V. Ghica and C. E. Dinu-Pirvu, "Introductory Chapter: Hydrogels - From First Natural Hydrocolloids to Smart Biomaterials," in *Hydrogels,* London, IntechOpen, 2019.

[15] V. Kumar, D. De and A. N. Gupta, "EFFECT OF IONIC STRENGTH ON SWELLING OF GELATIN HYDROGELS IN MARGINAL SOLVENTS," *International Journal of Advance Research In Science And Engineering,* vol. 4, no. 01, 2015.

[16] R. Skouri, F. Schosseler, J. P. Munch and S. J. Candau, "Swelling and Elastic Properties of Polyelectrolyte Gels," *Macromolecules,* vol. 28, pp. 197-210, 1995.

[17] F. Khoerunnisa, M. Nurhayati, R. N. Hiqmah, H. Hendrawan, F. Dara, H. A. Aziz, S. Yaya and M. Nasir, "Effect of pH, Temperature, and Electrolytes on Swelling and Release Behaviors of PVA/AAm/GO Based Hydrogel Composites," in *AIP Conference Proceedings*, 2021.

[18] I. C. Stancu, R. Filmon, C. Cincu, B. Marculescu, C. Zaharia, Y. Tourmen, M. F. Basle and D. Chappard, "Synthesis of methacryloyloxyethyl phosphate copolymes and invitro calcification capacity," *Biomaterials,* vol. 25, pp. 205-213, 2004.

[19] E. D. Giglio, S. Cometa, M. A. Ricci, A. Zizzi, D. Cafagna, S. Manzotti, L. Sabbatini and M. Mattioli-Belmonte, "Development and characterization of rhVEGF-loaded poly(HEMA–MOEP) coatings," *Acta Biomaterialia,* vol. 6, pp. 282-290, 2010.

[20] S. Susuki, M. R. Whittaker, L. Grondahl, M. J. Monteiro and E. Wentrup-Byrne, "Synthesis of Soluble Phosphate Polymers by RAFT and Their in," *Biomacromolecules,* vol. 7, pp. 3178-3187, 2006.

[21] M. Koch and M. Wlodarczyk-Biegun, "Faithful Scanning Electron Microscopic (SEM) visualization of 3D printed alginate-based scaffolds," *Bioprinting,* vol. 20, 2020.

[22] G. Ahuja and K. Pathak, "Porous Carriers for Controlled/Modulated Drug Delivery," *Indian Journal of Pharmaceutical Sciences,* vol. 71, no. 6, pp. 599-607, 2009.

[23] Y. Yu, C. M. Landis and R. Huang, "Salt-Induced Swelling and Volume Phase Transition of Polyelectrolyte Gels," *Journal of Applied Mechanics,* vol. 84, no. 5, 2017.

[24] D. F. Evans, G. Pye, R. Bramley, A. G. Clark and T. J. Dyson, "Measurement of gastrointestinal pH profiles in normal ambulant human subjects," *Gut,* vol. 29, pp. 1035-1041, 1988.

[25] M. B. Huglin and J. M. Rego, "Influence of temperature on swelling and mechanical properties of a sulphobetaine hydrogel.," *POLYMER,* vol. 32, no. 18, 1991.

[26] G. J. Alonso, J. L. Rivera-Armenta, A. M. Mendoza and M. L. Mendez-Hernandez, "Effect of temperature and pH on swelling behavior of hydroxyethyl cellullose-acrylamide hydrogel," *E-Polymer,* vol. 144, 2007.

[27] H. v. d. Linden and J. Westerweel, "Temperature-Sensitive Hydrogels," in *Taylor Flow in Microchannels*, Boston, MA, Springer, 2008, pp. 2006-2009.

[28] P. Ravichandran, K. L. Shantha and K. P. Rao, "Preparation, swelling characteristics," *International Journal of Pharmaceutics,* vol. 154, no. 1, pp. 89-94, 1997.

[29] Y. Zhao, F. Fu and O. Bucur, "Expansion Pathology: Nanoscale Imaging of Clinical Specimens with Optical," *Microscopy and Miscoanalysis* , vol. 27(S1), pp. 1902-1903, 2021.

[30] P. Dedecker, J. Hofkens and J.-I. Hotta, "Diffraction-unlimited Optical Microscopy," *Materialstoday,* vol. 11, pp. 12-21, 2008.

[31] B. R. Gallagher and Y. Zhao, "Expansion microscopy: A powerful nanoscale imaging tool," *Neurobiology of Disease,* vol. 154:105362, 2021.

[32] A. T. Wassie, Y. Zhao and E. S. Boyden, "Expansion microscopy: principles and uses in biological research," *Nature Methods,* vol. 16, pp. 33-41, 2019.

[33] E. Sivridis, M. S. Koukourakis, C. E. Zois, I. Ledaki, D. J. Ferguson, A. L. Harris, K. C. Gatter and A. Giatromanolaki, "LC3A-Positive Light Microscopy Detected Patterns of Autophagy and Prognosis in Operable Breast Carcinomas," *The American Journal of Pathology,* vol. 176, no. 5, pp. 2477-2489, 2010.

[34] W. Qiao, Q. Shang, F. H. Lei, A. Trussardi-Regnier, J.-F. Angiboust, J.-M. Millot and M. Manfait, "Imaging of P-glycoprotein of H69/VP small-cell lung cancer lines by scanning near-field optical microscopy and confocal laser microspectrofluorometer," *Ultramicroscopy,* vol. 105, no. 1-4, pp. 330-335, 2005.

[35] F. Chen, P. W. Tillberg and E. S. Bodyen, "Expansion Microscopy," *Science,* vol. 347, no. 6221, pp. 543-548, 2015.

[36] S. M. Asano, R. Gao, A. T. Wassie, P. W. Tillberg, F. Chen and E. S. Boyden, "Expansion Microscopy: Protocols for Imaging Proteins and RNA in Cells and Tissues," *Current Protocols in Cell Biology e56,* vol. 80, 2018.

[37] P.-J. Zhao, C. Li, Y.-L. Wang, C. Fan, X. Li, H. Gong, Q. Luo and M.-Q. Zhu, "Poly[N-(2-acetamidoethyl)acrylamide] supramolecular hydrogels with multiple H-bond crosslinking

enable mouse brain embedding and expansion microscopy," *Materials Chemistry Frontiers*, vol. 5, no. 4, pp. 1795-1805, 2021.

[38] S. Truckenbrodt, C. Sommer, S. O. Rizzoli and J. G. Danzl, "A practical guide to optimization in X10 expansion microscopy," *Nature Protocols*, vol. 14, pp. 832-863, 2019.

[39] Y. Wang, Z. Yu, C. K. Cahoon, T. Parmely, N. Thomas, J. R. Unruh, B. D. Slaughter and R. S. Hawley, "Combined expansion microscopy with structured illumination microscopy for analyzing protein complexes," *Nature Protocol*, vol. 13, pp. 1869-1895, 2018.

[40] A. S. Hoffman, "Hydrogels for biomedical applications," *Advanced Drug Delivery Reviews*, vol. 64, pp. 18-23, 2012.

[41] H.-J. Kong, K. Y. Lee and D. J. Mooney, "Decoupling the dependence of rheological/mechanical properties of hydrogels from solids concentration," *Polymer*, vol. 43, no. 23, pp. 6239-6246, 2002.

[42] D. J. Siegwart, J. K. Oh and K. Matyjaszewski, "ATRP in the design of functional materials for biomedical applications," *Progress in Polymer Science* , vol. 37, no. 1, pp. 18-37, 2012.

[43] S. A. Bencherif, N. R. Washburn and K. Matyjaszewski, "Synthesis by AGET ATRP of Degradable Nanogel Precursors for In Situ Formation of Nanostructured Hyaluronic Acid Hydrogel," *Biomacromolecules*, vol. 10, no. 9, pp. 2499-2507, 2009.

[44] A. Khabibullin, E. Mastan, K. Matyjaszewski and S. Zhu, "Surface-Initiated Atom Transfer Radical Polymerization," in *Controlled Radical Polymerization at and from Solid Surfaces*, Springer, Cham, 2015, pp. 29-76.

[45] M. Flejszar, P. Chmielarz, M. Giebl, K. Wolski, J. Smenda, S. Zapotoczny and H. Colfen, "A new opportunity for the preparation of PEEK-based bone implant materials: From SARA ATRP to photo-ATRP," *Polymer*, vol. 242, 2022.

[46] J. Y. Kim, B. S. Lee, J. Choi, B. J. Kim, J. Y. Choi, S. M. Kang , S. H. Yang and I. S. Choi, "CytocompatiblePolymerGraftingfromIndividualLivingCellsbyAtom-TransferRadicalPolymerization," *Angewandte Chemie International Edition*, vol. 55, pp. 15306-15309, 2016.

[47] R. Ramirez, J. Woodcok and S. M. Kilbey II, "ARGET-ATRP synthesis and swelling response of compositionally varied poly(methacrylic acid-co-N,N-diethylaminoethyl methacrylate) polyampholyte brushes," *Soft Matter*, vol. 14, pp. 6290-6302, 2018.

[48] N. Chan, M. F. Cunningham and R. A. Hutchinson, "ARGET-ATRP synthesis and swelling response," *Macromolecular*, vol. 209, pp. 1797-1805, 2008.

[49] M. Fantin, A. A. Isse, A. Venzo, A. Gennaro and K. Matyjaszewski, "Atom Transfer Radical Polymerization of Methacrylic Acid: A Won Challenge," *Journal of American Chemical Society,* vol. 138, no. 23, pp. 7216-7219, 2016.

[50] C. Britten, Y. Leng and K. B. Walters, "Direct Synthesis of Phosphate Pendant Hydrogels by Acidic Atom Transfer Radical," *Materials Today Chemistry.*

[51] V. Panic, B. Adnadjevic, S. Velickovic and J. Jovanovic, "The effects of the synthesis parameters on the xerogels structures and on the swelling parameters of the poly(methacrylic acid) hydrogels," *Chemical Engineering Journal,* vol. 156, no. 1, pp. 206-214, 2010.

[52] C. M. Ninciuleanu, R. Ianchis, E. Alexandrescu, C. I. Mihaescu, C. Scomoroscenco, C. L. Nistor, S. Preda, C. Petcu and M. Teodorescu, "The Effects of Monomer, Crosslinking Agent, and Filler Concentrations on the Viscoelastic and Swelling Properties of Poly(methacrylic acid) Hydrogels: A Comparison," *Materials,* vol. 14, 2021.

[53] X. Qin, "Coaxial Electrospinning of Nanofibers," *Electrospun nanofibers,* pp. 41-71, 2017.

[54] McMahan, S., Taylor, A., Copeland, K. M., Pan, Z., Liao, J., Hong, Y., "Current Advances in Biodegradalbe Synthetic Polymer-based Cardiac patches," *Journal of Biomedical Materials Reaserach,* vol. 108, no. 4, pp. 972-983, 2020.

[55] Borriello, A; Guarino, V; Schiavo, L; Alvarez-perez, M A; Ambrosio, L., "Optimizing PANi Doped Electroactive Substrates as Patches for the Regeneration of Cardiac Muscle," *Journal of Material Science,* vol. 22, no. 4, pp. 1053-1062, 2011.

[56] D. Ramnath, "Polypyrrole-Chitosan Hydrogel Functions as a Semi-conductive Bridge Within Fibrotic Matrix and Cardiac Tissue," 2019.

[57] A. E. Cassano, C. A. Martin, R. J. Brandi and O. M. Alfano, "Photoreactor Analysis and Design: Fundamentals and Applications," *Industrial and Engineering Chemistry Research,* vol. 34, pp. 2155-2201, 1995.

[58] Cui, Z., Ni, N. C., Wu, JJ., D, G. Q., He, S., Yau, T. M., Weisel, R. D., Sung, H. W., Li, R. K., "Polypyrrole-Chitosan Conductive Biomaterial Synchronizes Cardiomyocyte Contraction and Improves Myocardial Electrical Impulse Propagation.," 09 04 2018.

[59] Strandwitz, N. C., Nonoguchi, Y., Boettcher, S. W., Stucky, G. D., "In Situ Photopolymerization of Pyrrole in Mesoporous TIO2," *American Chemical Society,* vol. 26, no. 8, pp. 5319-5322, 2010.

[60] I.M Ibrahim, S Yunus and M.A Hashim, "Relative Performance of Isopropylamine, Pyrrole and Pyridine as Corrosion Inhibitors for Carbon Steels in Saline Water at Mildly Elevated Temperatures," *International Journal of Scientific & Engineering Research,* vol. 4, no. 2, 2013.

[61] Bruno, F. F., Fortier, J. M., Nagarajan, R., Roy, S., Kumar, J., Samuelson, L, A., "Biomimetic Synthesis of Water Soluble Conductive Polypyrrole and Poly (3,4ethylenedioxythiophene).," *Material Research Society* , vol. 736, 2003.

[62] Sang, N. X., Anh, L. T. L., Thai, T. T., Nghia, P. T., Son, V. T., "Facial Synthesis and Characterization of Polypyrrole/zinc oxide (ZnO) Nanorode and Flower-like Shape Composites," *VNU Journal Of Science: Mathematics-Physics*, vol. 34, no. 1, pp. 40-45, 2018.